UNIVERSITÀ DI PARMA

# UNIVERSITA' DEGLI STUDI DI PARMA

DOTTORATO DI RICERCA IN

"*Scienza e Tecnologia dei Materiali*"

CICLO XXXII

## Microsystems for electrically activated drug delivery and their application to post-surgery pain control


Coordinatore:
Chiar.mo Prof. Enrico Dalcanale

Tutore:
Dr. Salvatore Iannotta

Co-Tutore:
Dr. Victor Erokhin

Dottoranda: Valentina Ricci


Anni 2016/2019

*Ai miei nonni,*

# CONTENTS

# LIST OF FIGURES

# ABSTRACT

Acute postoperative pain is a complex phenomenon characterized by occurrence of inflammatory events and pathophysiological alterations that can lead to the increase of post-operative morbidity, an increase in mortality and a delay in patient recovery. Nowadays, among the several approaches to manage postoperative pain, one of the most efficient strategies is the regional administration of local anaesthetics, in particular the continuous wound infusion. Since the wound is the fundamental source of the pain stimulus, by blocking the stimulus at its origin the analgesic efficacy could be improved and hence preventing at the same time the systemic effects induced by intravenous administration. On the other hand, the continuous wound infusion is carried out through the classic intralesional catheters that show several limits, such as the risk of infection, the reduction of the patients' normal activities that influences their compliance, difficulty in administration and possible systemic toxicity.

In this PhD thesis we have demonstrated the feasibility of a novel type of devices that could be fruitfully used in the post-operative pain treatment by delivering locally much reduced quantities of drugs. All the main features needed for a successful application of the envisaged devices have been demonstrated, including: the biocompatibility, both by using materials that have already been certified in literature and by tests in our labs; the ability of drug loading and sealing; the mechanism of delivery actuated by electrical signals that could be eventually easily controlled remotely.

The different strategies that we explored to fabricate the final device are discussed in this thesis. We have demonstrated that we are able to load model agents both in form of crystals and liquids and we have developed various methods to seal the microcontainers. Finally, we have demonstrated for the first time the possibility of inducing the activation of the drug release by means of electric stimuli making it possible to control the drug administration remotely. We believe that the development of our new device can guarantee a safe, complete and effective administration contrasting the onset of both acute and chronic post-operative pain. We believe that all the research work carried out could have a much wider impact on the development in micro-nano medicine and in particular in local drug release methods.

# CHAPTER n°1

## 1 INTRODUCTION TO POST-OPERATIVE PAIN

In medical treatments the specific way of drug delivery is becoming more and more a matter of research because it has been recognized that the efficacy of the treatment itself, the limitation of the side effects and the duration of drugs effect are dependent on the administration route.

In recent years, the development of new technologies based on nanoscience applied to medicine, including systemic, local and targeting methods, are driving a truly change of paradigm in this field.
In this fast developing field, the application of such technologies to pain control and treatment is becoming a matter of research.

Pain is becoming a branch of medicine that was previously undervalued.
As an example, in Italy, particularly, the Law 38/2010 has made pain therapy a right for every citizen for the first time. As can be read on the website of the Italian Ministry of Health, "this is a highly innovative law, which for the first time guarantees access to palliative care and pain therapy by the patient, within the essential levels of assistance, in order to ensure respect for dignity and autonomy of the human person, the need for health, equity in access to care, quality of care and their appropriateness with regard to specific needs."
Pain is the main reason that leads patients to consult the doctor, it is also the main symptom that affects the quality of life of people by threatening their physical and mental integrity.[1]
It is difficult to establish an exact and complete definition of pain given the individuality and subjectivity of the event. The International Association for the Study of Pain (IASP) has created an agreement within the scientific community by defining pain as "an unpleasant sensory and emotional experience of actual or potential tissue damage or an experience expressed in such terms".

The pain comes from the union of two main components: a sensory, nociception, linked to the transduction, transmission and modulation of the stimulus from the periphery to the

central axis, and affective and experience-related components that significantly change perception.

## 1.1 HINTS ON PAIN PHYSIOPATHOLOGY

The pain sensitive system relies on peripheral mechanisms that transmit the stimulus to the pain central structures where different modulation pathways converge.
Potentially harmful stimuli (thermal, mechanical and chemical) generate somatic pain through the activation of primary nociceptive afferents located mainly in the skin, muscles and joints.
There are, albeit in smaller numbers, primary nociceptive afferent localized at visceral levels that can be triggered by phlogistic events generating visceral pain. In both cases, the primary nociceptive afferents are constituted by free nerve endings of neurons that present their cellular body in the ganglia of the dorsal spinal roots or cranial nerves. Primary afferent neurons are classified according to their diameter, degree of myelination and conduction velocity.[2]

Myelin is an insulating structure arranged around the axons and composed of proteins and lipids. The myelin coating around the axons can be a monolayer or made of several concentric layers that lead to a myelin sheath. Depending on the numbers of myelin layers, nervous fibres can be divided into unmyelinated fibres if myelin coating is composed by only one myelin layer or myelinated fibres if axons are coated by myelin sheath (multiple concentric layers of myelin). In the case of unmyelinated fibres, the nervous tissue appears grey, usually defined as "grey matter", while in the case of myelinated fibres, it appears white, commonly described as "white matter". The main function of myelin is to allow the correct conduction of nervous stimuli, enhancing their transmission speed by means of the "*salutatory*" conduction. In myelinated fibres, in fact, myelin sheath is not uniform along the whole length of axons, forming myelin segments. The interruptions of the myelin sheath between two adjacent segments are called Ranvier nodes (unmyelinated areas). In this way, the nerve impulse, instead of traveling along the entire length of the fibre, can proceed along the axon jumping from one segment to the other, from node to node (**Figure 1.1**).

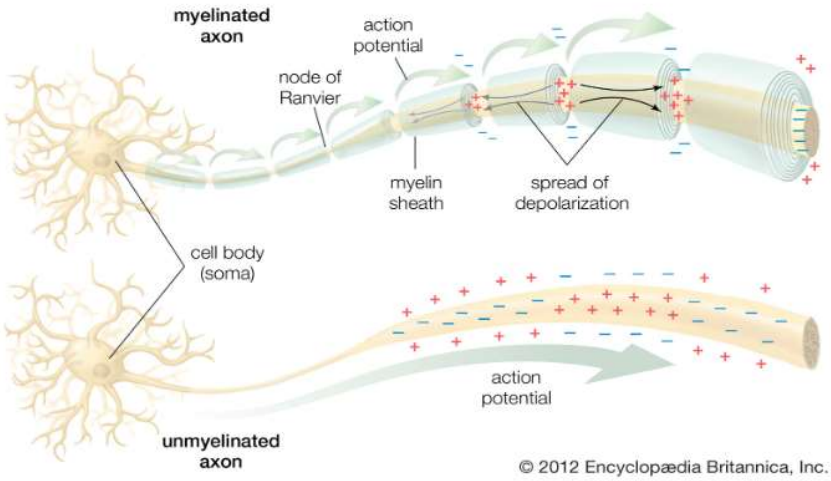


***Figure 1.1**: Basic structure of myelinated and unmyelinated axon and propagation of nerve impulse.[3]*

The axons that carry pain information, therefore the primary somatic and visceral nociceptive afferents, belong to the classes of Aδ fibers, thin myelinated fibers, and C fibers, unmyelinated.

The first type of fibers, Aδ, being myelinated, transmits the signal more rapidly. Therefore, it is believed that they are responsible for the first, acute pain as schematically described in **Figure 1.2**. The unmyelinated C fibers generate a slower signal transmission and this is therefore the basis of a more widespread and prolonged secondary pain; it is precisely the prolonged activation of these C fibers that causes the development of chronic pain.[2]

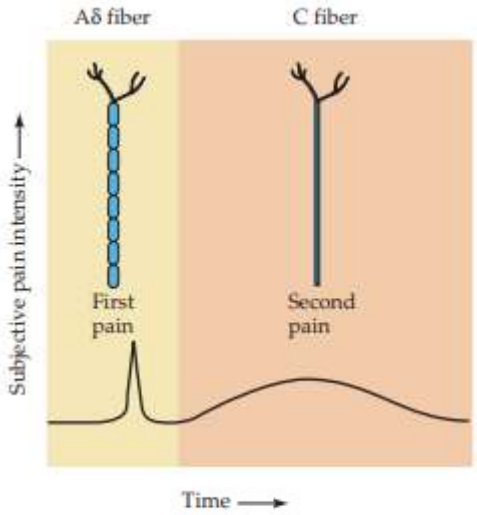


***Figure 1.2**: Pain intensity: first, acute pain is carried by myelinated Aδ fibres while second pain with duller, burning quality is carried by unmyelinated C fibres.[4]*

Repeated, intense and/or prolonged stimuli induce the release of various substances (phlogistic mediators, prostaglandins, nerve growth factor, etc) that, by interacting with nociceptors, lower their response threshold, contributing to the sensitization process. This process can take place both at the peripheral and central levels, in the spinal cord dorsal spine and in general causing a response to less intense stimuli. This process is of significant clinical importance because it contributes to hypersensitivity, pain and hyperalgesia (greater sensitivity to pain as a response to a noxious stimulus).[2]

The primary nociceptive afferents transmit the painful signal to the medullary neuron in the grey matter of spinal cord, releasing neurotransmitters. Sensitive impulses from different primary afferent fibers reach the same medullary neuron; this mechanism of convergence of impulses is the basis of the phenomenon of radiating pain that is a spatial displacement of the pain sensation with respect to the injured area.

The painful impulse once arrived at the spinal cord is sent through the spinothalamic tract to the thalamus.

The brain performs several different functions with respect to pain: through the somatosensory cortex, it defines the site, the intensity and the specific features of the pain; the anterior cingulate cortex and frontal lobes are responsible for emotions, in fact it is precisely the frontal cerebral cortex that gives emotional or unpleasant emotional value to the pain, determining also the behavioural response to the painful event.[5, 6]

Finally, individual pain perception is modulated by a dense network of connections between the various structures of the central nervous system that determine the subjective aspects of the experience. These networks are responsible for the perceived intensity of pain in dependence of expectation or other psychological variables. One of these networks, or circuits, has links to the hypothalamus, midbrain, and medulla, and it selectively controls spinal pain-transmission neurons through a descending pathway. These circuits are responsible for pain modulation, both in intensification and suppression, as they can release endogenous opioid peptides, such as enkephalins and endorphins, and opioid receptors are present in these structures.[2] In **Figure 1.3**, a schematic representation of transmission and modulation of pain is reported.

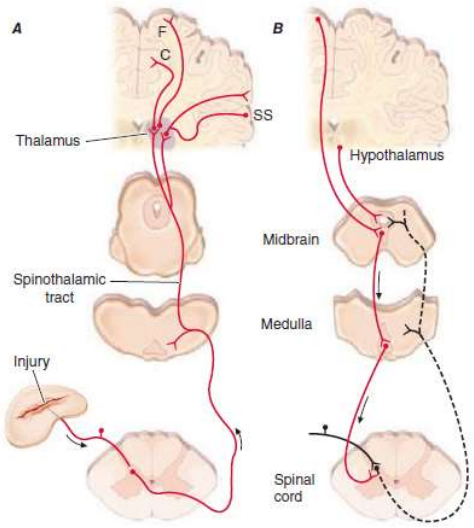


***Figure 1.3**: A) Transmission system of nociceptive stimuli. Noxious stimuli activate the sensitive peripheral ending of first afferent nociceptive fibres that transmit the message to the spinal cord where the message is carried to the spinothalamic tract. The message is sent to the thalamus and then to the anterior cingulate (c), frontal insular (f) and somatosensory cortex (ss). B) Pain-modulation network. Inputs from the frontal cortex and hypothalamus activate cells in the midbrain that control spinal pain-transmission through cells in the medulla.[2]*

## 1.2 POST-SURGERY PAIN

Acute Post-Surgery Pain (PSP) is a complex phenomenon characterized by occurrence of inflammatory events and physiopathological alterations that can lead to the increase of post-operative morbidity, an increase in mortality and a delay in patient recovery. In fact, the painful stimulus coming from the surgical sites triggers systemic responses that involve the cardiovascular system, the endocrine system and the metabolic balance; poor pain control can also compromise proper ventilation function and delay mobilization. Furthermore a not properly treated post-operative pain often leads to the so called Chronic Post-Surgical Pain syndrome (CPSP)[7], implicating an increase in terms of costs for the community. An adequate postoperative pain treatment contributes significantly to the reduction of perioperative morbidity, complications and duration of hospitalization thus contributing to accelerating the patient's global recovery. In an attempt to reduce PSP as much as possible, in many countries the introduction and training of a multidisciplinary team, composed of anaesthesiologists, specialists, surgeons, physiotherapists and nurses, coordinated by a resuscitation anaesthetist, was recommended to provide the Acute Pain Service.[8]

On the basis of the mechanisms of generation and transmission of pain signalling as described in Paragraph 1.1, also the tissue damages caused by surgery result in the release of substances and mediators of noxious stimuli that excite nociceptors, giving rise to *nociceptor pain.* Furthermore, pain can be ascribed directly to the damage of peripheral or central nervous system, generating *neuropathic pain.*

If not treated, postoperative pain can lead to sensitization of both peripheral and central nervous system that causes the reduction of stimuli intensity needed to produce pain. Therefore, stimuli that in normal conditions would not induce pain, begin to induce it. This phenomenon is called *allodynia* and typically occurs immediately after the painful event and can last several hours after the painful stimulus.[4, 9]

So far, there are no diagnostic instruments able to identify the grade of postoperative pain or the proper amount of analgesic drugs necessary to guarantee efficacy and to avoid side effects at the same time.

## 1.3 POST-OPERATIVE PAIN MANAGEMENT

To get a good postoperative pain control, different drugs or classes of drugs are available, including nonsteroidal anti-inflammatory drugs (NSAIDs) (in particular the cyclooxygenase-2 inhibitors that directly target the enzyme responsible for inflammation and pain), weak and strong opioids and local anaesthetics that can be associated or not to adjuvants. [10]
It is possible to achieve an effective PSP control, reducing drug doses and therefore limiting the side effects, preferring the associated use of systemic and local therapies or the combination of two or more drugs that exploit different mechanisms of action: these strategies are called *balanced analgesia* or *multimodal analgesia*.[8]

Acute postoperative pain can be treated in several different ways. Some of the most exploited strategies to manage postoperative pain are described in the following.

*Oral administration* is one of the most used administration pathways because it is non-invasive and well accepted by the patient that could also self-administrate it. Unfortunately, very often this administration route cannot be used whenever the patient is not able to swallow that is often the case in postoperative conditions. Furthermore, very common post-surgery complications are represented by nausea and vomiting, thus making impossible to pursue this route. Another problem arises from the delay of the analgesic effects compared to other administration way.
*Rectal administration* shows the advantage of avoiding first hepatic metabolism, and the disadvantages are the same as for the oral one. Additionally, it's not usually appreciated by the patient.
*Intramuscular injection* is very common in the treatment of postoperative pain. This route provides an effective analgesia even if the absorption is affected from the administration site and even in patient that cannot take oral drugs.
*Subcutaneous injection* or *intravenous administration* are preferable to prevent multiple punctures. In fact, in case of subcutaneous and intravenous routes, it is possible to leave a needle or a cannula for repeated administrations. Moreover, intravenous administration shows an almost immediate onset of the analgesic effect and it is efficient at lower doses.

Nowadays, intravenous *Patient-Controlled Analgesia* (ivPCA) is the method of choice for pain management. PCA allows the patients to decide when to deliver the analgesic, opioid, by

their own. Of course, the physician sets basic parameters such as the bolus dose administered when the patient pushes the button, the interval time when the instrument will not release any further dose even if the patient demands it, and the maximum number of doses in a certain period of time. Furthermore, the device can be set to release a background analgesic dose. The only requirement for this administration way is the cooperation of patient (that can be children as well, over 6 years old) and the capability of using the device. This route of administration is characterized by a great satisfaction of the patient and by a high analgesia quality. The disadvantages are related to the properties of opioids, such as the reduction of immune defenses and the induction of anatomical-functional changes of the central nervous system.[11]

Since the nociceptive inputs of the wound play a crucial role in the perception of pain it is important to act peripherally, and therefore locally, to prevent these inputs from reaching the central nervous system, thus triggering the conscious perception of pain.

The *regional administration* of analgesics acts on the origin of the pain cascade (peripheral nociception) preventing all the events related to the pain.[12] It can be performed by different techniques, such as wound infiltration before its closure or continuous wound infusion. The advantage of delivering analgesic directly into the wound (close to the nerves terminations) is that one can prevent the systemic effects, obtaining a better analgesia compared to intravenous administration. The duration of the analgesic effect depends on the technique used for the administration, if single shot or continuous. For safety reasons, the continuous wound infusion (CWI) is preferred to the single injection. Moreover, in terms of duration, infiltration of local anesthetics into the wound before its sealing shows a short-term postoperative pain relief.[9]

As already mentioned, the wound (the peripheral nociceptor) is the fundamental source of the pain stimulus and therefore the one on which the action of the treatment is most effective. This receptors activation is also able to be reactivated when the effect of the drugs is lost, exacerbating the pain and prolonging the sensitization effect in the central structures.[13] Therefore, blocking the stimulus at the origin through wound infusion increases analgesic efficacy, and continuous maintenance prevents the reactivation mechanisms, with a probable lower hyperalgesia and a more rapid resolution of the symptomatology.

Moreover, experimental models of pain have shown that the CWI of local anesthetics is

able to contrast peripheral inflammation and sensitization during the onset of acute post-operative pain.[14, 15] The consolidated use of this strategy would also be important in decreasing the quantities of morphine commonly used for post-operative pain control.

Despite all these advantages, continuous administration through the classic intralesional catheters has several limits, such as the risk of infection (external device), the reduction of the patient normal activities (problems of patient compliance), difficulty in administration and possible systemic toxicity.[13]

Therefore, new systems are desirable that could guarantee safe, complete and effective administration contrasting the onset of both acute and chronic post-operative pain.

In this framework, our perspective is the development of a micro-system loaded with the drug (local anesthetic or pain killer), able to be implanted in a specific area, could allow a total control on the release modalities and a specific modulation of the doses supplied. Indeed, micro-nanotechnologies play a fundamental role in the development of specific, personalized and consequently more effective therapies.

## 1.4 AIM OF THE WORK

Postoperative pain is a crucial clinical, social and economic problem. Today the recovery of the patient lacks accurate pain management that is carried out by prolonged treatments mainly through external devices, like catheters, implying a series of related problems including the potential onset of infections, the difficult management of the administration and the poor compliance with the patient.
The study and development of an alternative method of administration of post-operative pain medications, capable of overcoming these limits, could contribute to a better treatment of the patient while contributing to the reduction of morbidity and hospitalization times with a clear advantage in the clinical setting.

Therefore, in this PhD project, we aim at developing an innovative device for the post-operative pain treatment that would be able to block the pain cascade acting locally since it will be placed by the surgeon directly inside the wound, close to nociceptors responsible for the first pain transmission, avoiding the limits of the currently used catheters for continuous wound infusion. In particular, we want to reduce the risk of infection due to the presence of external device and improve patients' normal activities enhancing their

compliance. Furthermore, the catheters occlusion and dislodgment may occur during the therapy and their removal could induce further injury to the patients themselves. At the same time, we want to reduce the amount of drug administrated and hence minimizing the risk of toxicity, administrating drugs only when needed, being able to personalize the treatment for each patient, a goal not yet reached in pain medicine.

The device we proposed is based on polymeric microchambers that act as drug reservoirs. We studied two different possibilities for the device basic architecture. The first one (*Device Type* 1) is based on supported freestanding polymeric microchambers while the second one (*Device Type 2*) is based on microwells built inside a polyimide substrate that are sealed by a softer polymeric film. The two basic architectures are depicted in **Figure 1.4**.
The major aim of the project is to activate the drug release by exploiting an electric stimulus, so that it will be possible to perform the remote control of the drug administration.

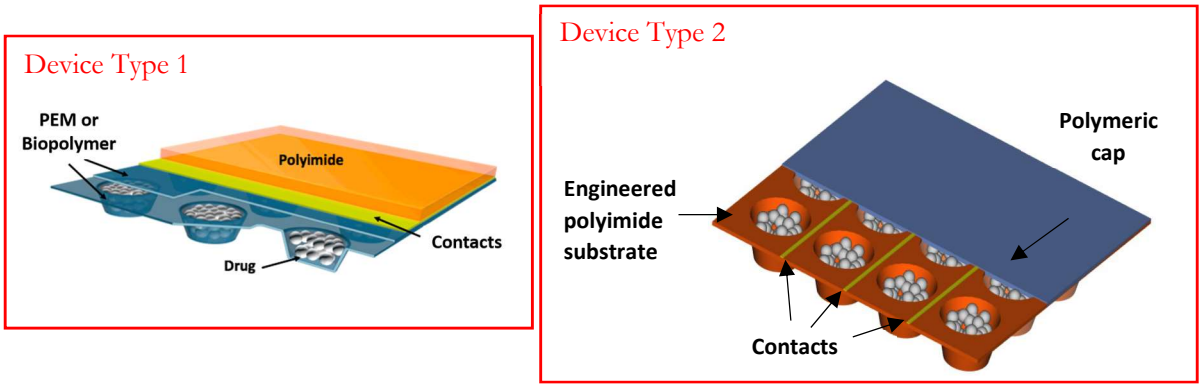


***Figure 1.4**: Device basic architectures.*

Although we have focused on specific pain therapy, many developments of this thesis can also be relevant in the field of both systemic and local drug delivery.

# CHAPTER n°2

## 2 DRUG DELIVERY SYSTEMS

Safety and efficacy are two major requirements in the field of drug delivery. Drug micro-packaging can improve both when developing a new drug delivery system (DDS). In fact, direct administration of therapeutic agents often induces side effects since their distribution in the body is not properly controlled.

Moreover, even drugs that show low toxicity are effective only if their bioavailability is in the therapeutic window. The bioavailability is the fraction of the administered drug dose that reaches the systemic circulation unmodified, and therefore it is available to be effective at the target site. The therapeutic window is the drug concentration range between the lower threshold limit above which the drug takes effective action and the upper toxic limit, above which toxic effects start to occur (**Figure 2.1**).[16-19]

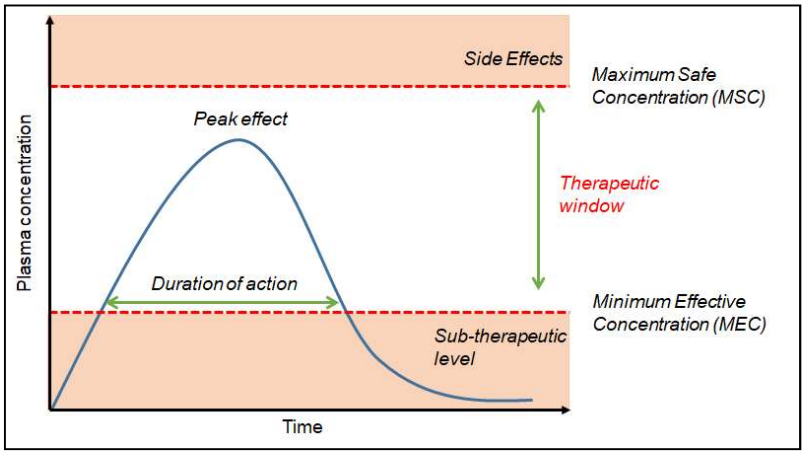


***Figure 2.1**: Therapeutic window scheme.*

The wider the therapeutic window, the safer the drug is. Instead, in case of drugs with a narrow therapeutic window, a small variation in dose or blood concentration may lead to serious adverse side effects. Therefore, therapies involving drugs with narrow therapeutic window require care. It is worth emphasizing that the therapeutic window for the same drug can be different from a patient to the other. It can move upwards if the drug finds any kind of resistance in the body of the patient or interacts with an antagonist so that a higher dose of drug is required to obtain therapeutic effectiveness. On the contrary, the therapeutic

window can shift downwards if the patient is hypersensitive to the drug or if a synergic interaction with another drug occurs.[18, 20]

In order to guarantee the therapeutic level of a drug, the necessary amount of the drug must reach the systemic circulation and the target site. To help in this direction, drug can be delivered through carriers that encapsulate the drug and guide it only towards the target site where the effective need of the drug is demanded.[21]
These carriers must fulfil several requirements:

- To be biocompatible and biodegradable;
- To load an adequate amount of drug;
- Release the drug following a proper pharmacokinetic in order to guarantee the therapeutic efficacy;
- Avoid that the undesired physiological metabolism of the drug would take place before reaching the target site.

A correct protocol of drug administration must also take into consideration that the biodistribution of drugs in the body could be different depending on whether the carrier is plane (*passive targeting*) or functionalized (*active targeting*), independently from the modalities with which such administration is implemented.

Passive targeting is also referred to as Enhanced Permeability and Retention effect (EPR). It exploits the natural tendency of particles-shaped carriers to accumulate in the part of the body characterized by hyper permeable vessels and lack of lymphatic drainage, such as tumour or inflamed tissues.[22, 23]
To exploit EPR effect as passive targeting, the carriers should stay in the body for a time long enough to reach the tumour site that is preventing their removal by the mononuclear phagocyte system (MPS). In the case of systemically administered nanoparticles, a surface coating with polyethylen glycol (PEG) increases the systemic circulation time while reducing immunogenicity. Hence, "PEGilation" of the carrier surface can prevent the carrier, and so the drug itself, from being aggregated, opsonized and phagocyted.[24-26] Nevertheless, passive targeting is not fully selective toward unhealthy tissues even upon PEGilation.

This is why active targeting exploits carriers' functionalization to promote specific recognition of the diseased cells, and hence avoiding effecting healthy cells. This makes possible to maximize the concentration of therapeutic agent at the target site, decreasing at the same time its distribution in other parts of the body hence reducing side effects. For example, cancer therapy involves the administration of cytotoxic drugs such as daunorubicin and doxorubicin. Such drugs kill efficiently cancerous cells, but their selectivity towards cancerous cells is quite low, so they induce apoptosis also in healthy cells.[27]

Therefore, the controlled delivery and release are very important and they are a matter of increasingly active research aiming at developing an ideal drug delivery system. As mentioned before, functionalizing the carrier makes possible to target the delivery system towards the desired cells, avoiding side effects in the healthy cells since the total amount of the administered drug decreases while its therapeutic efficacy improves.
Several systems, such as liposomes, micelles, dendrimers, nanoparticles (gold as well as paramagnetic iron-oxide nanoparticles or mesoporous silica), carbon nanotubes or quantum dots have been proposed in literature as drug carriers, each of which showing some drawbacks.[28] In general the major question to face is to reach a lifetime long enough in the body to guarantee their efficacy. Lifetime is strongly limited by the reaction itself of the body via the immune reactions.

In 1998, Sukhorukov et al.[29] made a significant step toward the fabrication of ideal drug containers by manufacturing nanoengineered polymeric capsules made of alternate layers of polyelectrolytes with opposite effective charge, using the so-called Layer-by-Layer (LbL) technique.[21]
Polyelectrolytes microcapsules, compared to traditional liposomes, have controllable stability and show high permeability towards polar molecules.[30, 31] This is one of the reason why they have attracted great attention for the encapsulation of various materials.[32]

## 2.1 LAYER-BY-LAYER SELF-ASSEMBLIES (LBL)

LbL is a bottom-up versatile physisorption-based technique that allows the production of ultrathin films onto solid substrates. The assembly is built up based on electrostatic interactions between molecules showing opposite charges producing a multilayer film.

This technique was introduced in 1966 by Iler, who assembled silica and alumina colloidal particles onto a glass substrate.[33] Later on, at the beginning of '90s, Decher et al. [34-36] applied the technique to bipolar amphiphilic molecules having two equal charges at each end. The film formation was accordingly promoted by adsorption of alternate layers with opposite polarity, giving thus a multi-layered film, as schematically represented in **Figure 2.2**.

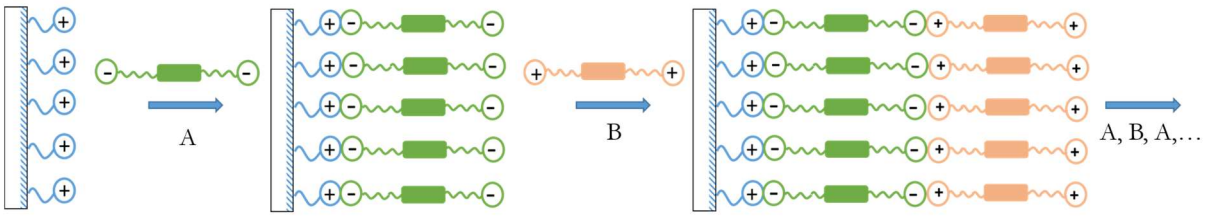


***Figure 2.2**: Schematic representation of adsorption of amphiphilic molecules.*

An improved variant involving the replacement of either the cationic or anionic amphiphilic layer by a positively charged or a negatively charged polyelectrolyte, respectively, was proposed later. In fact, the adsorption of a polyelectrolyte with a given polarity onto a charged surface having an excess of opposite charges takes place at a sufficiently high concentration of polyelectrolyte solution. This is possible because the adsorption of polyelectrolytes onto a charged surface induces the reversion of charge. Indeed, at a sufficiently high concentration of a polyelectrolyte solution, only a part of charged residues attaches to the surface while the remaining residues stay exposed to the solution interface. Finally, they assembled multilayer nanoscaled films by adsorbing alternatively anionic and cationic polyelectrolyte alone.

The build-up of multilayers involves the immersion of a positively charged flat substrate into a solution of the negatively charged polyelectrolyte (polyanion). As a result, a negative monolayer is adsorbed and part of the negative ion groups still expose to the interface. After rinsing in abundant water, the substrate is dipped into the solution containing the positively charged polyelectrolyte (polycation). Again, a monolayer of polyelectrolyte is

adsorbed and the original positive charge is restored.[36] Repetition of this procedure in a cyclic way leads to the fabrication of the so-called polyelectrolytes multilayers film (PEM). A schematic representation of LbL procedure is reported in **Figure 2.3**.

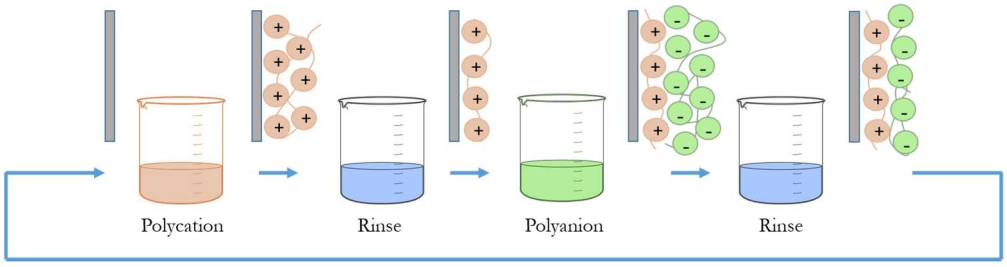


***Figure 2.3**: Schematic representation of polyelectrolytes adsorption by layer-by-layer procedure.*

Before the introduction of the LbL technique, the manufacturing of films controlled at the molecular level was carried out by the Langmuir-Blodgett (LB) method and self-assembly techniques. LB technique involves the formation of a monolayer at the interface between air and water and its consequent transfer onto a solid substrate.[37, 38] Indeed, self-assembly techniques exploit chemisorption or coordination chemistry. Both LB is based on a special equipment and shows constriction in terms of size and geometry of the substrate as well as the film properties and stability. Self-assembled techniques are based on the chemisorption with reaction yield of 100% to maintain functional density on the surface. Since the number of reactions showing a 100% yield is strictly limited, this method applies only to some of particular classes of molecules.[39, 40]

The LbL technique is applicable is a versatile method to produce films based of different types of molecules. The fabrication is very simple, does not require any special equipment or substrate features, because its size, nature and topology are not a restriction since the process involves adsorption from water solution. Deposition of multilayers onto a glass slide or in general onto a flat substrate can be carried manually or using an automated setup as the one reported by Portnov et al.[41]. Different kinds of materials have been used to create multilayer films since the only condition to be suitable for the LbL technique is that they must be charged. Therefore, synthetic polyelectrolytes, biopolymers such as proteins, nucleic acids, lipids and also inorganic particles have been employed.[42-49]

In 1998, Sukhorukov et al. [50] coated for the first time a non-flat substrate by this technique. In detail, they coated micron-sized polystyrene latex particles modified with sulphate group with poly (sodium styrene sulfonate) (PSS) and polyallylamine

hydrochloride (PAH). They hence demonstrated that it is possible to grow polyelectrolytes multilayers films onto particles, paving the way towards the fabrication of a novel class of colloids with controlled and tuneable features at the interface and, most relevant, to the possibility of obtaining micro or nanocontainers for a large variety of applications, i.e. microreactors and drug carriers.

### 2.1.1 POLYELECTROLYTES MULTILAYERS CAPSULES FOR DRUG DELIVERY

Still in 1998, the same group reported for the first time the fabrication of hollow microcapsules made by LbL technique. The method involves the adsorption of polyanion and polycation onto colloid microparticles, acting as a template, in a typical core-shell configuration. After the deposition of each layer, the removal of the unabsorbed polyelectrolyte occurs by centrifuging and washing the dispersed microparticles several times. The schematic representation of capsules shell fabrication is described in **Figure 2.4**.

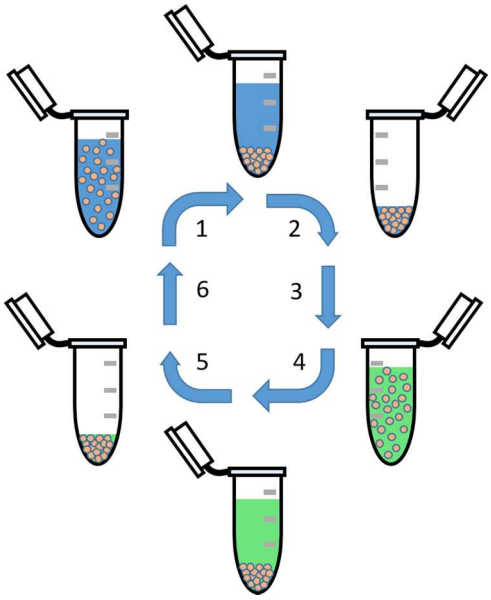


***Figure 2.4**: Polyelectrolytes multilayers shell formation. After adding polycation solution and stirring for 15 min: 1) centrifugation; 2) removal of the supernatant; 3) three washing steps, addition of the polyanion solution; 4) centrifugation; 5) removal of the supernatant; 6) three washing steps, addition of the polycation solution; reiteration until the desired number of layers is deposited.*

After the deposition of the desired number of layers, the dissolution of the template (referred to as "passive" template) occurs, enabling the formation of hollow polymeric shells. In their specific case, melamine formaldehyde (MF) particles were the templates and PSS and PAH were the polyanion and the polycation, respectively. The dissolution of the MF template takes place in water media at pH lower than 1.6.[29] The effect of the pH on

the LbL shell is discussed in the following paragraphs.

The discovery of this method to fabricate hollow microcapsules attracted a lot of interest mainly in the field of drug delivery, since they seemed to be the ideal candidate to host drug and act as carriers. Various materials, both organic and inorganic, can be used to fabricate capsules. The possibility of selecting different kinds of cores leads to the fabrication of capsules of different size and geometry. Besides MF particles already mentioned, other examples for organic templates are polystyrene[51, 52] and polylactic acid particles[53]. Organic templates show several limitations mainly due to dissolution issues. For instance, MF particles dissolution leads to the formation of large oligomers that slowly diffuse out of the polymeric shells, hence the multilayer is exposed to high mechanical stress that can also lead to the capsules damage and rupture. Indeed, polystyrene and polylactic acid cores' dissolution takes place in organic media that are known to modify the structure and the stability of the polymeric shells.[52]

Unlike the case of organic template, the dissolution of inorganic cores takes place easily in aqueous solution and the dissolution products, having a low molecular weight, diffuse through the capsules shells without affecting the stability of the shells themselves. Among the inorganic templates reported in literature, there are carbonate-based particles such as $CdCO_3$, $CaCO_3$, $MnCO_3$, silica micro and nano particles and gold nanoparticles. Nonetheless even inorganic templates show several limitations. For example, carbonate templates formation leads to a polydisperse distribution with not perfectly spherical particles that can result in lack of stability and aggregation problems. However, the advantages are numerous including their porosity that can be used to encapsulate chemicals by absorption.[54, 55] As far as the $SiO_2$ particles is concerned, the main disadvantages arise from the dissolution that takes place by etching the silica core with hydrofluoric acid and by the fact that they could aggregate as well.[56, 57] Gold nanoparticles can be useful for their nanometric size that makes them suitable for circulation. However, they also show some limitations. In fact, their dissolution occurs using very hazardous solutions, such as potassium cyanide.[58] The main advantage of using inorganic cores is that the osmotic pressure after the dissolution of the core is avoided and the dissolution itself of the core is completely achieved.[59]

Another class of sacrificial cores is represented by biological cells, such as human red blood cells[60]. However, the dissolution of a template made of human red blood cells involves

their incubation into a sodium hypochlorite solution that, on its turn, can oxidize the outer polyelectrolyte shell.[61, 62]

Beyond the solution of using sacrificial "passive" templates, removed once the polyelectrolytes multilayers is generated, LbL assembly can be used to directly coat active substances, for example in form of crystals or pre-loaded particles, realizing thus "active" templates.[50, 59, 63-65]

Layer-by-layer method is universal and very simple to carry out, so there are no restrictions about charged materials that can be used to fabricate LbL assemblies. The mostly used polyions to create nanoshells are poly(styrene sulphonate) (PSS), poly(acrylic acid) (PAA), dextran sulphate, sodium alginate, gelatine and DNA portions as polyanions, and polyethyleneimine (PEI), poly(dimethyldiallylammonium chloride) (PDDA), poly(allylamine) hydrochloride (PAH) and chitosan as polycations.[59]

The typical polyions are chosen depending on the desired features to implement into the capsules, so it is possible to tailor the composition of the shell. Every material gives its own functionality to the capsules. For example, weak polyelectrolytes leads to the formation of pH sensitive capsules. Therefore, by changing pH, it is possible to open or close shell's pores to promote drug load or release, respectively.[66] Furthermore, the typical materials for the fabrication of the shells, can be combined with other ones that can give special functionality to the capsules. In this way, for example, it is possible both to load the drug inside the capsules and release it upon triggering by an external stimulus. Moreover, by using a polymer with reactive group as outermost capsule's layer, one can modify the surface with specific ligand, receptor or whatever to exploit targeted drug delivery.[67]

#### 2.1.1.1 STIMULI FOR ENCAPSULATION AND RELEASE

The external stimuli for encapsulating a payload inside the capsules and then for releasing it, can be of different nature depending on the kind of polyelectrolytes and on the kind of materials incorporated in between the layers. Stimuli can be chemical, physical or biological as summarized in **Figure 2.5**.

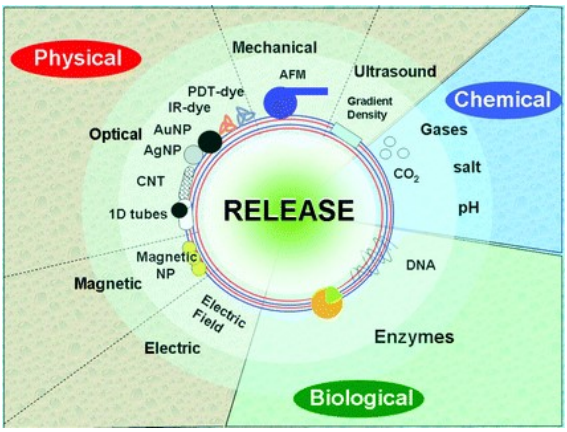


***Figure 2.5**: Scheme of the different release methods.[68]*

Among chemical triggers, there are the already mentioned pH, the ionic strength and solvent action.

The fabrication of pH-sensitive capsules is possible involving weak polyelectrolytes such as PAH, PAA, or poly(methacrylic acid) (PMAA). The pH can be used to control the capsules permeability. In fact, the change of pH leads to the accumulation of charges in between the multi-layered shell, so that the repulsion of charges causes capsules expansion with opening of pores and consequent increase in permeability.[66, 67] Regarding to ionic strength, it is well known that the increase of salt ions screens the electrostatic interactions between the oppositely charged polyelectrolytes that form the multilayers shell. In fact, polyelectrolytes show different conformation in salt solution compared to in water. In water, the conformation of polyelectrolyte is relatively relaxed while in presence of salt their conformation becomes more coiled as the salt concentration increases, inducing an increased permeability since the coiled conformation generates a less compact "packaging" letting molecules passing through the shell. Antipov et al. investigated the salt-induced change in permeability by monitoring the diffusion rate of a dye molecule through the shell while changing the salt concentration.[62, 67, 69] Changing salt concentration can also bring to opposite results when polyelectrolytes containing hydrophobic groups compose the multilayer shell. An example of such polyelectrolyte is PSS; in this case, increasing of salt concentration leads to reduction of the electrostatic interaction between the opposite layers. This results in shrinkage of the capsules by PSS' hydrophobic groups with consequent decrease in permeability.[62, 67, 70]

The most widely used media is by far water while organic solvents could tune capsules' permeability. Lvov et al. reported the use of a mixture of ethanol and water to increase

PSS/PAH capsules permeability and encapsulate big urease molecules inside the shell. After the ethanol removal and once the water environment is recovered, the shell's pores are closed again so that urease molecules are entrapped inside, while small urea molecules can diffuse through the membrane.[62, 67, 71]
It is worth pointing out that ionic strength and solvent induced changes in permeability could have useful applications in industry while their exploitation in nanomedicine and biological environment turns out to be rather tricky.

Physical triggers include magnetic field, a mechanical deformation, light, ultrasounds and temperature. Changes in temperature can induce permeability variation in hollow polyelectrolytes multilayers capsules. In the case of a PEM film onto a solid substrate, an increase of temperature will not affect the film thickness, while in a free PEM film in presence of water, as it is the case of capsules, an increase in temperature can lead to shell shrinkage that results in stiffening of capsules walls with consequent reduction in permeability up to its disappearance. Water is fundamental to achieve such effect that can be exploited to encapsulate and release molecules in and from the capsules.[62, 67, 72-75]

Although the temperature could be an important trigger for both encapsulation and release, its application *in vivo* is quite difficult, since the temperature in physiological media is almost constant. That is why it is necessary to explore remote triggering such us ultrasounds. Shchukin et al. and Skirtach at al. [76, 77] demonstrated the opening of polyelectrolytes multilayers capsules exploiting ultrasonic waves. The latter group demonstrated also the effect of enhancing ultrasound sensibility by incorporating $Fe_3O_4$ nanoparticles. The main challenge for ultrasounds application in medicine is keep frequency and power in the allowed range.
Another remote trigger investigated is the application of a magnetic field to capsules that incorporate magnetic particles in their shells. The main reason for incorporating magnetic nanoparticles in polymeric capsules is of course the possibility of targeting. The combination of targeting and possible release could enhance the performances of polymeric delivery systems. Lu et al. demonstrated that the permeability of PSS/PAH incorporated with ferromagnetic cobalt nanoparticles increases if they are exposed to alternating magnetic field (frequencies 100-130 Hz) for 30 min.[62, 67, 78] The main limitation to this kind of trigger arises from the long exposure time needed that induces an increase of temperature as well as the high frequencies required.

In addition, the laser light is another physical stimulus that allows release from polyelectrolytes capsules. The main requirement for biomedical applications is that the light must work in the near IR so that this minimizes the light absorption from cells and tissues (the so-called light bio-window). By incorporating noble metals nanoparticles in between the layers of the shells, their light absorption can trigger the release by the local heating of the irradiated nanoparticles, causing in turn the capsules rupture with the consequent rapid release of the whole payload.[79, 80] Light driven release has been deeply studied since it allows complete remote release, limited by the penetration of the light itself. Skirtach at al.[81] introduced an advanced technique for the release that allows a slower and controlled release of the cargo without the disruption of the capsules. Indeed, when the irradiation ends, there is no more heat generation and the multilayers become impermeable again. This could be explained by considering that once the laser is switched off, the temperature of the polyelectrolytes decreases under their transition temperature forcing the melted polyelectrolytes to seal back again.[81] Light irradiation allows also encapsulating drugs since light can induce variation in permeability of the shells. Bédard et al. exploited the incorporation of polymers containing azobenzene groups to encapsulate dye-labelled dextran. When irradiated by a proper wavelength, azo groups change their conformation modifying their geometry that results in the shrinkage of the capsules with encapsulation of dextran.[82]

Erokhina et al. incorporated bapteriorhodopsin into capsules' shell that acts as proton pump when irradiated by light. During the exposure to light, this protein starts to pump protons inside the capsule decreasing pH locally, thus increasing permeability through the shells.[83]

Studies about release of cargo from polymeric multilayer capsules also include physiological triggers as demonstrated by De Geest et al. They fabricated multilayer capsules sensitive to physiological pH and endogenous enzymes. In the former case, the capsules shell is made of poly(hydroxypropylmethacrylamide dimethylaminoethyl) (p(HPMA-DMAE) and PSS, while in the latter case they used poly-L-arginine and dextran sulphate.[84] The advantage of exploiting physiological trigger is of course that it will implicate no external stimuli.

In addition to delivering and releasing, fine targeting is also very important in the perspective of biomedical application to discriminate bad cells from healthy ones. Indeed, once the therapeutic agent is delivered to the specific site, it should ideally attack only the

bad cells. One of the best ways to develop fine targeting is to exploit the antigen-antibody recognition, which is very specific, by using receptors that are selective toward specific molecules. This could be done by including antibodies in the capsules shell by electrostatic interaction or by covalent bonding.[85, 86]

Polyelectrolytes multilayers capsules represent a good drug delivery system when the administration is via circulation and when targeting is needed. Sometimes only the induced release is the important requirement for example in the case of implants or prosthesis. When the main aim is to localize the drug and to release it when desired instead of drive it to the target, microchambers and arrays of microchambers are better suited.

### 2.1.2 FREESTANDING MICROCHAMBERS MADE BY LBL TECHNIQUE

Freestanding microchambers made by polyelectrolytes multilayers were developed driven by the will of combining microelectromechanical systems (MEMS) properties [27, 87, 88] with responsive materials to enable site specific release on demand. MEMS have been developed and employed as drug delivery systems in form of micro-pump or valves. In any case MEMS need external components to activate the release and their dimensions are usually in the order of tens of microns and above. On the side of the small sizes there are nano or microscaled systems as polymeric capsules, such as the polyelectrolytes multilayers capsules described above, hydrogels or mesoporous silica.[89-93]

Freestanding PEM films have been obtained by means of sacrificial layers.[94, 95] After the sacrificial layer dissolution, the LbL films are suspended and can be transferred onto any solid or porous support. For example, Nolte et al. [96, 97] fabricated freestanding membranes made of polyelectrolytes multilayers and they used them to seal microcontainers that perform as drug reservoir. These membranes can be used as diffusion barrier for macromolecules while they are still permeable to small compounds. Before 2011, different techniques to pattern prefabricated PEM films have been developed, such as contact printing, lift-off technique and solvent-assisted room temperature imprinting. All these techniques involved the fabrication of 2D films.[98]

Beginning from 2011, Kiryukhin et al. reported ways to fabricate arrays of hollow freestanding microchambers made of polyelectrolytes multilayers films.[17, 98, 99]. A schematic illustration of the process is reported in **Figure 2.6**.

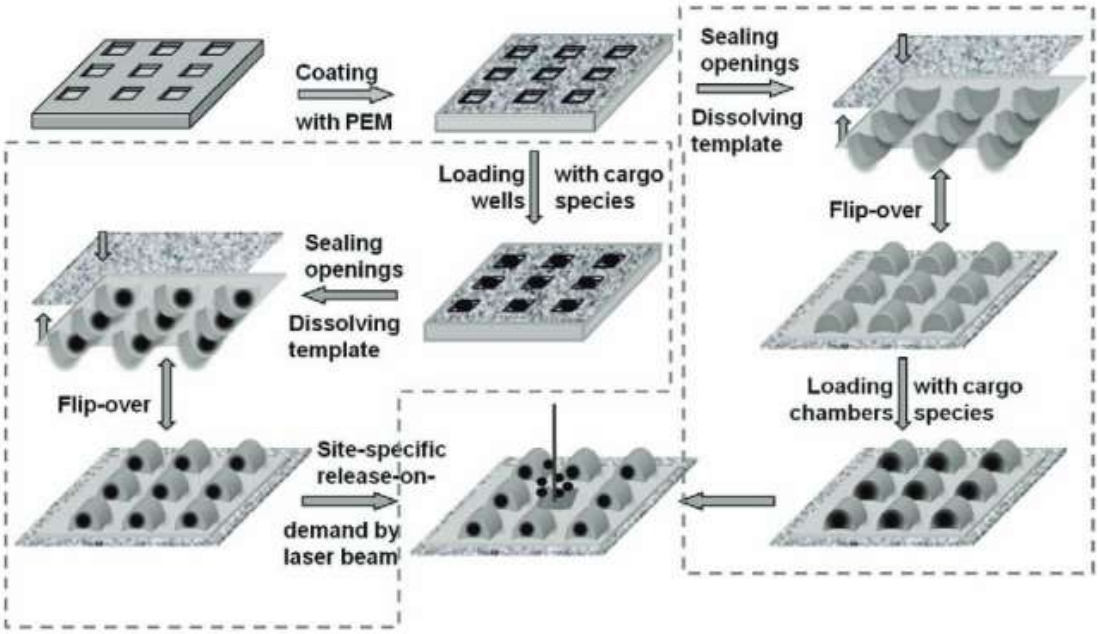


***Figure 2.6**: Schematic illustration of freestanding PEM microchambers, their loading and release on demand.[17]*

Firstly, a micropatterned template (poly(methylmethacrylate) (PMMA)) containing wells is fabricated. A polyelectrolytes multilayers film is then deposited by layer-by-layer technique on the template.

A crucial parameter for a successful microchambers fabrication is the deposition even inside and outside the template microwells. If the wells are poorly wetted by polyelectrolyte solution or if the wells size is smaller than polyelectrolytes coils, the resulting PEM film is not uniform. In particular the film obtained inside the wells is thinner than outside, and thus prevents the good fabrication of freestanding microchambers. On the contrary, if the excess of polyelectrolytes is not properly removed during the washing steps, a thicker film is formed inside the wells. To overcome these problems, the ionic strength of polyelectrolyte solution, the time of adsorption steps, as well as the time and number of washing steps can be properly tuned.[67, 99]. Furthermore, depending on the molecules chosen and the selected geometries, there is a critical number of layer needed to stabilize the chambers as shown by Kiryukhin et al.[98, 99]

Once the PEM film has been deposited onto the patterned substrate, chambers can be loaded with the desired cargo exploiting different techniques developed for both particles and liquids.[17, 67, 100, 101] The sealing of the loaded chambers is crucial in order to avoid leaking of the payload and hence have an effective cargo storage. This can be obtained by

pressure induced adhesion toward another PEM coated support.[102] Loaded freestanding microchambers can be therefore revealed by dissolving [98] or by mechanical pulling out [102] of the sacrificial template. The mechanical stamp lift off has several advantages compared to the conventional dissolving of the template. First of all organic solvents are avoided and the patterned substrate can be recycled and reused to fabricate new microchambers.

It is also possible to load already sealed freestanding microchambers exploiting tuneable permeability of PEM shells as discussed in the case of PEM capsules[103, 104], as for example pH, ionic strength, etc. In the case of freestanding microchambers obtained by dissolution of sacrificial template (i.e. with toluene) it is possible to load the sealed chambers by solvent-exchange method. This method was developed to load oils inside water-dispersed polyelectrolytes multilayers capsules using ethanol or acetone, as intermediate solvent compatible both with water and oil phase.[105] In the case of microchamber, the requirement of using water compatible solvent is avoided since microchambers are already filled with toluene. As an example, sunflower oils as well as perylene derivative showing green fluorescence have been encapsulated inside PEM freestanding microchambers by solvent-exchange methods.[17, 98] Even though it is preferable to adopt a loading strategy already well known, the feasibility of the technique in case of microchambers should be verified every time.[67]

The release of cargo from loaded and sealed microchambers has been demonstrated, for example, incorporating gold nanoparticle in between the microchambers walls during layer-by-layer assembly. The release was activated by means of focused laser radiation that leads to the opening of the selected chamber, while the others stay unaffected.[17, 67]

The fabrication of these systems offers the possibility of carrying out the controlled release over time and space of a precise amount of payload, making these PEM microchambers suitable for application where the systemic delivery can be avoided, such as in implants coating and bioscaffolds.

The main limitation to the final application of both polyelectrolytes multilayers capsules and freestanding microchambers is the difficulty of encapsulating small molecules (Mw < 1 kDa). In fact, the permeability of both microchambers and microcapsules is only slightly reduced by increasing the number of deposited layers. Furthermore, in the case of chambers

a minimum amount of layers is needed to have freestanding chambers and this results to be a cumbersome and time-consuming procedure.
This is the reason why Gai et al. [106] focused the attention on the fabrication of freestanding microchambers made of hydrophobic biodegradable polymers in order to encapsulate small hydrophilic molecules.

## 2.2 FREESTANDING MICROCHAMBERS MADE OF HYDROPHOBIC AND BIODEGRADABLE POLYMERS

Long-term drug encapsulation remains a challenge especially for small hydrophilic molecules. As already mentioned, a way to decrease PEM shell permeability is to increase the number of layers but also in this case small hydrophilic compounds are difficult to be kept encapsulated. Current attempts to decrease the permeability of PEM capsules were achieved by Gao et al. [106, 107] with the incorporation or *in situ* synthesis of quantum dots or by photochemistry. Both methods require procedures incompatible with biomolecules, impeding their use in biomedical applications.

To overcome these limits, Gai et al. [106] started studying the possibility of fabricating hydrophobic chambers made of poly-lactic acid (PLA) since hydrophobic polymers show efficient barrier properties for small hydrophilic molecules.
PLA is a thermoplastic polyester derived from naturally available lactic acid. PLA is biocompatible, biodegradable and hydrophobic that is approved by the U.S. Food and Drug Administration (FDA). The degradation occurs easily in physiological conditions by hydrolysis of the ester backbone leading to the formation of non-harmful and non-toxic compounds that can be excreted through kidney or eliminated in form of $CO_2$ and $H_2O$ through metabolic processes in animals.[108] The biocompatibility and the complete biodegradability make PLA an ideal material for biological and medical applications, such as implants, sutures and drug delivery systems.[108-111]

Gai et al.[106] fabricated PLA freestanding chambers by means of the one-step dip-coating technique that consists in dipping of a substrate patterned with microwells into a PLA solution in chloroform for 5 s. Then, also a flat substrate was dipped inside the same solution for 5 s. Microchambers were sealed by printing them onto the coated flat substrate

under pressure for 10 s and were revealed after lifting off the patterned substrate (**Figure 2.7**).

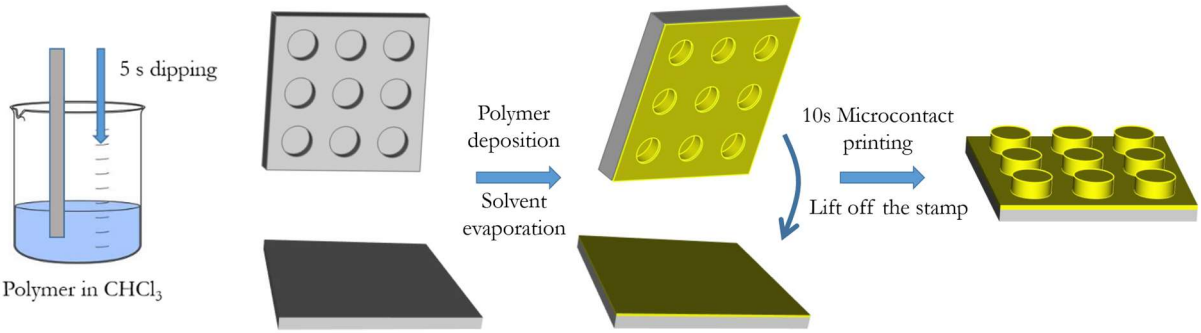


***Figure 2.7**: Schematic representation of microchambers fabrication by one-step dip-coating technique.*

This technique allows the fabrication of freestanding polymeric microchambers saving a lot of time compared to the production of drug containers made by LbL technique (5s, compared to several days for the PEM chambers[98] and about a day for PEM capsules[112]). Furthermore, the use of a hydrophobic polymer allows the encapsulation of a small hydrophilic drug.[106]

Regarding the release methods, only few strategies to open PLA freestanding microchambers have been reported so far: external high intensity as well as low intensity focused ultrasounds (HIFU, > 1MHz and LFUS, 20-100 kHz) and near infrared radiation (NIR).[106, 113-116] Ultrasounds are one of the most suitable mechanical stimuli to activate the cargo release from microchambers because of their thermal and non-thermal effects.[117-120] Instead, NIR lasers operating in the biological window, in which biological matter absorption is low, allow precise release stimuli exploiting the incorporation og gold nanoparticles as demonstrated by Gai et at.[114]; however, this kind of radiation only penetrates up to 1 cm in the body and therefore it can be used only for applications close to the skin.[114]

The fabrication of these PLA microchambers arrays paves the way to the possibility of investigating other types of biopolymers, to encapsulate small hydrophilic compounds and to ensure long-term encapsulation. Sindeeva et al. [121], for example, explored the poly(lactide-*co*-glycolide) (PLGA, 50:50 $T_g$ 40-60°C, $T_m$ 72-77°C) biopolymer to fabricate microchambers with the one-step dip-coating technique. PLGA is a copolymer of poly lactic acid (PLA) and poly glycolic acid (PGA). Its hydrophobicity is related to the amount

of lactide, and it increases with the increase of lactic acid. It is biocompatible and biodegradable and it is approved by the FDA.[122, 123]

### 2.2.1 BIODEGRADABLE POLYMERS

A biomaterial is defined as any biocompatible substance, either natural or synthetic, engineered to interact with biological systems.[124] Among the various studied materials, polymers show high potential because of their great diversity, chemically engineerable, as well as of their physical and mechanical properties.[125] Biodegradable polymers are of extreme interest because they can be divided and excreted or resorbed without removal or further surgery.[125]

When a biomaterial is used in biomedical applications, the bio-environment response depends on its chemical and biological properties. When a biomaterial is biodegradable, also the changes in the material induced by the degradation itself should be considered. In general, when designing a biodegradable biomaterial, several properties must be taken into account. The material must not induce a sustained inflammatory response; it must be characterized by an appropriate degradation rate, depending on its function; it must have appropriate mechanical properties; it must produce non-toxic degradation products that can be excreted or resorbed and it must have appropriate permeability and processability for its designed application.[125, 126] Biodegradable polymers can be divided into two main categories: hydrolytically degradable polymers and enzymatically degradable polymers. The latter ones, even though technically sensitive to hydrolytic degradation, require catalysis to go through a significant degradation in physiologically conditions.[125] In this paragraph we will focus on the hydrolytically degradable polymers since they are those of interest for this work. Several of the questions to be faced are in common with those occurring in tissue engineering about which there is a wide literature to confront with. In fact our devices are designed to be implanted for a typical time of few days.

One of the very first degradable polymers investigated for biomedical applications is polyglycolide (PGA) that shows a $T_g$ of 35-40°C and a $T_m$ higher than 200°C. PGA is characterized by a very rapid degradation rate that is limiting its application in drug delivery. Therefore, the main application of PGA is in the field of short-term tissue engineering.[125] However, PGA as biomaterial shows several drawbacks because its rapid degradation gives rise to significant local production of glycolic acid. Although glycolic acid is resorbable via

the citric acid cycle, high levels of this substance is correlated to strong, undesired inflammatory responses.[125, 127, 128].

Another biodegradable polymer widely investigated as biomaterial is the already mentioned polylactide (PLA). Since its monomer is chiral, it comes in four forms: poly(L-lactic acid) (PLLA), poly(D-lactic acid) (PDLA), poly(D,L-lactic acid) (PDLLA) that is a racemic mixture of the D and L forms, and meso-poly(lactic acid). In the biomedicine, only PLLA and PDLLA have been studied.[125] PLLA is characterized by a $T_g$ of 60-65°C and a $T_m$ of about 175°C. Compared to PGA, it has an additional methyl group that makes PLLA more hydrophobic and stable against hydrolysis. Slow degradation time limits the application of PLLA for short-term controlled delivery; in fact, PLLA of high molecular weight can take up to 5 years to be completely resorbed *in vivo*.[125, 129] A strategy to facilitate the degradation could be to shorten the polymer length and decrease its crystallinity, however, the complete *in vivo* resorption takes months after the delivery.[125] PDLLA having random positions of the two isomers shows a slightly lower $T_g$ of 55-60°C but even though it has a lower degradation time compared to PLLA, PDLLA still takes more than a year to be completely bioresorbed.[125] This is the reason why it is mainly applied in the field of tissue engineering as scaffold or coating for inorganic implants.[125, 130]

Copolymerization of PGA and PLA (both L and D, L forms) leads to the already mentioned poly(lactide-*co*-glycolide) (PLGA) that is the one of the most investigated biodegradable polymers in the biomedical field. PLGA has been used in sutures, drug delivery and tissue engineering as scaffolds.[125] Since PGA and PLA possess quite different properties, it is possible to finely tune the features of the PLGA form of interest, changing the percentage of the two homopolymers in the PLGA composition. In particular, the variation of the PLA:PGA ratio can tune the degradation time. 50:50 PLGA, 75:25 PLGA and 85:15 PLGA show degradation time of 1-2 months, 4-5 months and 5-6 months respectively.[125, 131, 132] Unfortunately, PLGA as drug delivery systems suffers from bulk erosion meaning that the degradation occurs throughout the whole material equally thus making it difficult to control the release of payload.[125]

Another class of investigated biodegradable polymers is the one of polyhydroxyalkanoates that can be produced both from bacterial and synthetic pathways.[125] The most studied polymer of this class is poly(3-hydroxybutyrate) (PHB), a semicrystalline isotactic polymer

that shows a $T_g$ of around 5°C and a $T_m$ range of 160-180°C.[125, 133] The degradation of PHB by hydrolysis leads to a normal blood constituent, the D-(-)-3-hydroxybutiryc acid.[125, 134] PHB is biocompatible and easily processable and because of its degradation rate its main applications are in the field of long term tissue engineering.[125, 135, 136] On the contrary, it is too stable to be employed in controlled delivery uses. To extend the possible application of PHB, very often it has been copolymerized with 3-hydroxyvalerate to form poly(3-hydroxybutyrate-*co*-3-hydroxyvalerate) (PHBV) that shows lower $T_g$ and $T_m$ ranges of -5-20°C and 80-160°C respectively, depending on the hydroxyvalerate content since it is less crystalline than PHB.[125, 137] Even though the addition of HV enhances the potential of PHB, the degradation time is still too long for short-term biomedical applications.[125]

An additional biodegradable polyester is polycaprolactone (PLC), a semicrystalline polymer very easily dissolvable in organic solvent. PCL has a $T_g$ of about -54°C and a $T_m$ ranging between 55 and 60°C.[138] Due to its very low degradation rate, PCL main applications are in the long term implanted delivery devices as, for example, the commercial PCL-based contraceptive Capronor® that delivers contraceptive drug *in vivo* for more than a year and it has been on the market for over 25 years. [125, 139, 140] Researchers have also investigated PCL in form of drug delivery systems with sizes ranging from micro to nanometers where the degradation rate remains higher than 2-3 years.[125]

Poly(propylene fumarate) (PPF) is another polyester that shows the possibility to be crosslinked through the unsaturated bonds in its structure and both the crosslinker and crosslink density affects the degradation rate together with the molecular weight.[141] PFF is a liquid that turns to solid during crosslinking. Due to these properties its main applications are in filling bone defects and long-term delivery, for example of ocular drugs.[125, 142, 143]

Another family of biodegradable polymers is those of polyanhydrides, the degradation of which is highly dependent on the polymer structure and can vary up to a factor 6.[125] Main application of polyanhydrides is in the field of drug delivery systems in form of particles. On the contrary, due to their usually low molecular weights that lead to poor mechanical properties, their application in tissue engineering is limited.[125] For the same reason, also polyacetals are mainly used as drug delivery vehicles. In particular, the degradation of particles based on polyacetals is catalysed by acid environment (such as

lysosomal pH).[125, 144, 145] Poly(ortho esters) show degradation catalysed by acidic pH as well and they are mainly used as drug delivery systems while their application as scaffold is limited due to their weak mechanical properties, combined with the fact that they induce inflammatory response.[125, 146] Among hydrolytically degradable polymers, polycarbonates are also worthwhile. Even though their bonds are hydrolytically stable, it seems that the *in vivo* degradation occurs faster than expected probably due to enzymatic degradation.[125, 147] The most investigated polycarbonate is poly(trimethylene carbonate) (PTMC) that shows great flexibility, slow degradation times but weak mechanical properties and it has been produced in form of particles for drug delivery applications.[125]

Polyurethanes are another class of interesting biomaterials that have been mainly used in prostheses and could be considered for our application. On the market, for example there is NovoSorb™ made of two components that cure *in situ* at physiological temperature leading to a material similar to cements that promotes cells adhesion and proliferation at the same time.[148] Polyurethanes in general are resistant to degradation in most conditions thus making their application in drug delivery difficult.[125]

Another class of biodegradable polymers for biomedical application can be found in polyphosphazenes whose peculiarity arises from the fact that their backbone is completely inorganic and consists of phosphorous and nitrogen. This phosphonitrilic backbone is not intrinsically sensitive to hydrolysis. On the other hand by choosing the proper side groups the degradation time can be tuned so that they can be used both for drug delivery and tissue engineering. Another property of polyphosphazenes is that their degradation products are neutral and act as pH buffer when combined with polymers that have acidic degradation products. Unfortunately, they can show significant and sustained foreign body responses.[125, 149, 150]

Finally, polyphosphoesters are another interesting class of biopolymers containing phosphorous in their monomers. As in the case of polyphosphazenes, it is possible to vary the degradation time selecting the proper side groups. The degradation products are phosphates, alcohols and diols that are completely bioresorbable or can be excreted. So far, polyphosphoesthers have been produced for drug delivery applications in form of particles, micelles and films but also they have been used as scaffolds in tissue engineering.[125, 151]

The summary of applications, advantages, disadvantages and structure of some of the hydrolytically biodegradable polymers here discussed, are reported below in **Table 1**.

***Table 1**: Summary of some of biodegradable polymers and their applications, advantages, disadvantages and structure.[125]*

| Polymer | Applications | Advantages | Disadvantages | Structure |
|---|---|---|---|---|
| Polylactide | Tissue engineering; Drug delivery | Highly processable; Many commercial vendors available | Limited degradation; Highly acidic degradation products | 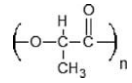 |
| Polycaprolactone | Tissue engineering | Highly processable; Many commercial vendors available | Limited degradation | 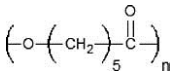 |
| Polyanhydrides | Tissue engineering; Drug delivery | Significant monomer flexibility; Controllable degradation rate | Low molecular weights; weak mechanical properties | 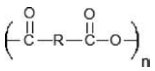 |
| Polyacetals | Drug delivery | Mild pH degradation products; pH sensitive degradation | Low molecular weights; Complex synthesis | 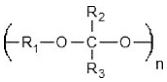 |
| Poly(ortho esters) | Drug delivery | Controllable degradation rates; pH sensitive degradation | Weak mechanical properties; Complex synthesis | 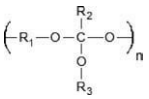 |
| Polycarbonates | Drug delivery; Tissue engineering; Fixators | Chemistry-dependent mechanical properties | Limited degradation; Require copolymerization with other polymers | 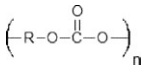 |
| Polyurethanes | Prostheses; Tissue engineering | Mechanically strong; Handle physical stresses well | Limited degradation; Require copolymerization with other polymers | 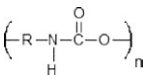 |
| Polyphosphazenes | Tissue engineering; Vaccine adjuvant | Synthetic flexibility; Controllable mechanical properties | Complex synthesis | 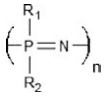 |
| Polyphosphoesters | Drug delivery; Tissue engineering | Biomolecule compatibility; High biocompatible degradation products | Complex synthesis | 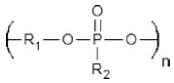 |

All the discussed polymers show advantages and disadvantages. In this thesis we decided to investigate a few of them starting from the materials used for other applications. In particular, starting from the work of Gai et al.[106] we tried first to reproduce microchambers made of PLA and then we explored their fabrication also with PHB, PLGA and PCL as will be further discussed in the following chapters. Finally, on the basis of the extended set of experiments carried out, we selected PCL as biopolymeric component for developing our final device.

# CHAPTER n° 3

## 3 MATERIALS AND METHODS

### 3.1 DEPOSITION OF MULTILAYERS MADE OF CONDUCTIVE POLYMERS ONTO A FLAT SUBSTRATE

Since we aimed at triggering the drug release by an electric stimulus, we begun by exploring the layer-by-layer technique for conductive polymers to develop the devices. We chose poly(3,4-ethylenedioxythiophene) polystyrene sulfonate (PEDOT:PSS) as the conductive polymer the chemical structure of which is shown in **Figure 3.1**.

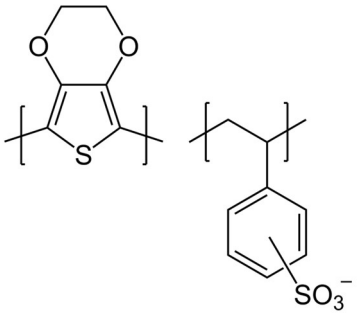


***Figure 3.1**: Chemical structure of PEDOT:PSS.*

Usually, a thin film of PEDOT:PSS can be prepared by different techniques such as spin-coating, solvent casting and dip-coating. However, the typical film morphology obtained is not good enough because of the colloidal nature of PEDOT:PSS dispersion in water. There are only a few research groups reporting on PEDOT:PSS as polyanion in layer-by-layer technique to get ultrathin films.[152-157] In fact, PEDOT:PSS is formed by PEDOT, a tiophene-based polymer, that would not be soluble in water without the presence of PSS. PEDOT carries positive charges while the PSS sulfonate groups show negative charges. Since the amount of PSS exceeds the PEDOT one, the overall charge is negative, so PEDOT:PSS can act as polyanion. We used PEDOT:PSS Clevios PH1000 purchased from Heraeus. We decided to try to deposit PEDOT:PSS using polyethyleneimine (PEI) as polycation. We proceeded by depositing a PEM film onto a flat substrate (glass slide) to figure out the best concentration to form a homogeneous film. We first used PEDOT:PSS as received but we observed that the film would break just after two bilayers since Clevios PH1000 appears to be quite viscous. After trying different dilutions in water, we determined

that only 1:10 dilution in water would give rise to a homogenous film formation. In the following experiments involving PEDOT:PSS, we always used Clevios PH1000 diluted 1:10 in water. Moreover, PEDOT:PSS diluted 1:10 was sonicated in a Branson 1800 ultrasonic bath for 5 min and filtrated with polypropylene membranes with 0.45 μm pore size purchased from VWR.

We prepared different samples depositing 5, 10 and 15 layers of PEI-PEDOT:PSS bilayers where PEI was at the concentration of 2 mg/ml. We proceeded by first deeply washing the glass slides with soap and water, and with ethanol. After their drying, we made the depositions by using PEI as first anchoring layer with the following parameters: 10 min and 30 s for each dipping and washing steps, respectively.
To study the mechanism of deposition we used Quartz Crystal Microbalance (QCM).

### 3.1.1 QUARTZ CRYSTAL MICROBALANCE (QCM)

Quartz Crystal Microbalance is a mass balance that is very sensitive to small mass variations. The working principle is based on the oscillation frequency of piezoelectric materials, such as quartz. To fabricate quartz crystal resonators that are employed in QCM, wafers are obtained by cutting them from the bulk quartz at a certain orientation with respect to crystallographic axis. Usually, quartz discs used in QCM are manufactured with the method called "AT-cut", that cuts quartz wafers approximately at 35° with respect to the z-axis.[158] Once the quartz disc is ready, metal contacts are evaporated directly on the top and bottom sides of the quartz disc. Being connected to the generating circuit, quartz can oscillate at a precise frequency that is its resonance frequency. Typically, resonance frequencies are in the range of MHz and are inversely proportional to the quartz thickness. Small changes in mass on the electrodes affect the quartz oscillation frequency. This variation in frequency can be monitored and is directly related to the mass variation using the equation developed by Sauerbrey in 1957:

$$\Delta f = \frac{-2f_0^2}{A\sqrt{\mu_q \rho_q}} \Delta m \cong -C\Delta m$$

where:

- $f_0$ is the resonance frequency of the crystal (Hz)
- $\Delta f$ is the frequency variation (Hz)

- $\Delta m$ is the mass variation (g)
- $\mu_q$ is the shear modulus for quartz for AT-cut crystals ($\mu_q$=2.947x10$^{11}$ g·cm$^{-1}$·s$^{-2}$)
- $\rho_q$ is the quartz density ($\rho_q$ = 2.648 g/cm$^3$)
- A is the piezoelectric active area, defined by the overlapping area between the two electrodes.

When developing his equation, Sauerbrey assumed that the very small mass amount on the electrodes can be treated as a change in the mass of the crystal itself. Therefore, for the equation to be valid, it is necessary that the mass is rigidly adsorbed on the crystal, that the mass variation is small compared to the crystal mass and that the mass is homogenously distributed over all the piezoelectric active area. **Figure 3.2** shows a schematic representation of Sauerbrey's findings.

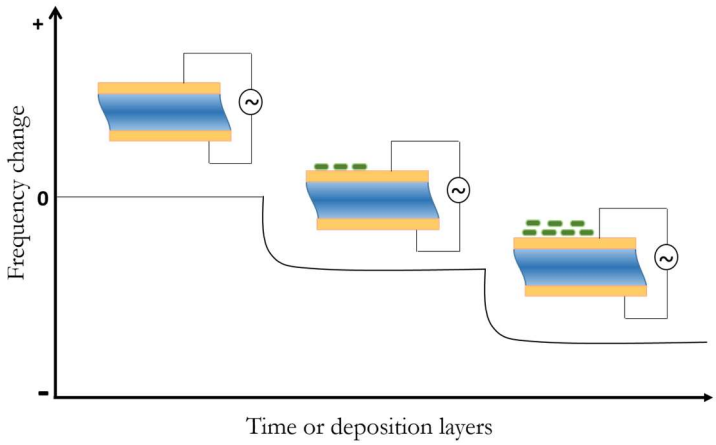


***Figure 3.2**: Schematic illustration of Sauerbrey's model: quartz oscillates at a constant frequency (its resonance frequency) when the appropriate voltage is applied. When molecules adsorb onto the crystal surface, oscillation frequency decreases and further decreases as more molecules adsorb on its surface.*

In our experiments we deposited 16 layers of polyethileneimine (PEI) and PEDOT:PSS onto quartz crystals. Quartz crystals with resonance frequency of 10 MHz were purchased by RS Components. Quartz came inside a HC-49U package that we removed before the deposition. To perform deposition on quartz crystals, since they are quite small, we used 2 ml Eppendorf tubes as polyelectrolytes containers and we filled them completely with polyelectrolyte solutions, placing quartz crystal upside down inside the Eppendorf tubes.

We started with depositing the first PEI layer that acts as anchoring layer, then we proceeded with the deposition of PEDOT:PSS as polyanion and PEI as polycation. We employed a PEI solution at the concentration of 2 mg/ml and the PEDOT:PSS (Clevios

PH1000 diluted 1:10, sonicated 5 min and filtered with polypropylene filters with 0.45 μm pore size prior to the deposition). Each deposition step took 10 min, then we let dry in air for 30 s and then we washed the sample 3 times, for 30 s each step. Before measuring the frequency by means of QCM, we dried the sample with filtered dry air. We acquired the signal after 10 s.

## 3.2 FABRICATION OF CAPSULES BY THE LAYER-BY-LAYER TECHNIQUE

The fabrication of capsules has been carried out with the traditional layer-by-layer technique to obtain the classical core-shell systems using calcium carbonate microparticles as sacrificial templates.

### 3.2.1 TEMPLATES FABRICATION

Inside a beaker, 3 ml of $CaCl_2$ aqueous solution 0.33 M were added to the same amount of $Na_2CO_3$ aqueous solution 0.33 M while vigorously stirring. The colour of the solution turned white due to the formation of a dispersion of $CaCO_3$ microparticles, according to the following reaction:

$$CaCl_{2\,(l)} + Na_2CO_{3\,(l)} \longrightarrow CaCO_{3\,(s)} + 2NaCl_{\,(l)}$$

After stirring for further 30s, the dispersion was divided into aliquots inside Eppendorf tubes. The separation between particles and supernatant was carried out by centrifugation. We washed the templates three times, centrifuging at 5000 rpm for 30s withdrawing supernatant and refilling with MilliQ water.

In order to prevent $CaCO_3$ particles crystallization, that may occurs, we immediately coated them with the first polylectrolyte layer that in our case is always polyethyleneimine (PEI), widely used as anchoring layer.

### 3.2.2 SHELL FORMATION

To fabricate the polyelectrolytes multilayers shells we followed the standard protocol, already reported in literature (see Paragraph 2.1.1 and **Figure 2.4**): after the addiction of the polyelectrolyte solution, the templates dispersion was stirred for 15 min. Then, three washing steps took place in order to remove the unadsorbed polyelectrolyte. Each washing step involves the centrifugation at 5000 rpm for 30s with withdrawal of supernatant and refill with MilliQ water. The procedure is repeated until the desired number of layers is deposited.

To create polyelectrolyte capsules, we employed the following polyelectrolytes:

- Polyethylenimine (PEI) 50% v/v solution in water from Sigma-Aldrich
- Polyallylamine hydrochloride (PAH) ~ 56000 Da from Sigma-Aldrich
- Polystyrenesulphonate (PSS) ~ 70000 Da from Sigma-Aldrich
- PEDOT:PSS Clevios PH1000 from Heraeus
- FITC-PEI, we prepared according to a procedure described hereafter.
- TRITC-PAH

All the polyelectrolyte solutions except PEDOT:PSS, were prepared at the concentration of 2 mg/ml. To fabricate PSS-PAH capsules, the salt content was NaCl 0.5 M, while PEI-PEDOT:PSS capsules were prepared without salt addition. In the latter case, we did not add salt because, from a test we made, we figured out that the presence of salt in PEDOT:PSS solution leads to precipitation of PEDOT, probably due to overcompensation of PEDOT and PSS charges by $Na^+$ and $Cl^-$ ions.

### 3.2.3 CORE DISSOLUTION

Once the polylectrolytes multilayers shell is fabricated, hollow microcapsules were obtained by removing the sacrificial core. Both HCl 1 N and an ethylenediaminetetraacetic acid (EDTA) solution 0.05 M can be used to dissolve the template.

HCl 1N is added dropwise until the formation of bubbles can be seen, since the reaction leads to the formation of gaseous $CO_2$.

$$CaCO_3 + 2HCl = CaCl_2 + H_2O + CO_2\uparrow$$

Indeed, the use of EDTA involves the incubation of the templated-systems in EDTA solution 0.05 M for 20 min to allow the complexation reaction of EDTA with $Ca^{2+}$ ions to take place (**Figure 3.3**). At least two washing steps with EDTA are needed: for each step, we centrifuged the dispersions at 4000 rpm for 2 min, we removed the supernatant and refilled with EDTA.

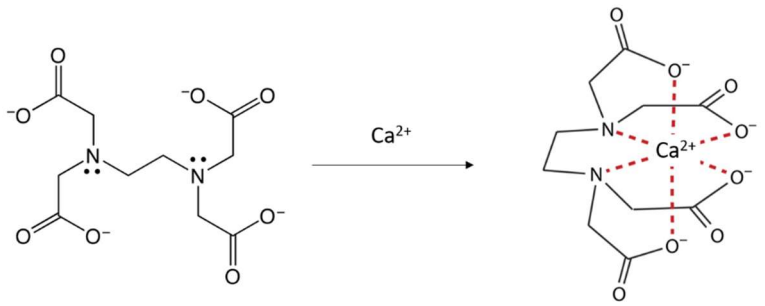


***Figure 3.3**: Ca-EDTA complex formation mechanism.*

In both cases, the dissolved ions were finally removed by three centrifugations and washing steps with ultrapure $H_2O$ from MilliQ system at 4000 rpm for 2 min.

After core dissolution, hollow microcapsules were characterized by scanning electron microscopy using a Zeiss Auriga Compact instrument and by optical microscopy with a Nikon Eclipse Ni-E microscope equipped with a Nikon DS-Qi2 Camera.

### 3.2.4 LABELLING POLYELECTROLYTE WITH FLUORESCENT DYE

We labelled polyelectrolytes with fluorescein isothiocyanate (FITC) according to the following procedure. We dissolved 100 mg of polyelectrolyte (PEI) in 25 ml of MilliQ $H_2O$. The pH was adjusted to 9 with a solution of NaOH 1M and confirmed with pH test paper. A solution of 5 mg of fluorescein isothiocyanate in 5 ml of dimethyl sulfoxide (DMSO) was added to the polylectrolyte solution, while magnetically stirring at 1000 rpm in ice bath and kept stirring for at least 30 min. To remove the FITC unlabelled, the final solution was dialyzed against $H_2O$ MilliQ for 3 days with a dialysis tube with a cut-off of 8-14 kDa (Carl Roth GmBH&Co. KG, Germany) purchased from Sigma-Aldrich. Before using the dialysis bag, it was necessary to heat it at 100°C inside a beaker filled with water for 15 min in order to remove the oil protecting its surface. During this procedure, the dialysis bag was filled with water to the 2/3 of its volume. For the whole dialysis time, the setup was kept in the dark, and the water was changed 2 times per day. Then, the polylectrolyte-FITC solution was stored in the dark at 4°C prior to its use.

We also labelled PAH with TRITC (tetra-methylrhodamine isothiocyanate) dye purchased from Sigma-Aldrich, following the procedure reported in Ref. [55]. Briefly, the fluorescent-labelled PAH was prepared by overnight incubation at room temperature of its mixture with TRITC (0.1 M carbonate buffer, pH=9) followed by dialysis against 0.01 M Tris-HCl, pH 7,5 using a dialysis bag with MW cut-off 14000.

### 3.2.5 LOADING PAH-PSS CAPSULES WITH VITAMIN B12

The shells capsules are composed by 5 bilayers of PAH-PSS. Loading was performed by leaving the formed hollow microcapsules in a vitamin B12 (cyanocobalamin) solution (4 mg/mL, pH 3.0) for 24 h with continuous shaking. Afterward, the capsules were precipitated and the water was replaced by a buffer at pH = 8 (borate/hydrochloric acid from Merck). Vitamin B12 (cyanocobalamin) was purchased from Alfa Aesar.

Images were taken by Fluorescence Optical Microscope Nikon Eclipse Ni-E equipped with a Nikon DS-Qi2 Camera, in transmission geometry. The exposure time was set at 300 ms. For the characterization, capsules were dried on a glass slide the surface of which was previously positively charged by deposition of PEI-PSS-PEI layers. The same treatment was used for samples for SEM studies, too.[159]

## 3.3 FABRICATION OF NANOENGINEERED SMART FILTERS

### 3.3.1 3D NETWORK (GLASS FIBRE FILTERS)

We aimed at experimenting the feasibility of nanoengineering smart filters by modifying commercial glass fibres filters to finely tune their permeability.

We used commercial glass fibre filters (GFF, APFF02500, glass fibre filters, without binder made by EMD Millipore) that we purchased from Sigma-Aldrich. These filters are hydrophilic, with a diameter of 25 mm, thickness of 380 μm and pore size of 0.7 μm. Since the average thickness of a bilayers of polyelectrolytes is nanometer-sized, it is not possible to directly coat the filters with the polyelectrolytes. Therefore, we decided to exploit the principle of fabrication of hollow polyelectrolyte multilayers capsules, growing sacrificial templates in between the filters' glass fibers. Again, we used calcium carbonate particles as sacrificial templates. We put the filters in a 90 mm plastic petri dish. We added 15 ml of $CaCl_2$ 0.33 M, that is the amount of solution needed in order to completely submerge the filter. While vigorously shaking, we added 15 ml of $Na_2CO_3$ 0.33 M and we kept stir for 1 min. The solution turns immediately white indicating the formation of $CaCO_3$ particles (**Figure 3.4**).

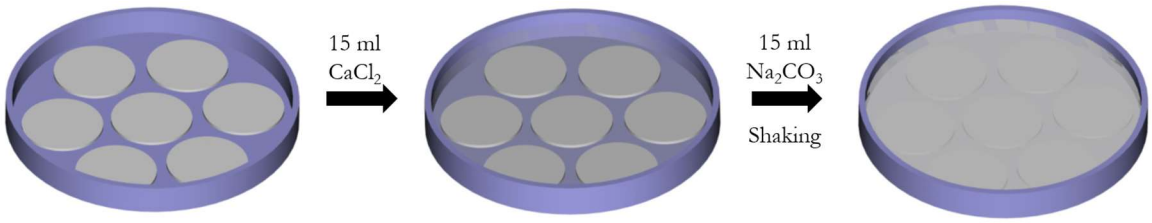


***Figure 3.4**: Particles formation procedure.*

After washing filters in MilliQ $H_2O$, they were dipped in PEI solution at 5 mg/ml for 2 hours, in order to avoid $CaCO_3$ crystallization. After that, the filters were washed again in $H_2O$ MilliQ and we let them dry at room temperature overnight.

Before the polyelectrolytes deposition, we needed to create a border both in order to have the possibility of manipulating the filter with tweezers easily during deposition and to delimit the "filtration area". To do so, we used polydimethylsiloxane (PDMS), Sylgard 184 from Dow Corning Corporation purchased from VWR. Sylgard 184 comes as an elastomer kit with a base and curing agent that have to be manually mixed in a 10 (base): 1 (curing agent) ratio by weight. After preparing the PDMS mixture, we deposited it at the edge of the filters with a pipette tip, placing the filters between two 15 ml falcon tubes lids as filter holders and rotating them (**Figure 3.5**). Filters with fresh PDMS border are let dry at room temperature for the weekend (two days).

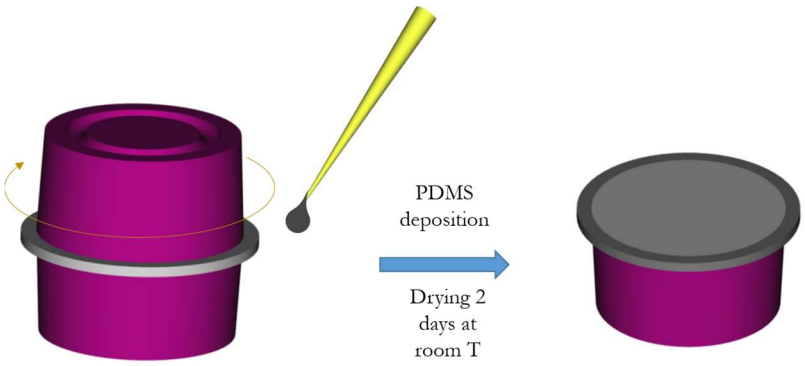


***Figure 3.5**: PDMS borders deposition.*

We deposited PDMS both after and before particles formation to figure out if the filter will be still wettable or not and whether the result depends on the presence of particles or not. Polyelectrolytes deposition was carried out using 2 mg/ml PSS and PAH solutions. The first 5 layers were deposited without salt content, while the following layers were deposited with NaCl 0.5 M. To simultaneously deposit onto 5 filters, we fabricated 2 different Teflon containers (see **Figure 3.6**).

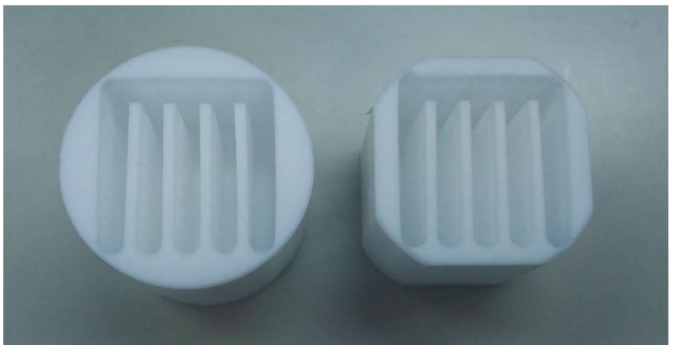

***Figure 3.6**: Teflon containers for simultaneous deposition on 5 filters.*

As for already discussed the capsules fabrication and layer-by-layer deposition onto flat substrate, the deposition onto filters involves their dipping in polyanion solution (PSS) for 10 min followed by three washing steps to remove the unadsorbed polyelectrolyte. Then, the filters are dipped into the polycation solution (PAH) and again washed trice with $H_2O$ MilliQ. The procedure is repeated until the desired number of layers is obtained. We deposited 5, 10, 15, and 20 PSS-PAH bilayers. Therefore, we finally obtained systems with the following shell composition:

$(PEI\text{-}PSS)_1^{H2O}$ $(PAH/PSS)_2^{H2O}$ $(PAH/PSS)_n^{NaCl\ 0.5M}$.

Filters characterization was carried out by SEM analysis with a Zeiss Auriga Compact.

### 3.3.2 2D NETWORK (POLYCARBONATE MEMBRANE)

We decided to deposit polyelectrolytes multilayers onto another kind of substrate, a polycarbonate membrane. We selected Isopore filter membranes GTTP01300 from Millipore for this experiment. These membranes are made of polycarbonate, they have pore size of 0.2 μm and they are hydrophilic with a diameter of 13 mm. Since the pores are made by laser, the control over their size is very precise. In contrast to the deposition onto GFF, in this case we tried to deposit without sacrificial cores since the pores are smaller than for the GFF ones. Moreover, we did not even create the PDMS border because GTTP filters are not fibrous and are easy to handle with tweezers without the risk of damages.

### 3.3.3 FILTRATION TESTS

Preliminary filtration tests were made using the dye Coomassie Brilliant Blue R-250 at a concentration of 0.05 mg/ml. In the case of the 3D filters, the filtration was made by gravity, dropping the dye onto the filter and collecting the filtered solution for UV-VIS analysis that were carried out with a Jasco 7850 spectrophotometer. Before the filtration, wax borders were deposited to confine the filtration area.

3D filters have been also used to estimate the water filtration speed through the nanoengineered filter depending on the pH. To this end, we used water at pH 3 with addition of HCl 1 N, pure water (pH 6,5) and water at pH 9 with the addition of NaOH 0.1 M. The filters were placed in a Buchner funnel inserted in a 250 ml flask. The flask was connected to a water pump kept at a pressure of 15 kPa. We filled bottle with septum with 50 ml of solution to be filtered that was then added dropwise through an administration set and a needle fixed above the filter. The time needed for the water at different pH to be filtered was hence recorded.

Our filtration tests on 2D filters were carried out placing filters in a stainless steel filter holder. The filtrates were collected and analysed by UV-VIS spectroscopy using a Jasco 7850 spectrophotometer. In particular, 120 μl of each filtrate were diluted to 1ml as final volume prior to the measurement that was carried out in the range of 350-700 nm, with 100 nm/min scan speed and slit 2.

## 3.4 FABRICATION OF MICROCHAMBERS

To fabricate microchambers we used PDMS stamps showing microwells. We began with the fabrication of small round microchambers using a PDMS stamp produced from a silicon master. Later, in order to maximize the volumes and the geometries we produced bigger and squared microchambers using PDMS stamps that we produced from Kapton substrate engineered with microwells as discussed later.

### 3.4.1 FABRICATION OF MICROPATTERNED PDMS STAMPS FROM A SILICON MASTER

PDMS stamps patterned with microwells were fabricated following a procedure slightly modified from that reported in literature.[160] The procedure consists of casting a PDMS mixture of precursor and curing agent in the ratio 10:1 onto a silicon master with micropillars. The PDMS was then degassed for 45 min in vacuum (until no more bubbles are visible) and cured at 70°C for 3 hours. The PDMS was hence cut with a surgical blade and lifted off from the silicon master (**Figure 3.7**).

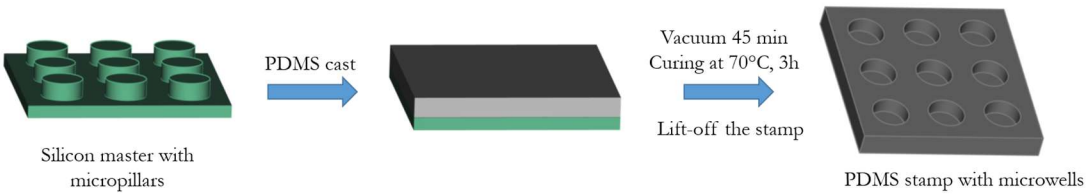


***Figure 3.7**: Stamp fabrication from silicon master.*

### 3.4.2 FABRICATION OF MICROPATTERNED PDMS STAMPS FROM KAPTON BASED MICROWELLS

The Kapton based substrate with microwells fabrication will be discussed later. Kapton substrates were deeply cleaned by washing with $H_2O$ MilliQ and sonicating for 60 seconds; then they were dried with filtered and dry air. Then, the Kapton substrates were placed into a plastic petri dish and the PDMS mixture (precursor:curing agent 10:1 ratio) was cast onto them. Afterwards, the PDMS was outgassed for 45 min (until no more bubbles were visible) and cured at 70°C for 3 hours. Subsequently, the PDMS was carefully cut with a surgical knife and lifted off from the Kapton substrates, obtaining PDMS "stamp 1" type showing micropillars. PDMS "stamp 1" was then exposed to an oxygen plasma at 50W for 10 min (Diener Plasma Cleaner). On the other hand, we fabricated PDMS "stamp 2" type with microwells by pouring PDMS mixture onto PDMS "stamp 1", following the previously described steps of degassing and curing. "Stamps 2" were finally obtained by carefully cutting and lifted off from the stamp 1 (**Figure 3.8**).

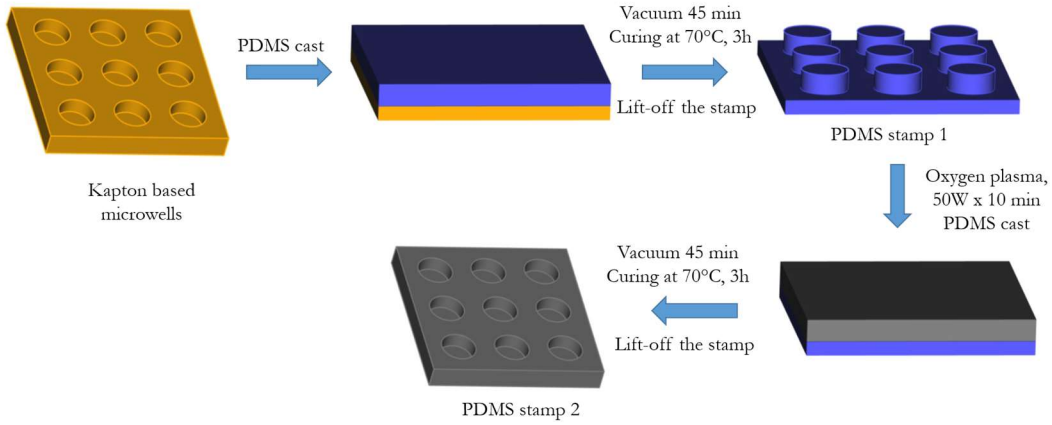


***Figure 3.8**: Fabrication of PDMS stamp 1 e 2.*

### 3.4.3 FABRICATION OF POLYELECTROLYTES MULTILAYERS MICROCHAMBERS BY THE LAYER-BY-LAYER TECHNIQUE

Our aim was to build microcontainers with conductive properties needed for the activation of the delivery process. We hence began by trying to build microchambers using PEDOT:PSS and polyaniline (PANI) as polymers conferring conductivity to our systems. In case of PEDOT:PSS as conducting polymer, commercial Clevios PH1000 from Heraeus was used to fabricate microchambers. Before the deposition, Clevios PH1000 was sonicated and diluted 1:10 with $H_2O$ MilliQ; then, it was filtrated with polypropylene filters with 0.45 μm pore size (VWR) to remove the biggest PEDOT aggregates. We used polyethyleneimine (PEI) as positive polyelectrolyte at the concentration of 2 mg/ml in water.

As regard to polyaniline, in standard formulation it is soluble in organic solvent such as N-methyl-2-pyrrolidone (NMP) and N,N-dimethylacetamide (DMAC). Instead, we used a water soluble PANI form following a modified version of the protocol developed by Rubner et al.[161], aiming at taking the main advantage of the layer-by-layer technique of using polymers in water solutions. Therefore, we started from a solution of polyaniline in its base form (emeraldine base, ~ 100000 Da, from Sigma-Aldrich) in DMAC (Alfa Aesar), at the concentration of 20 mg/ml. The solution was stirred overnight then sonicated for 8-10 hours. PANI larger particles were removed by filtering the dispersion with filters with decreasing pore sizes. We began by using paper filters with 25 μm pore size and we ended up using simultaneously 2 paper filters with pore size <1 μm. The obtained solution is blue, indicating that PANI is still in its non-conductive form. In order to get the final conductive PANI dipping solution, we slowly added one part of the filtered PANI solution to nine part of water at pH 3.2. Immediately the solution turns green indicating that polyaniline turned in its conductive form. The final pH was adjusted to 2.7 adding 2 drops of HCl 1N. It is important not to go below pH 2.5 or above pH 4 to prevent PANI precipitation. As counter polyelectrolyte we used a polystyrene sulfonate (PSS) at the concentration of 2 mg/ml. The pH of the PSS solution was adjusted with HCl 1 N to get pH 2.7. The as-prepared solution will expire in 3 days when the polyaniline will precipitate.

We carried out the microchambers fabrication by the deposition of polyelectrolytes multilayers onto both a microwells patterned PDMS stamp and a flat substrate where the microchambers will be finally transferred to.[162] As a flat substrate we used generally a glass slide deeply washed with soap and MilliQ water, and finally in ethanol before

beginning the deposition. The PDMS stamps were washed by sonicating them into ethanol for 30 s and then let drying in air before carrying out the deposition.
For both the PDMS stamp and the flat substrate, the first layer is always polyethyleneimine (PEI), working as an anchoring layer. Therefore, both substrates were dipped into a PEI solution 2mg/ml for 20 min in order to confer homogeneous positive charge to the surfaces. The substrates were dipped into a polyanion solution (acidic PSS or PEDOT:PSS) for 10 min, then a 30 s drying step in air took place before rinsing them three times. Each rinsing step lasted 30 s. In case of PANI deposition, the water solution was adjusted at pH 2.7 by adding HCl 1N, in order to prevent PANI dedoping. Subsequently, each substrate was dipped into a polycation solution (PANI or PEI) for 10 min, then dried for 30 s and rinsed trice again. The procedure was repeated until the desired number of layers was obtained.

The deposition was performed both manually and using an automated dip-coating robot, similar to the one proposed by Portnov et al.[41], and programmed with LabView.

In order to make sealable the microchambers onto the flat substrate, the last layer for the PDMS stamp and the flat substrate have to show oppositely charges so that an electrostatic interaction could give rise to adhesion and hence sealing. The chambers are hence sealed by microcontact printing by applying pressure, putting weights on top of the samples, overnight in presence of 5µl of water.[163] Freestanding microchambers are finally obtained by lifting off the stamp. The schematic reproduction of the microchambers fabrication is reported in **Figure 3.9**.

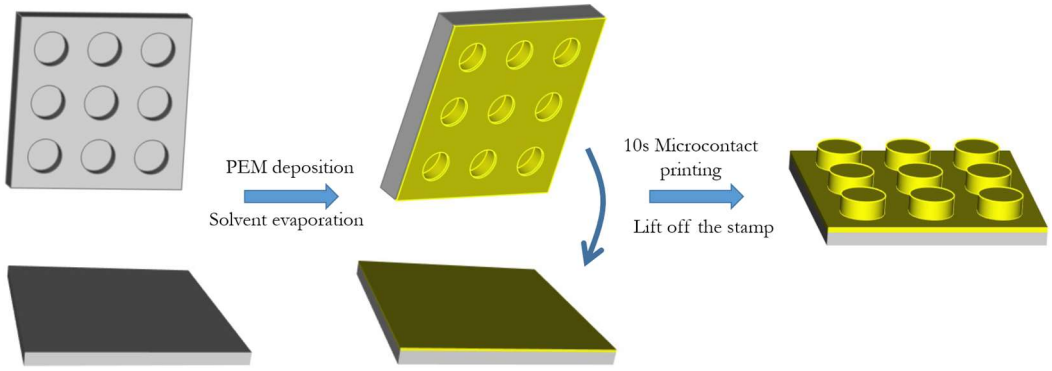


***Figure 3.9**: Microchambers fabrication process.*

Resuming, we finally got two different types of chambers, PANI-based and PEDOT:PSS-based respectively:

- PEI/(PSS-PANI)$_{60}$ microcontact printed onto PEI/(PSS-PANI)$_{10}$/PSS;
  where PEI was in a 2 mg/ml solution, PSS 2 mg/ml and pH 2.7 and PANI was prepared as mentioned before.
- (PEI-PEDOT:PSS)$_{20}$ microcontact printed onto (PEI-PEDOT:PSS)$_{10}$/PEI;
  where PEI was in a 2 mg/ml solution and PEDOT:PSS Clevios PH1000 was diluted 1:10 and filtrated with filter having 0.45 μm pores size.

The freestanding PEM microchambers were characterized by Scanning Electron Microscopy using a Zeiss Auriga Compact microscope.

### 3.4.4 FABRICATION OF MICROCHAMBERS BY ONE-STEP DIP COATING TECHNIQUE

The fabrication of microcontainers by one-step dip coating is realized by dissolving polymers that are biocompatible, biodegradable, hydrophobic and approved by the Food and Drug Administration. The polymers of choice have been polylactic acid (PLA), poly-ε-caprolactone (PCL), polyhydroxybutyrate (PHB) and poly lactic-*co*-glycolic acid (PLGA). The technique adopted is based on microwells patterned PDMS stamps, fabricated as described above, and PDMS sheet as flat substrates. These polymers are dissolved in organic solvent such as chloroform at different concentrations, since the concentration is known to be one of the main parameters influencing the film thickness. The best concentration for forming reproducible freestanding hollow microchambers with PLA, turns out to be 2% w/w. [106]

Therefore, we dissolved PLA, as well as PCL and PHB in chloroform at the concentration of 2% w/w, while we dissolved PLGA at the concentration on 5% w/w. In the case of PCL we also prepared solutions at 1 and 3 % w/w. Once the polymer is completely dissolved, the microwells patterned PDMS stamp is dipped into the chloroform polymer solution for 5 s and then pulled out. The same method was also used for the flat PDMS sheet to coat it with the same polymer. Both the stamps and the flat substrates were dried in air. Finally, freestanding sealed microchambers are obtained by 10s microcontact printing and the subsequent lifting off the stamp (see **Figure 2.7**). In this case, microcontact printing is performed by simply pressing for 10s.

Polylactic acid biopolymer (PLA), polycaprolactone (PCL, $M_w$ ~ 45000 Da), Poly(D,L-

lactide-co-glycolide) (PLGA, lactide/glycolide (50:50), $M_w$ ~ 30000-60000 Da) and poly-3-hydroxybutyrate (PHB, $M_w$ ~ 300000 Da) were purchased from Sigma-Aldrich.

## 3.5 TOWARDS THE FINAL DEVICE

Since our final device should be handled by a surgeon in the delicate phases of a surgery, the device should be easy to handle and robust enough. We hence focused our work on the architecture based on the most robust substrate satisfying all the other requirements already mentioned. This is why our choice was for the device based on polyimide microwells. We followed two different strategies to develop the substrate with microwells: the first one is a chemical synthesis of the polyimide by a liquid polyamide precursor and an imidization process [164]; in the second one we obtained microwells by hot-embossing a commercially available polyimide sheet.

### 3.5.1 SUBSTRATE ENGINEERING: POLYIMIDE MICROWELLS FROM A LIQUID PRECURSOR

The liquid precursor used was polyamic acid in DMSO (kindly provided from Dr. Sergio Bocchini of the Italian Institute of Technology IIT that synthesised it in his laboratory on the basis of the recipe reported in the paper of Cheng et al.[164]). To fabricate the polyimide with patterned microwells, firstly we manufactured a silicon master by Deep Reactive Ion Etching (DRIE) as described elsewhere [165] with the process reported in **Figure 3.10**.

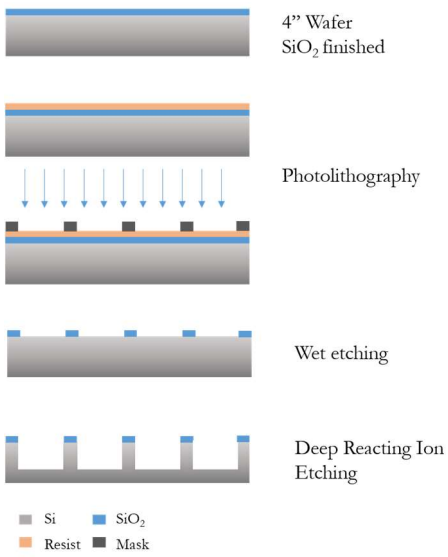


***Figure 3.10**: Process flow for the Si master fabrication.*

This technique is a typical clean room process developed for fabricating high aspect ratio features on Si.[166] This master showed squared wells with dimensions 50x50x40 μm, 20

µm apart from each other. We then cast PDMS Sylgard 184 elastomer kit in the ratio of elastomer:curing agent 10:1 onto the silicon master. The PDMS replica of the master, showing squared pillars, was obtained after outgassing PDMS mixture for 45 min, curing it at 70°C for 3 h and lifting off the Si master. To facilitate the release from the Si master, a Teflon-like coating obtained as described in literature [167] was deposited by DRIE C4F8 30 s at 100 sccm, 10 W RF power - 1000 W ICP power, 20 mTorr, step.

Thereafter, polyamic acid in DMSO was cast onto PDMS stamp and it was baked at 150°C to remove the solvent and allow the imidization process. Finally, it was possible to release the polyimide microwells from the PDMS master because of the high flexibility and elasticity of PDMS itself hence the microwells patterned freestanding polyimide was obtained (**Figure 3.11**).

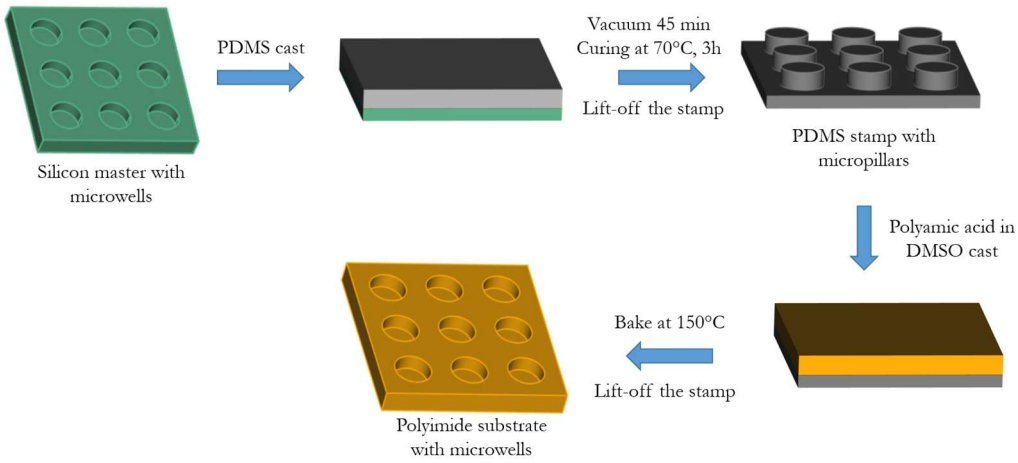


***Figure 3.11**: Substrate engineering from liquid precursor (wells are represented cylinder-like for simplicity).*

### 3.5.2 SUBSTRATE ENGINEERING: POLYIMIDE MICROWELLS FROM A POLYIMIDE SHEET

Microwells made of polyimide were also obtained by the tailored hot-embossing process. This method provides different advantages especially in term of cost efficiency and scalability, good reasons for selecting this technique for the final device development. We used a commercially available polyimide sheet, Kapton, the structure of which is reported in **Figure 3.12**, in particular we used Kapton HN 25 µm thick from Dupont.

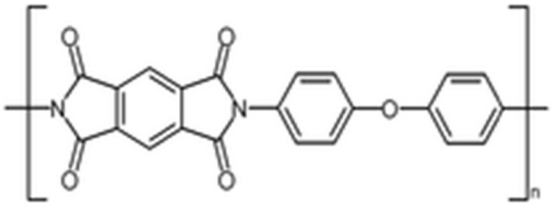

***Figure 3.12**: Chemical structure of Kapton.*

We exploited hot-embossing technique to print patterns to polyimide sheet making use of a HEX01 JENOPTIK Mikrotechnik machine (**Figure 3.13**) present at Chilab laboratory (https://areeweb.polito.it/ricerca/micronanotech/main-page). This technique allows to replicate pattern from a master onto a polymer by increasing polymer temperature, above its glass transition temperature $T_g$, and applying pressure at the same time. The Hot-embossing machine used is also equipped with a vacuum chamber, which optimized the filling of the mould during emboss process avoiding air entrapment.

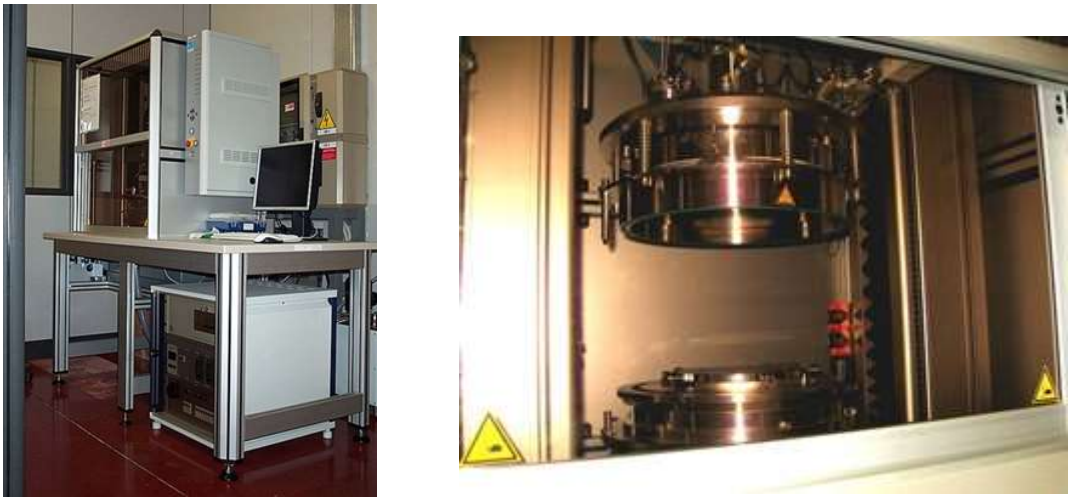

***Figure 3.13**: Hot embossing equipment presents at Chilab laboratory.*

The first hot-embossing experiments, aimed at testing the process, were made on Cyclic Olefin Copolymer (COC, Topas, 5013) since the glass transition temperature of Kapton is very high (>300°C) and we needed specific modifications of the apparatus to reach those temperatures.

Topas COC is a family of amorphous, transparent copolymers based on both linear and cyclic olefins, the bone structure of which is reported in **Figure 3.14**.

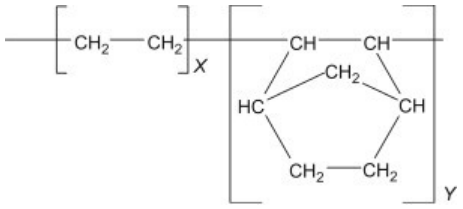


***Figure 3.14**: Bone structure of Cyclic Olefin Copolymer (COC).*

Topas COCs show a glass transition temperature in the range from 80°C to 180°C or, if expressed in terms of heat deflection temperature (0.45MPa), the range goes from 75°C to about 170°C. In particular we selected Topas COC 5013 characterized by a heat deflection temperature of 130°C which makes it easier to mold by hot-embossing compared to a Kapton sheet.

To hot-embossing the COC sheet, we used a Si master processed as described above, showing squared pillars with 50x50x30 μm size. The hot-embossing parameters were:

- Temperature: 170 °C
- Time: 300 s
- Load: 7500 N

Thereafter, we performed hot-embossing on Kapton sheet with the following parameters:

- Temperature: 320 °C (limit of the machine)
- Time: 20 min
- Load: 20000 N

These parameters are the upper limits for the instruments, after the modifications that were realized, so it is not possible to further increase the temperature, pressure or time to prevent damages to the machine.

Another side effect is the fragility of the Si master that breaks after only few presses. To avoid the breakage of pillars during the hot-embossing procedure, we used a 15 μm thick PDMS (Sylgard 184, elastomer kit, elastomer:curing agent 10:1 ratio) film deposited on a Si substrate that act as a soft counter mould.

### 3.5.3 LOADING TECHNIQUES

#### 3.5.3.1 LOADING OF MODEL AGENTS IN THE FORM OF CRYSTALS

Loading tests were performed using model agents since they could be clearly visible and loading could be hence easily assessed.

We used Rhodamine B and sodium chloride for this purpose. They were both purchased from Sigma-Aldrich. To perform loading tests, we prepared solutions dissolving Rhodamine B in MilliQ $H_2O$ at the concentration of 0.5 mg/ml and NaCl at the concentration of 3 M. Loading tests were carried out both using the PDMS stamps and the hot-embossed polyimide sheet, hereafter called *substrates*. The substrates are dipped into the model agent solution and sonicated for 1 min in the case of PDMS stamps since they are made of smaller wells and for 30 s in the case of polyimide sheet made of bigger wells. Sonication allows the removal of bubbles from the microwells and the cargo loading at the same time. Sonication was performed at 40 kHz using a Branson 1800 sonication bath. Substrates are then withdrawn out the model agent solution and the excess of the solution is carefully removed with a cotton stub. The solvent inside the wells hence evaporates and the drug remains in the form of crystals at the bottom of the wells (**Figure 3.15**).

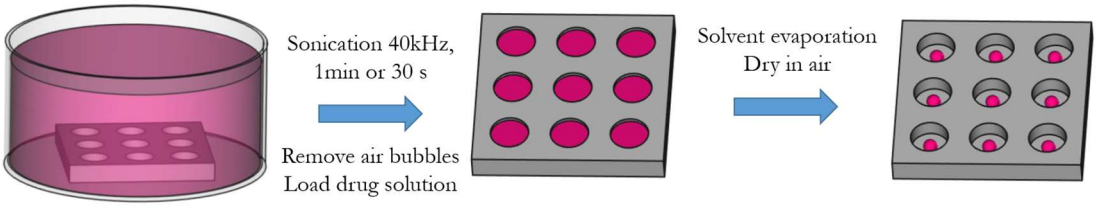


***Figure 3.15**: Schematic representation of loading drugs in form of crystals.*

#### 3.5.3.2 LOADING OF MODEL AGENTS IN THE LIQUID FORM

The principle of loading the model agents in liquid form is basically the same as the one previously described. In this case we used fluorescein sodium salt at the concentration of 0.1 mg/ml in MilliQ water. However, since the solvent (water in our case) evaporates very fast, in the order of a few seconds, the loading of the liquid drugs is performed simultaneously with the sealing procedure.

### 3.5.4 SEALING TECHNIQUES

We developed different strategies to seal the loaded microwells called the "*ring method*" and the "*blanket coverage method*" respectively. The procedures are different depending on the state of the cargo, if the model agents are in form of crystals or in liquid form.

#### 3.5.4.1 THE "RING METHOD"

The *ring method* was performed using a Teflon trough and a craft manufactured ring. The trough is the one usually used for Langmuir-Blodgett and Langmuir-Shaeffer deposition of the dimension of 20x3.5 cm. The ring is made of a copper wire stuck to a metal bar, as holder. The trough is filled with MilliQ water. The desired polymer solution in chloroform is spread at the surface (**Figure 3.16**, 1). After film stabilization (**Figure 3.16**, 2) two Teflon bars are placed parallel at a distance of 3 cm from each other. The film was cut on a side with a very sharp blade to facilitate the insertion of the ring below the film (**Figure 3.16**, 3). Finally, freestanding polymeric film is obtained by lifting off the film itself (**Figure 3.16**, 4).

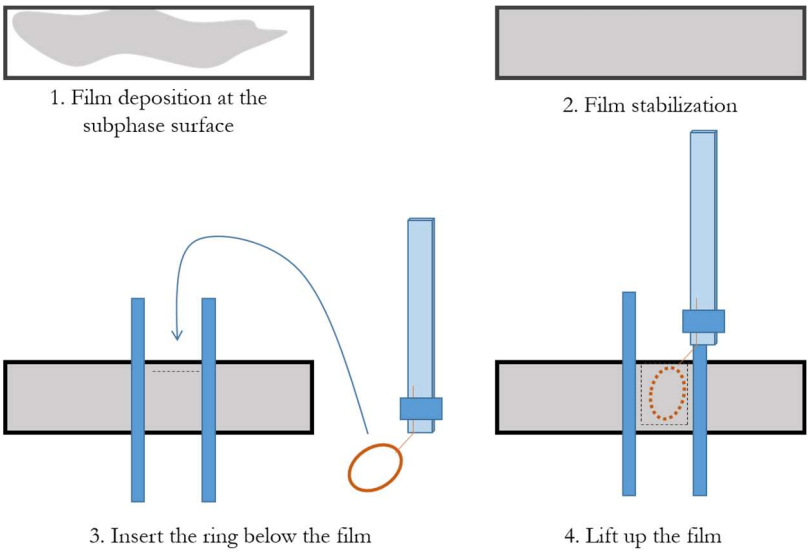


***Figure 3.16**: Schematic representation of Ring method procedure.*

After the drying in air of the film, it is possible to seal the microwells already loaded with model agents in form of crystals, simply pressing the film onto the substrate, as described in **Figure 3.17**.

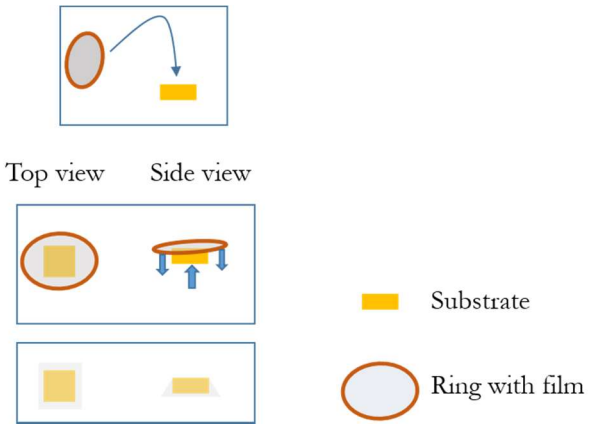


***Figure 3.17**: Schematic representation of sealing microwells with Ring method.*

We prepared the films by spreading poly-ε-caprolactone (PCL, $M_w$ ~ 45000 Da from Sigma-Aldrich) at the concentration of 2 and 1 % w/w in chloroform ($CHCl_3$, AnalaR Normapur, purchased from VWR). Only 1% w/w concentration leads to an appropriate thickness that is possible to cut with a very sharp blade. The 2 % w/w concentration leads to a thicker film that could not be easily cut without ruining it. Therefore, we decided to focus our work on the PCL 1% w/w and we created films made of PCL 1%, spreading 80 µl of polymer solution.

### 3.5.4.2 THE "BLANKET COVERAGE METHOD"

This sealing procedure is carried out by placing the substrate onto a stainless steel little support with holes, as the one reproduced in **Figure 3.18**, inside a 9 cm diameter glass Petri dish.

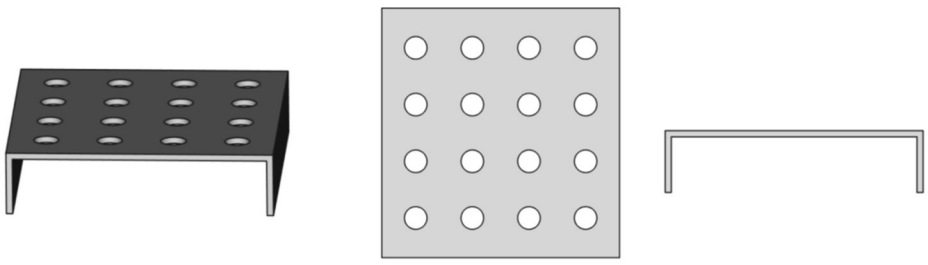

***Figure 3.18**: From left to right, schematic representation of the stainless steel support used in the "Blanket coverage method" sealing preocedure, its top view and side view.*

The method consists in filling the Petri dish with a subphase, completely submerging the substrate. The first experiments were carried out using MilliQ water as subphase to develop

the technique. After waiting the stabilization of the subphase for a few minutes, the polymer solution is carefully and slowly spread onto the subphase surface, with a 250 µl syringe (Hamilton 1725 TLL, purchased from VWR). After the stabilization of the film, the subphase is removed by drawing it up. At the same time the film "*blanket*" goes down together with the subphase level, until it completely covers the substrate and the small supporting table. After the blanket drying, the substrate is sealed **Figure 3.19**.

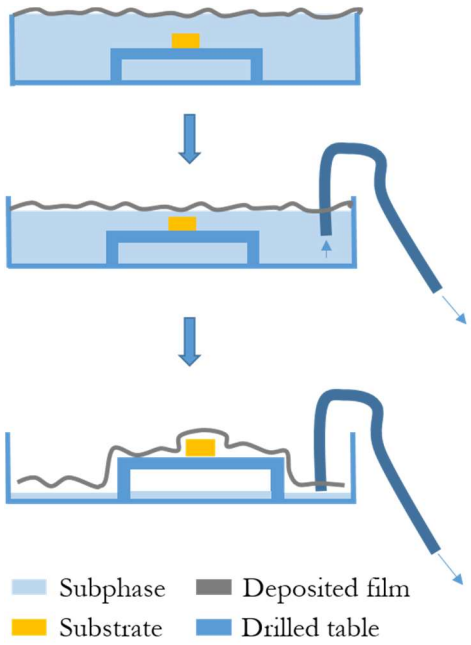


***Figure 3.19**: Schematic representation of the "Blanket Coverage Method" for sealing.*

We explored this method with poly-ε-caprolactone solutions. Therefore, we prepared polymer solutions dissolving it in chloroform ($CHCl_3$, AnalaR Normapur, purchased from VWR) at the concentration of 1 and 2 % w/w. We prepared the "*blanket*" with different amount of polymer solution decreasing the amount to get the thinnest blanket possible: 200, 150, 100 and 50 µl. As it will be discussed later, we performed opening tests on sealing films made of 200 and 50 µl. Both the MilliQ water and polymer solution were stored at a temperature of 4 °C before performing the sealing procedure.

#### 3.5.4.3 THE "BLANKET COVERAGE METHOD" FOR SEALING WHILE LOADING DRUG IN LIQUID FORM

To perform loading of drug in liquid form, fluorescein sodium salt was employed as model agent. The subphase was then replaced by fluorescein solution 0.1 mg/ml in water. The solution was stored in the dark at 4°C before its use. To load liquid fluorescein into the polyimide microwells, the substrate was dipped into fluorescein salt solution and sonicated

with Branson 1800 sonicator at 40 kHz for 30 s. Then, it was immediately placed on the drilled table inside the glass petri dish; therefore, it was submerged by fluorescein solution. All the operations regarding fluorescein were performed in the dark to prevent fluorescein photobleaching. 50 µl of poly-ε-caprolactone 1% w/w was spread at the fluorescein solution surface with a 250 µl syringe. The subphase was withdrawn and finally the sealed substrate with the loaded liquid fluorescein is obtained.

### 3.5.5 RELEASE ACTIVATION

The aim of the PhD project is to activate the release of chemicals loaded into microcontainers by applying an electric stimulus. This is the reason why the deposition of metallic contacts is required. We followed different approaches to deposit gold and titanium contacts designing different layouts depending on the desired opening mechanisms. The layout for gold contacts is shown schematically in **Figure 3.20**. The orange lines represent lines of microwells with the dimension of 50x50x40 µm, while the yellow lines represent the contacts.

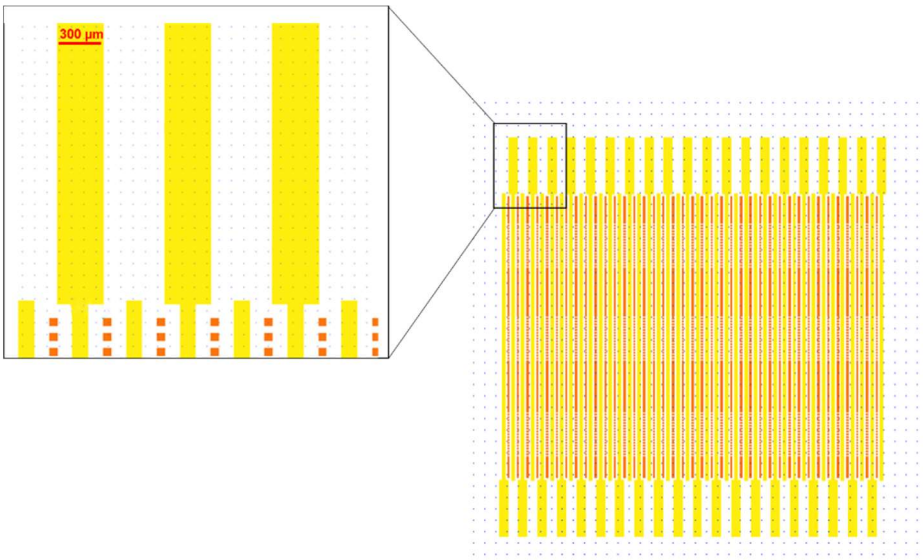


***Figure 3.20**: Schematics of the gold contacts layout.*

#### 3.5.5.1 GOLD CONTACTS DEPOSITION STRATEGIES

- Hot-embossing and evaporation through shadow mask

The first approach was to deposit gold contacts after the hot-embossing of the polyimide film. Therefore, gold was evaporated through a shadow mask using a ULVAC EBX-14D system e-beam evaporator to get contacts in between the microwells lines (**Figure 3.21**).

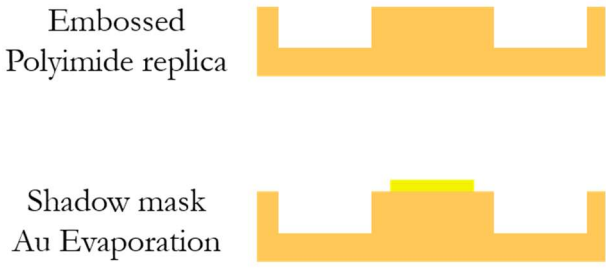


***Figure 3.21**: Schematics of the first strategy for gold contacts deposition.*

- Hot-embossing, evaporation, photolithography and etching

In this procedure, again first of all the polyimide sheet was hot-embossed, then gold was evaporated on the whole substrate's surface. Hence the Au contacts are obtained by means of photolithography and etching step (**Figure 3.22**).

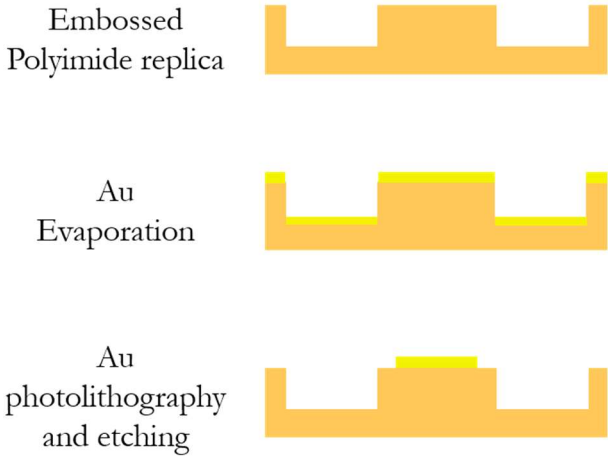


***Figure 3.22**: Schematics of the second strategy for gold contacts deposition.*

- Evaporation, hot-embossing, photolithography and etching

At the beginning, gold is evaporated onto the flat polyimide sheet. Then, the substrate is hot-embossed to get lines of microwells. Therefore, Au contacts are obtained by means of photolithography and an etching step (**Figure 3.23**).

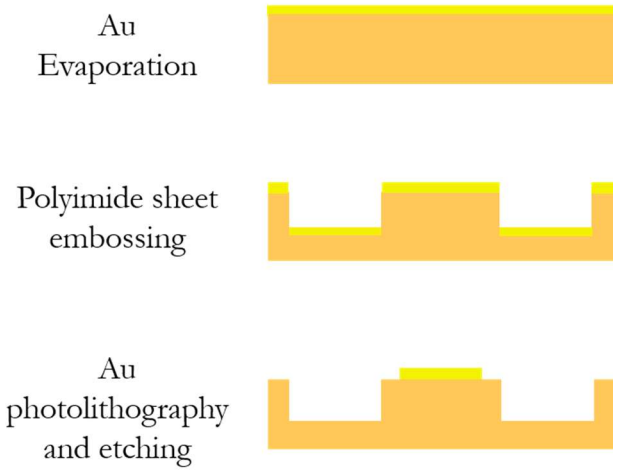


***Figure 3.23**: Schematics of the third strategy for gold contacts deposition.*

- Evaporation, photolithography and etching followed by hot-embossing

First of all, gold is evaporated onto the flat polyimide sheet. Then, gold contacts are obtained by photolithography and etching and finally, the flat sheet is hot-embossed to get microwells (**Figure 3.24**).

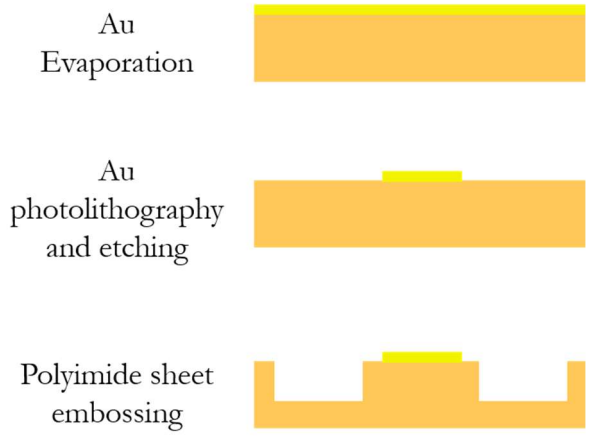


***Figure 3.24**: Schematics of the fourth strategy for gold contacts deposition.*

### 3.5.5.2 Ti CONTACTS

Aiming at performing microwells opening by electrical actuation based essentially on a Joule effect, we decided to deposit contacts of titanium for its well known good biocompatibility but also to obtain both a good adhesion on the substrate and a controlled resistivity, higher respect to Au, in a range that would keep the applied voltage low enough not to induce unwanted effects such as electrolysis and activation of other bioelectronics effects.

The designed layout (**Figure 3.25**) differs from the previous one: in this case Ti contacts are designed to overlap the lines of microwells.

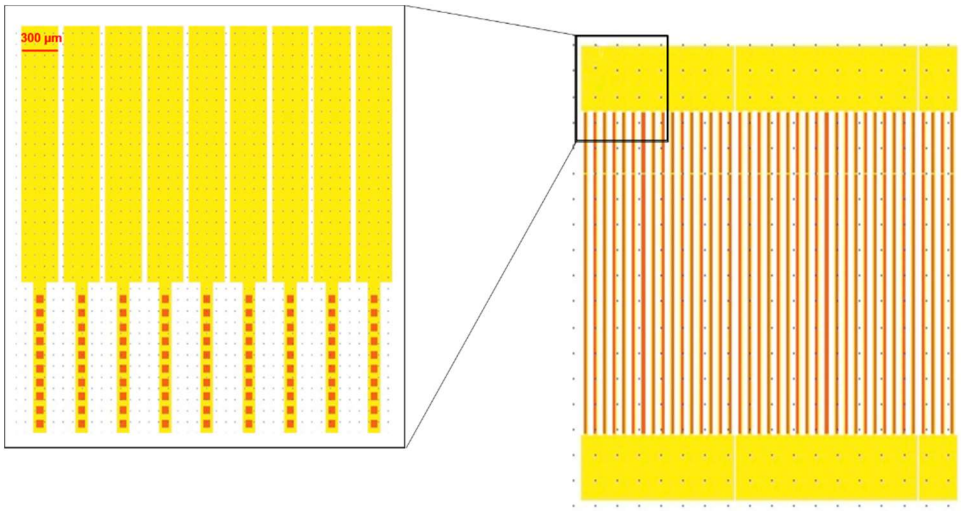


***Figure 3.25**: Schematic titanium contacts layout where the Ti contacts are in yellow and the lines of wells are in deep orange.*

To deposit Ti contacts, both sputtering and evaporation processes have been explored. In both cases, Ti was deposited onto the already hot-embossed microwells patterned substrate. Therefore, Ti contacts were obtained by photolithography and etching (**Figure 3.26**).

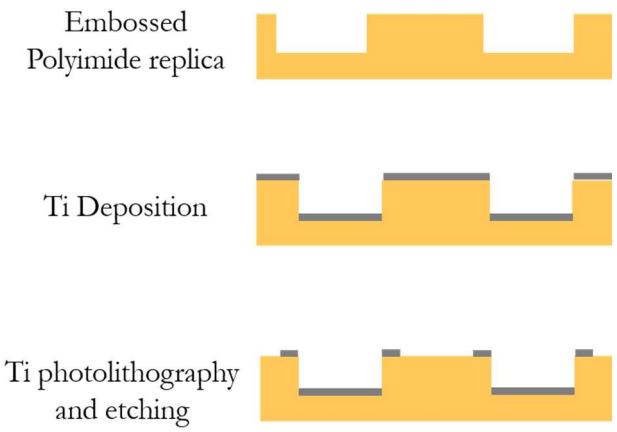


***Figure 3.26**: Schematic Ti deposition mechanism.*

The first opening tests were performed on substrates with Ti contacts deposited by RF MAGNETRON SPUTTERING.

### 3.5.5.3 OPENING EXPERIMENTS

In a first series of experiments we joined together a series of contacts on one side and on the other so that several lines of microwells could be activated together. To this end, before the polymeric film deposition, we short-circuited several Ti/microwell pads with lines of silver paste, in order to obtain a series of conductive stripes that can be connected to a source meter.

In detail, we connected the edges of the parallel pads to the source meter by using silver paste, as indicated in the schematic representation of **Figure 3.27**.

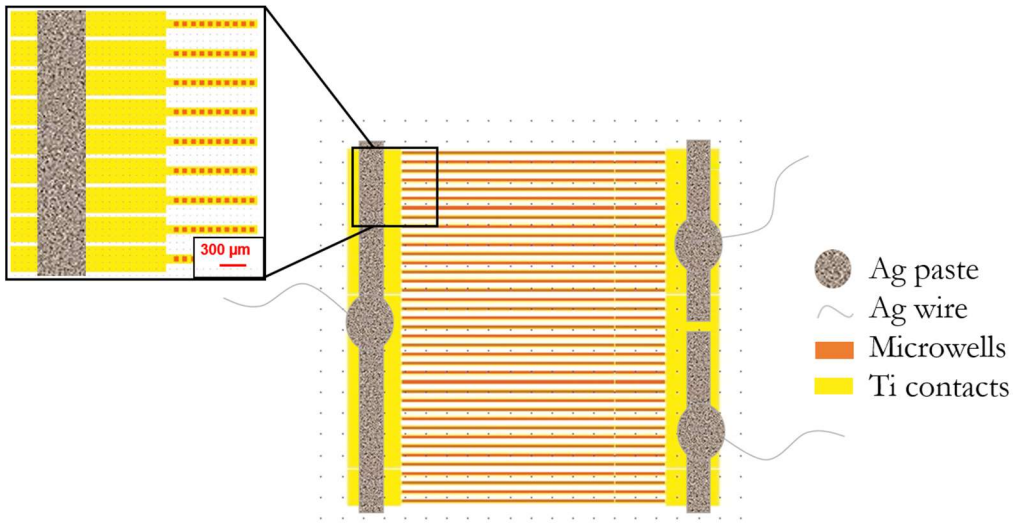


***Figure 3.27**: Schematic representation of connected pads.*

In this way, the connection of the metallic contacts to the voltage supplier through crocodile connectors is, on one hand, easier if compared to connecting every single pad and on the other hand, it allows to perform a statistical analysis of the opening mechanism efficiency.

The effect of the voltage supply on the sealing cap has been checked in real time by placing the device under an optical microscope Nikon Eclipse Ni-E equipped with a Nikon DS-Qi2 Camera. The voltage supply was performed with a Keysight B2912a controlled by a Quick IV Measurement software provided by Keysight.

We first performed opening trials on a sealing cap made of 200 µl PCL 1% w/w. We applied 1V for 600s; after which, we applied a voltage from 0 to 10V in about 60 s. Then, we focused the analysis on another area of the sample by taking images after the application of 10V for 600s. Then, we decided to further increase the voltage to 35V for 3 min.

As discussed later, no observable opening appeared for sealing films made of 200µl PCL

1% w/w, therefore we performed opening tests on another sample consisting in microwells covered by a sealing film made of 50 µl of PCL 1% w/w. We applied 5V for 600s collecting images during and after the measurement. Then, we repeated the procedure by applying 15V for 600s, again taking pictures before and after measurements.
We then decided to change the protocol applying voltage from 0 to 40V with 1V as scan step and 5s as scan time taking pictures before, during and after the application of the voltage steps.
The post process analysis was performed by Scanning Electron Microscopy carried out using a Zeiss Auriga Compact.

To better visualize the opening process, we carried out other opening experiments by acquiring real-time videos of the film melting. The sample was sealed in all the cases by the "*Blanket coverage method*" using pure water stored at 4°C as subphase and sealing films were always made of 50 µl of PCL 1% w/w.
We applied voltage using the following voltage scan steps and scan times:

- Scan step= 2V; scan time= 10s
- Scan step= 1V; scan time= 15s

In order to evaluate the opening of the microwells in conditions similar to those of the final application, we also performed opening test on a substrate loaded with fluorescein sodium salt in liquid form. We placed a PDMS container on the loaded and PCL-sealed substrate and we filled it with MilliQ water (**Figure 3.28**). Therefore, we applied the voltage with scan steps of 1V and scan time of 30s.

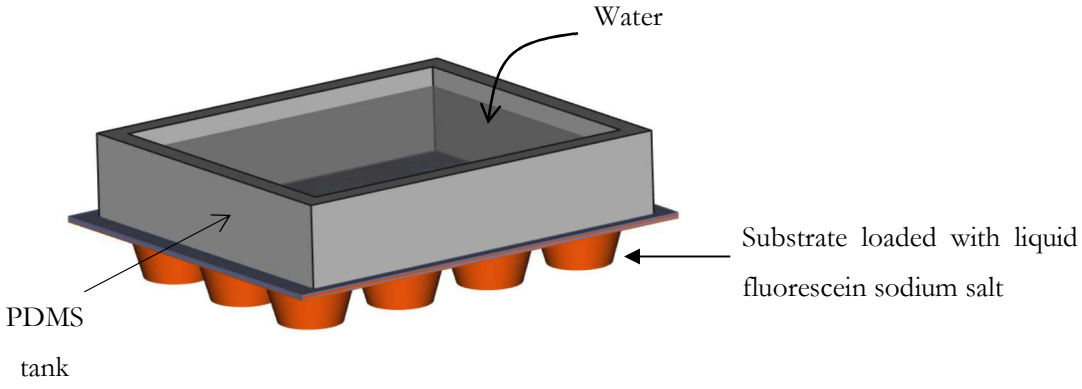


***Figure 3.28**: Experimental set-up for in liquid opening activation.*

# CHAPTER N° 4

## 4 RESULTS AND DISCUSSION

In this PhD project we aim at developing an innovative device for the post-operative pain management based on microchambers as drug reservoirs directly positioned in the wound so that the local pain control by the drug could be carried out remotely with the greatest efficiency and the minimum amount of drug. To this end, one of the major aims of the project itself is the activation of the drug release by means of an electric trigger. We hence designed two different basic architectures where the main difference is the way the microchambers have been built. In the first architecture, the whole chambers are entirely made by soft polymers, such as polyelectrolytes multilayers or biopolymers. Instead, the second architecture involves on one hand a more robust polymer playing the role of a substrate where the microchambers are formed that has been chosen to be polyimide, and on the other hand a softer polymer playing the role of the sealant of the chambers. The schematic basic architectures are reported in **Figure 1.4**.

We first explored the possibility of making the microchambers directly by the same polymers since it is one of the strategies being explored in literature (Paragraph 2.1.2 and 2.2).

In particular, we first studied polyelectrolytes multilayers in form of films, capsules and microchambers. We explored conventional polyelectrolytes as well as unconventional ones, such as the conductive polymer PEDOT:PSS, in principle well suited to fulfil the final aim of the project of activating the release using electric stimuli.

As previously mentioned, PEDOT:PSS is not a real polyelectrolyte, but since PEDOT is doped with an excess of PSS, that is negatively charged, on the whole, it can play the role of the polyanion in the layer-by-layer deposition technique, in combination with a polycation. Only few papers on PEDOT:PSS used in layer-by-layer technique report on its use in layer-by-layer growth of films [154-157] so that we firstly studied the deposition mechanism of this conductive polymer as polyanion.

## 4.1 LAYER-BY-LAYER DEPOSITION OF PEDOT:PSS

As already described previously, we used PEDOT:PSS Clevios pH 1000 as unconventional polyanion in the layer-by-layer technique. We used polyethyleneimine (PEI) as counter polyelectrolyte that carries positive charges. We first used PEDOT:PSS Clevios pH 1000 as received by the supplier observing that its large viscosity makes not easy to create homogeneous films. In fact, just after 3 bilayers, the resulting PEM film tends to break. This is probably due to the fact that the exceeding PEDOT:PSS on the surface of the film, during the drying process could rip off the deposited film (probably due to the gravity). To demonstrate the validity of this conclusion, an image of a broken film made of (PEI-as received PEDOT:PSS)$_3$ is shown in **Figure 4.1**.

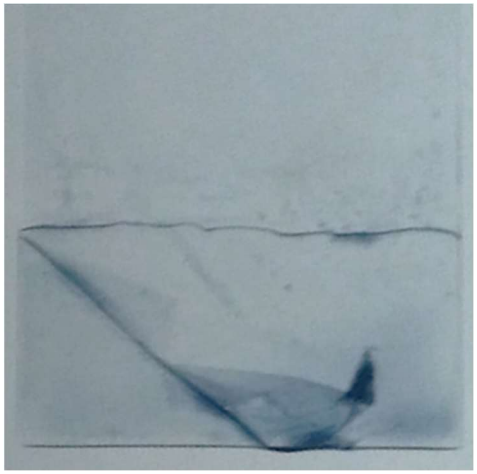

***Figure 4.1**: Broken film made of 3 bilayers of PEI and as received PEDOT:PSS.*

We hence decided to dilute the solution down to a concentration that could give rise to the deposition of a homogeneous film. This concentration was found to be the 1:10.

**Figure 4.2** shows images of polyelectrolytes multilayers (PEM) films deposited onto glass slides made of 5, 10 and 15 bilayers of PEI and PEDOT:PSS, where commercial Clevios PH1000 was diluted 1:10.

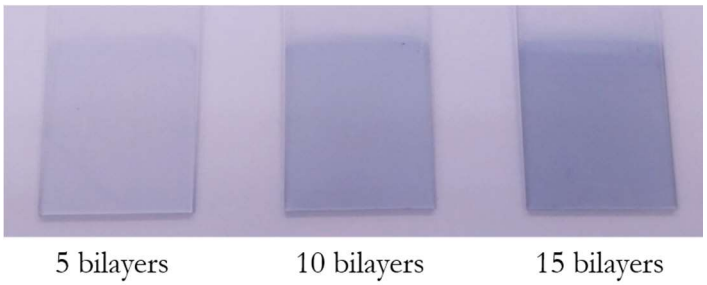


***Figure 4.2**: Films of PEI-PEDOT:PSS onto glass substrates, where commercial PEDOT:PSS was diluted 1:10.*

Therefore we decided to use this concentration to study the deposition mechanism of PEI-PEDOT:PSS with the Quartz Crystal Microbalance (QCM). The following graph in **Figure 4.3** represents the variation of frequency after each deposition step.

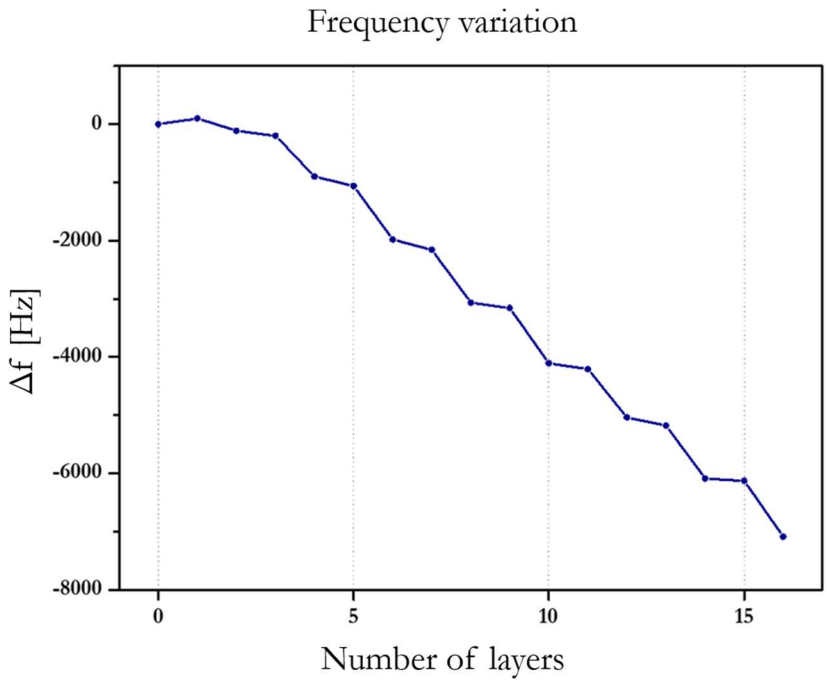


***Figure 4.3**: Frequency variation as a function of the number of deposited layers.*

Immediately, it is clearly evident that for the first 3 layers the change in frequency is observable but not pronounced. From the deposition of the 4th layer, the decrease in frequency follows a regular trend: the frequency decrease after the deposition of PEDOT:PSS is higher than the one observed after PEI deposition.

Using Sauerbrey's equation,

$$\Delta f = \frac{-2f_0^2}{A\sqrt{\mu_q \rho_q}}\Delta m \cong -C\Delta m$$

we correlated the variation of frequency to deposited of mass. Recalling that $\mu_q$ is the shear modulus that for AT-cut crystals is $2.947 \times 10^{11}$ g·cm$^{-1}$·s$^{-2}$ , $\rho_q$ is the quartz density that is 2.648 g/cm$^3$; $f_0$ is the quartz resonance frequency in Hz (10 MHz for our crystals) and the quartz active zone is 0.12566 cm$^2$, we calculated the coefficient C (~ $18 \cdot 10^8$ Hz/g). We could hence finally correlate the variation in frequency with the deposited mass. **Figure 4.4** shows the resulting dependence of the mass deposited as a function of the number of deposited layers.

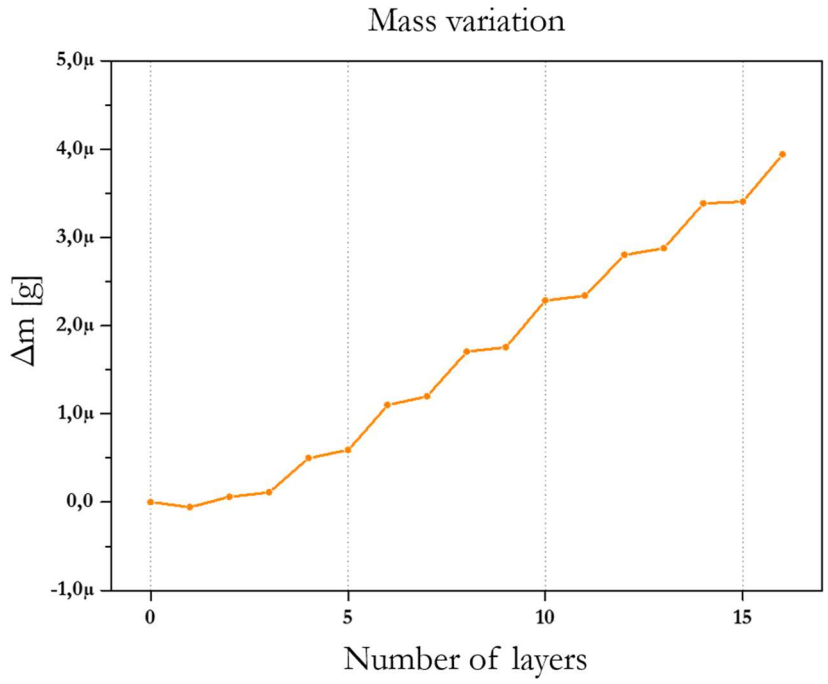


***Figure 4.4**: Graph of the deposited mass as a function of the number of layers.*

On this basis we calculated the average mass addition for both PEI and PEDOT:PSS (not considering the first three layers) and we determined that every deposition of PEDOT:PSS adds about 0.49 µg of material while deposition of PEI contributes with 0.064 µg. From these data we estimated the thickness of the deposited layers knowing the mass, the active area and the density of the materials. Therefore, we estimated by simple geometrical estimates that one layer of PEI is 2.0 ± 0.5 nm thick while PEDOT:PSS deposition leads to a layer 20.0 ± 0.5 nm thick.

## 4.2 FABRICATION OF MICROCAPSULES WITH THE LAYER-BY-LAYER TECHNIQUE

### 4.2.1 MICROCAPSULES MADE OF PEDOT:PSS AS UNCONVENTIONAL POLYANION

Once we determined the best concentration for forming homogeneous film made of PEI-PEDOT:PSS, we studied the way to create 3D structures, such as microcapsules and microchambers that could be used as containers for drug delivery. Therefore, we started with the formation of capsules as described in Paragraph 3.2. After the template dissolution, the formation of hollow microcapsules was verified with Scanning Electron Microscopy (SEM) and the results are shown in (**Figure 4.5**).

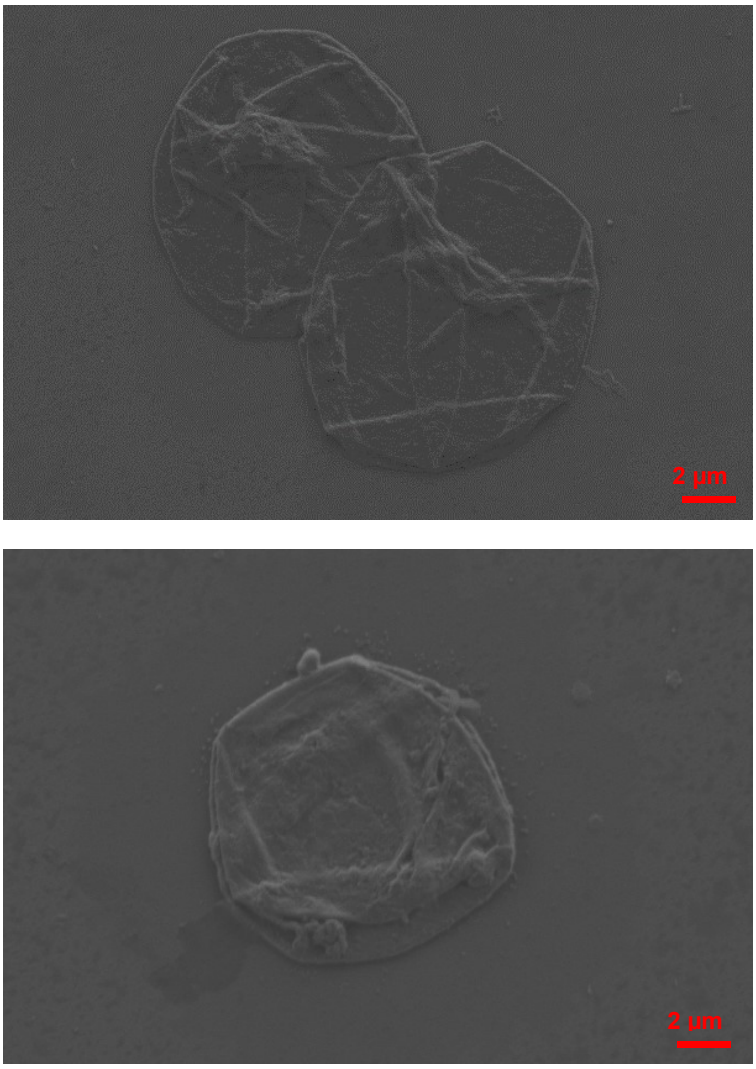


***Figure 4.5**: SEM images of capsules made of (PEI-PEDOT:PSS).*

The capsules appear to be well formed with a diameter of about 5 μm. The corrugations of the collapsed capsules upon template dissolution are clearly evident thus indicating that we succeeded in the complete dissolution of the $CaCO_3$ particles templates.

In literature several examples of conducting microsystems, also in form of capsules, mainly based on polyaniline (PANI) fabricated also with the layer-by-layer technique are reported.[168, 169]
These systems are considered as very promising for the development of nano and micro-sized electronic devices, sensors, energy storage devices due to their hollow structure and high surface area. As far as we know, there are no reports already available in literature regarding the fabrication of conductive hollow capsules made of PEDOT:PSS. We believe that our results could pave the way to the further study on these microsystems that could be suitable for significant applications in several fields.

### 4.2.2 PAH-PSS CAPSULES LOADED WITH VITAMIN B12

We also experimented the fabrication of capsules made of PSS in combination with PAH and we loaded them with Vitamin B12. Vitamins are an essential class of micronutrients controlling relevant processes in living organisms and that are present in very small amount in food. A reduced availability of the main vitamins in the human body often depends on a low concentration of vitamin complexes in food or, in some cases, on a reduced absorption in the intestine, interactions with antivitamin drugs, genetic deviations of the vitamin metabolism, etc. Each vitamin is required in a certain quantity to accomplish specific functions that are determined by genes, proteins and enzymes. In particular, Vitamin B12 performs its role mainly in bone marrow, liver, intestinal epithelium and in the nerve cells. Vitamin B12 is involved in the cell metabolism (DNA synthesis and regulation), in the normal functioning of the brain and nervous system, and in the formation of red blood cells. It is produced by specific bacteria in the human colon but not enough is absorbed to be considered a good source. Hence it has to be supplied through the diet and in particular from animals derived food, considered to be the major dietary source of vitamin B12.[159]

We labelled PAH with TRITC in order to observe the loaded capsules with fluorescence microscopy. Fluorescence optical microscopy and scanning electron microscopy were carried out for revealing the structure of the loaded capsules. **Figure 4.6** shows a

fluorescence microscopy image of the dried Vitamin B12-loaded capsules. A well visible corrugation on the surface of the collapsed shell layer was observed which is more evident in the SEM image in **Figure 4.7**.

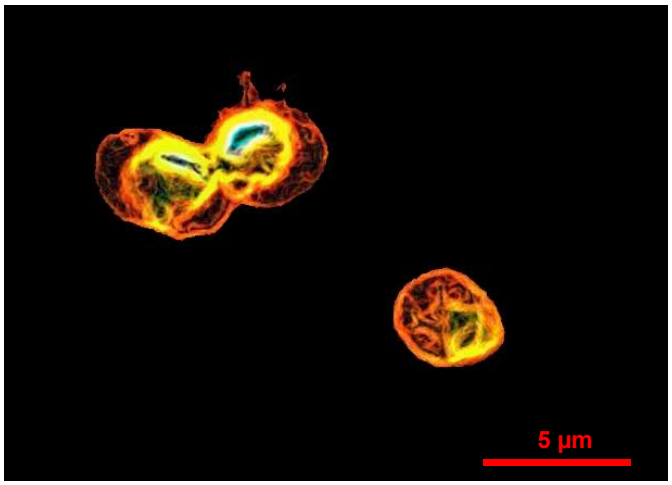


***Figure 4.6**: Fluorescence image of Vitamin B12-loaded capsules observed with Nikon Eclipse Ni-E microscope, transmission mode.*

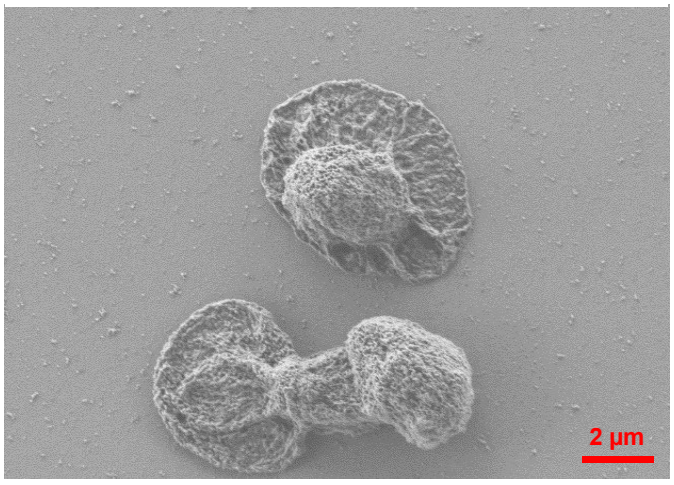


***Figure 4.7**: SEM image of Vitamin B12-loaded capsules.*

We have hence developed a smart carrier for the Vitamin B12 demonstrating the effectiveness of the encapsulation process. This is the first step towards the targeted delivery and the induced release of Vitamin B12. Once Vitamin B12 is loaded into these nanoengineered polymeric capsules, the targeted delivery could be achieved for example by incorporating magnetic nanoparticles into the polymeric shell and by using an external magnetic field. Moreover, with a proper chemical engineering of the capsule, the pore opening might be triggered directly by an active agent released as a consequence of the development of the disease itself. In particular, if the disease is characterized by a pH

decrease, the cargo release will be done in an automatic way. In other cases, it is necessary to modify/functionalize the shell so that its permeability would increase in the presence of the characteristic disease factors.[159]

## 4.3 FABRICATION OF NANOENGINEERED SMART FILTERS

Studying the properties of nanoengineered capsules, in particular their tuneable permeability, we have developed the idea of fabricating novel fine smart filters starting from commercial ones. To this end we coated the filters with different number of layers of polyelectrolytes since the number of layers is one of the parameters influencing capsules shell permeability.

### 4.3.1 3D NANOENGINEERED SMART FILTERS

We started this work by modifying commercial glass fibres filters having 0.7 μm pores sizes. Since the average thickness of polyelectrolytes bilayers is in the nano scale range, we could not directly coat these kinds of filters with polyelectrolytes multilayers. We hence implemented the same strategy used to fabricate the hollow polyelectrolytes capsules that is the use of sacrificial templates. We have then grown $CaCO_3$ particles *in situ*, between the filter's glass fibres before the polyelectrolytes deposition. After the polyelectrolytes deposition, the $CaCO_3$ particles are dissolved with the process already described before. Before PEM deposition, we have created a PDMS border in order to avoid any damage of the filter during manipulations and to confine the filtration area as described in Paragraph 3.3.1. We tried to create the PDMS border before and after the $CaCO_3$ particles formation. Only in the second case we have managed obtaining filters that remained wettable in the middle (see **Figure 4.8**); indeed, when we deposited PDMS before the formation of $CaCO_3$ particles, PDMS coated the whole filter area leading to a hydrophobic non wettable and unusable filter.

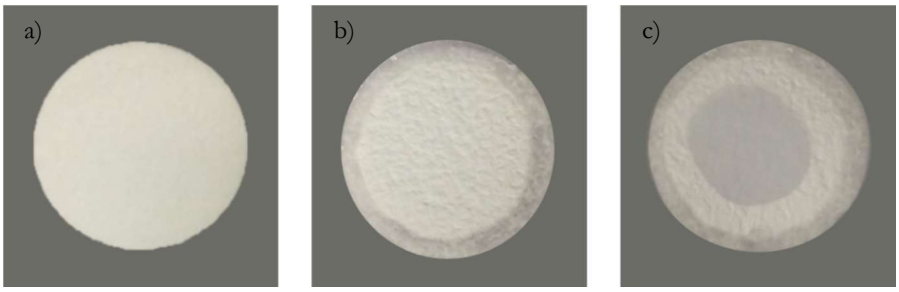


***Figure 4.8**: Pictures of APFF filter a) after $CaCO_3$ particles grown, b) after formation of PDMS border and c) after immersion in water.*

Every step of the formation of the polyelectrolytes multilayers 3D network was characterized by Scanning Electron Microscopy (SEM). **Figure 4.9** reports the case of the deposition of 15 bilayers of PAH-PSS.

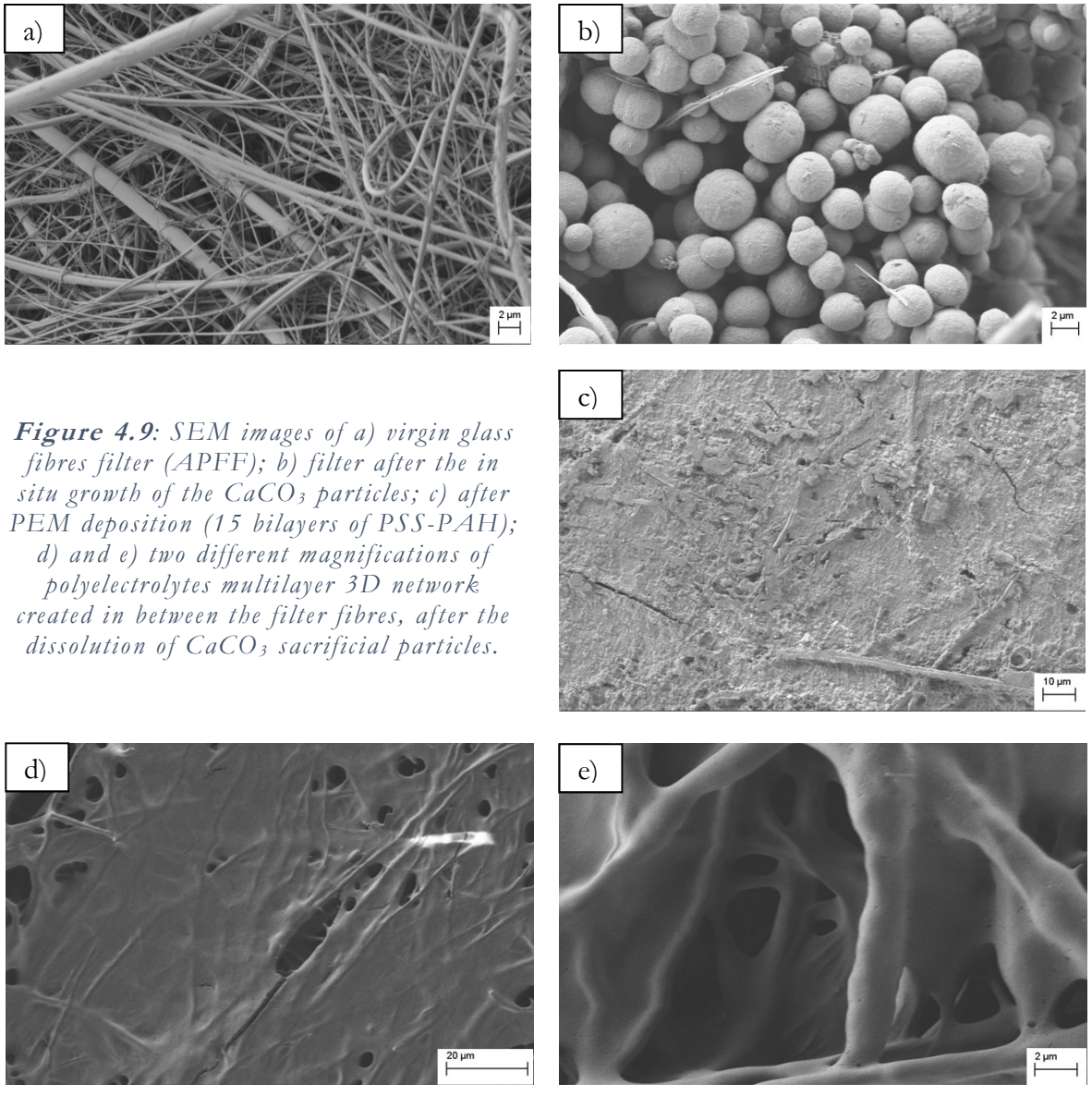


***Figure 4.9**: SEM images of a) virgin glass fibres filter (APFF); b) filter after the in situ growth of the $CaCO_3$ particles; c) after PEM deposition (15 bilayers of PSS-PAH); d) and e) two different magnifications of polyelectrolytes multilayer 3D network created in between the filter fibres, after the dissolution of $CaCO_3$ sacrificial particles.*

We made a series of experiments in particular as a function of the number of deposited layers, we report here only the ones giving the best results.

In the case of $(PSS\text{-}PAH)_{15}$ we also evaluated the difference in morphology depending on the storage mode. Before the SEM characterization, two identical filters coated with $(PSS\text{-}PAH)_{15}$ were stored at room temperature indipendently one immersed in water and the other one, in dry conditions until their further investigation (about one week). **Figure 4.10** shows the comparison of SEM micrographs taken from the two samples. It is clearly evident that storing the filter in wet conditions leads to a smoother network characterized by a much reduced roughness compared to the filter stored under dry conditions.

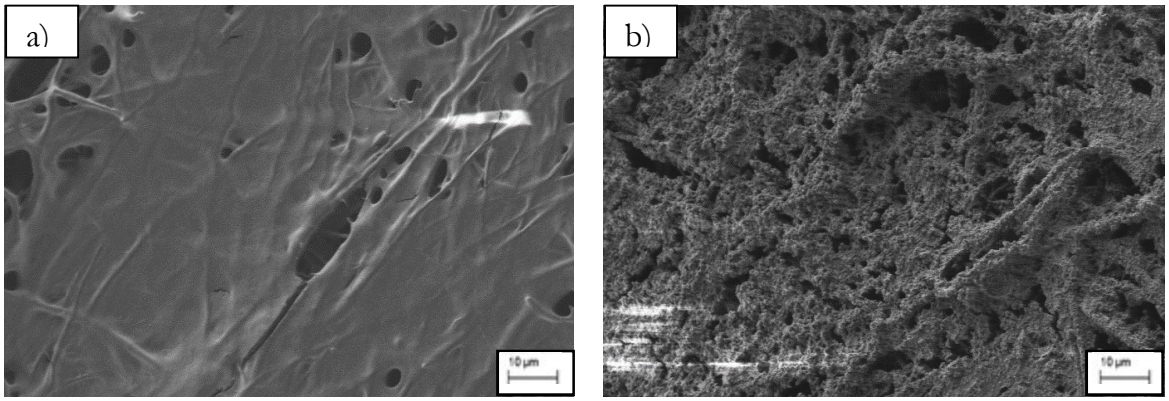


***Figure 4.10**: SEM images of glass fibre filters coated with $(PSS\text{-}PAH)_{15}$ a) stored in wet conditions and b) stored in dry conditions.*

We correlated the roughness of the filter stored under dry conditions to the presence of salt that during the drying process crystallized, increasing the roughness and breaking the polyelectrolytes multilayers film itself. We hence considered the filters stored in wet conditions as better suited for the experiments for qualifying the filtration properties.

#### 4.3.1.1 FILTRATION TESTS

The filtration tests have been performed using Coomassie Brilliant Blue (CBB) dye. One of the well-known properties of polyelectrolytes multilayers capsules is that they can host and keep stored large molecules but they remain permeable to small compounds even for a large number of layers forming the shell. In fact, since the polymeric shell is completely permeable only to low molecular weight molecules, they are in general used to encapsulate biotherapeutics with high molecular weight such as nucleic acids and proteins.[170-173] Anyways, there are no well-defined ways to predict the cut-off molecular weight to define whether a molecule will pass through the shell or not.[174]

Since one of the main aims of this PhD project involves the entrapment of local anaesthetics that usually are small molecules, we decided to test the filtration properties of the modified filters with CBB because it is characterized by a relatively small molecular weight.

Experimentally, we performed the filtrations through a pristine filter and through the filter modified with the 15 bilayers of (PSS-PAH) as described in Paragraph 3.3.3. **Figure 4.11** and **Figure 4.12** show the UV-VIS spectra of CBB solution and of the filtrates respectively.

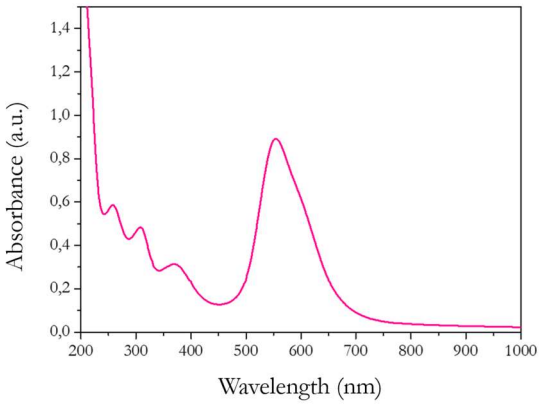


***Figure 4.11**: UV-VIS spectrum of CBB solution.*

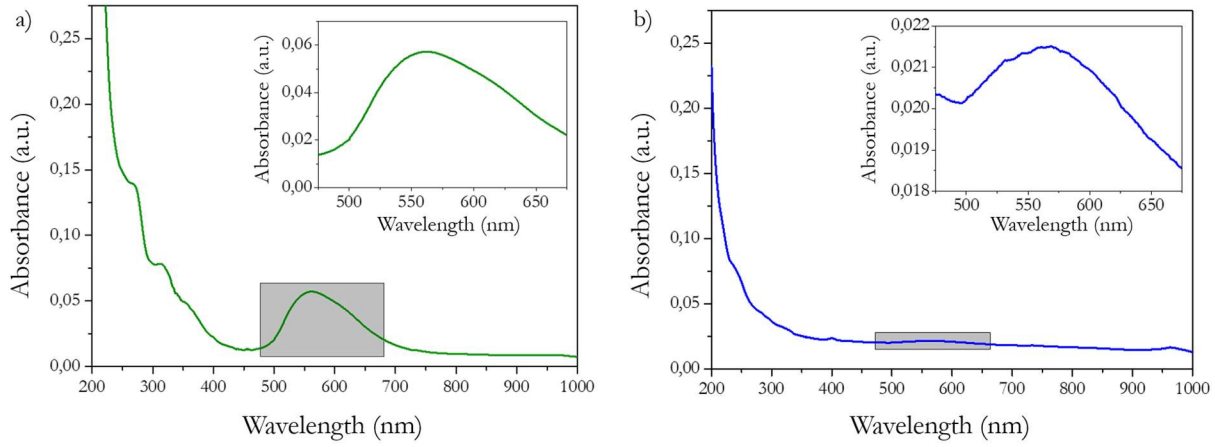


***Figure 4.12**: UV-VIS spectra of filtrates collected after filtration of CBB solution through a) pristine glass fibre filter and b) glass fibre filter modified with a 3D network made of 15 bilayers of (PSS-PAH).*

With these preliminary filtration tests, we have demonstrated that it is possible to finely tune the permeability of commercially available filters and this result could be considered as the first step towards selective nanofiltration.

Polyelectrolytes multilayers capsules made of PSS and PAH are known to be sensitive to the environmental pH. In fact, they change their permeability depending on the surrounding pH value. This effect has been employed for both loading compounds inside the capsules and for their release from them. [66, 83, 175]

For this reason, we decided to evaluate the filtration speed (that could be related to the flow rate), of the modified filters as a function of the pH of the solution to be filtered. For this experiment, we decided to use the glass fibre filters modified with a 3D network made of 5, 10, 15 and 20 bilayers of (PSS-PAH) and the results are reported in **Figure 4.13**.

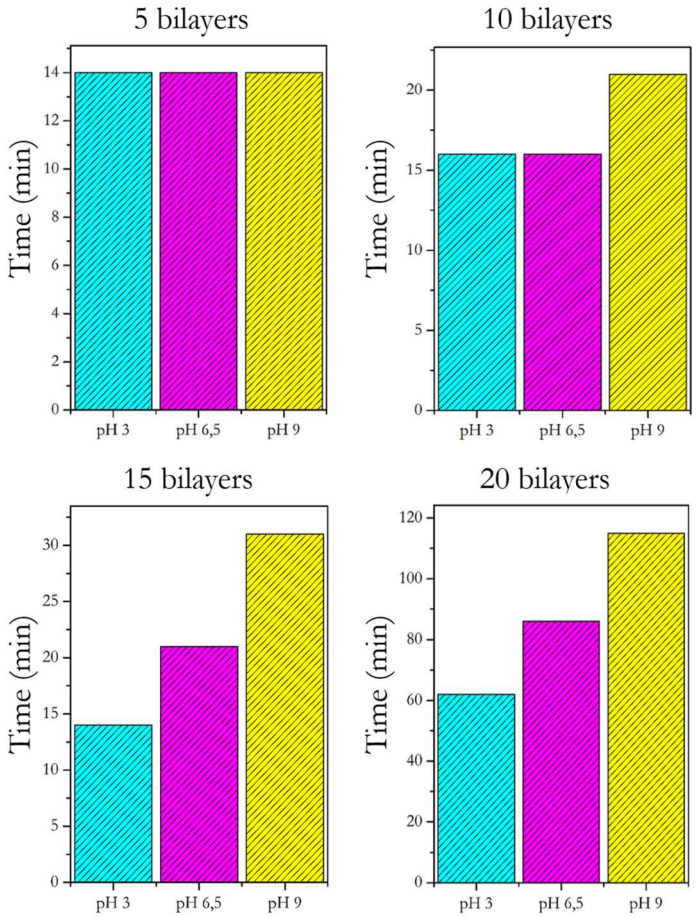


***Figure 4.13**: Graphs representing the filtration time in function of the pH of the filtered solution for different modified filters.*

These graphs represent the time required for each modified system to filter 50 ml of water at different pH values. It is clear that 5 bilayers of PSS-PAH are not enough to modify the filtration speed depending on the pH and for every pH values the time required to filter 50 ml of solution is the same and it is about 15 min. Also in the case of 10 bilayers the difference of filtration speed in negligible. This is probably due to the fact that neither the deposition of 5 bilayers nor of 10 bilayers leads to the formation of a homogeneous 3D network that could cover the filter pores, as it happens instead presumably in the case of 15 and more bilayers. In fact, comparing the graphs corresponding to 15 and 20 bilayers, a clear difference in the filtration speed is evident and the trend reflects what was expected: at pH 3 the pores of the 3D network are fully opened allowing the solution to pass faster through it. By increasing the pH, pores progressively close until they become fully closed. Of course, the polyelectrolytes multilayers network is still permeable to water (in this experiment the filtered solution was water) but the time required for the solution to pass through increases. Therefore we have demonstrated that it is possible to tune the permeability of commercially available filters in which the filtration speed depends on the pH of the solution to be filtered. This result paves the way to the fabrication of filters with tuneable filtration capability.

### 4.3.2 2D FILTERS

We performed filtration tests onto 2D filters composed of polycarbonate film, which has a smooth, glass-like surface. These kind of filters show 0.2 μm pores size and we decided to modify them without the growth of any sacrificial templates since pores dimensions are smaller than the ones of the glass fibre filters used for the previous experiments. Furthermore, since pores are manufactured by a laser technology (see morphological characterization in **Figure 4.14** taken from Ref. [176]) and the membrane itself is quite robust, we did not create the PDMS border and we deposited polyelectrolyte multilayers directly onto the as received filters.

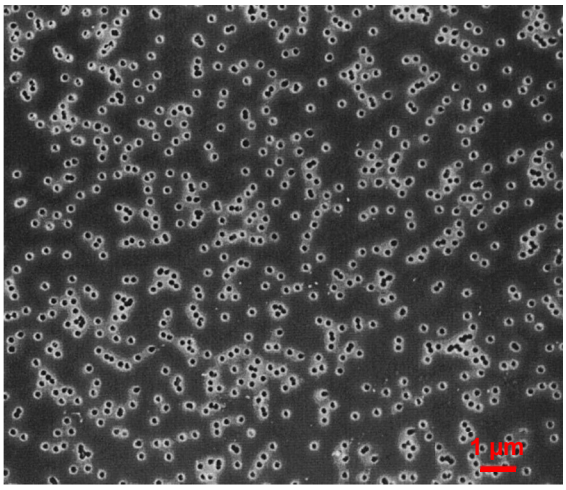


***Figure 4.14**: SEM image of the Isopore polycarbonate membrane.[176]*

The filtration tests were carried out as described in Paragraph 3.3.3 using filters modified with 5, 10, 15 and 20 bilayers of (PSS-PAH). We used Coomassie Brilliant Blue as the solution to be filtered and the resulting UV-VIS spectra are depicted below (**Figure 4.15**).

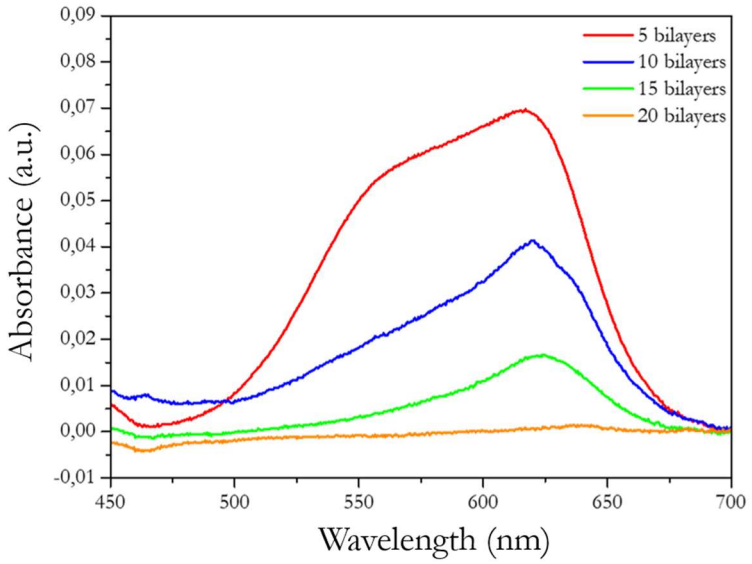


***Figure 4.15**: UV-VIS spectra of filtrates collected after filtration of CBB solution through Isopore membranes modified with 5, 10, 15 and 20 bilayers (from top to bottom, respectively).*

From these spectra it is evident that filter permeability towards Coomassie Brilliant Blue dye was decreased increasing the number of $(PSS\text{-}PAH)_n$ bilayers as expected. Therefore, even in this case, we have demonstrated that it is possible to tune finely the filter permeability towards relatively small compounds, by the deposition of polyelectrolytes multilayers and that it is possible to select the desired filtration powers choosing the proper number of deposited bilayers. From these preliminary experiments it is thinkable to tailor the design of very fine filters by changing the polyelectrolyte coatings in terms of the specific polymers, number of layers and so on.

## 4.4 MICROCHAMBERS MADE OF POLYELECTROLYTES MULTILAYERS AND BIOPOLYMERS

As previously discussed, the main aim of this PhD project is the development of a device for the local efficient treatment of post-operative pain overcoming the present limitations. To this end we envisage that the activation of the drug release should be triggered electrically. We hence designed two different basic architectures and we began exploring the development of microchambers entirely made of polyelectrolytes multilayers or biopolymers, following the procedure described in Paragraph 3.4. To fabricate the microchambers we used PDMS stamps. SEM characterizations of every manufacturing step are reported in **Figure 4.16** where the PDMS stamps are obtained starting from Kapton based microwells.

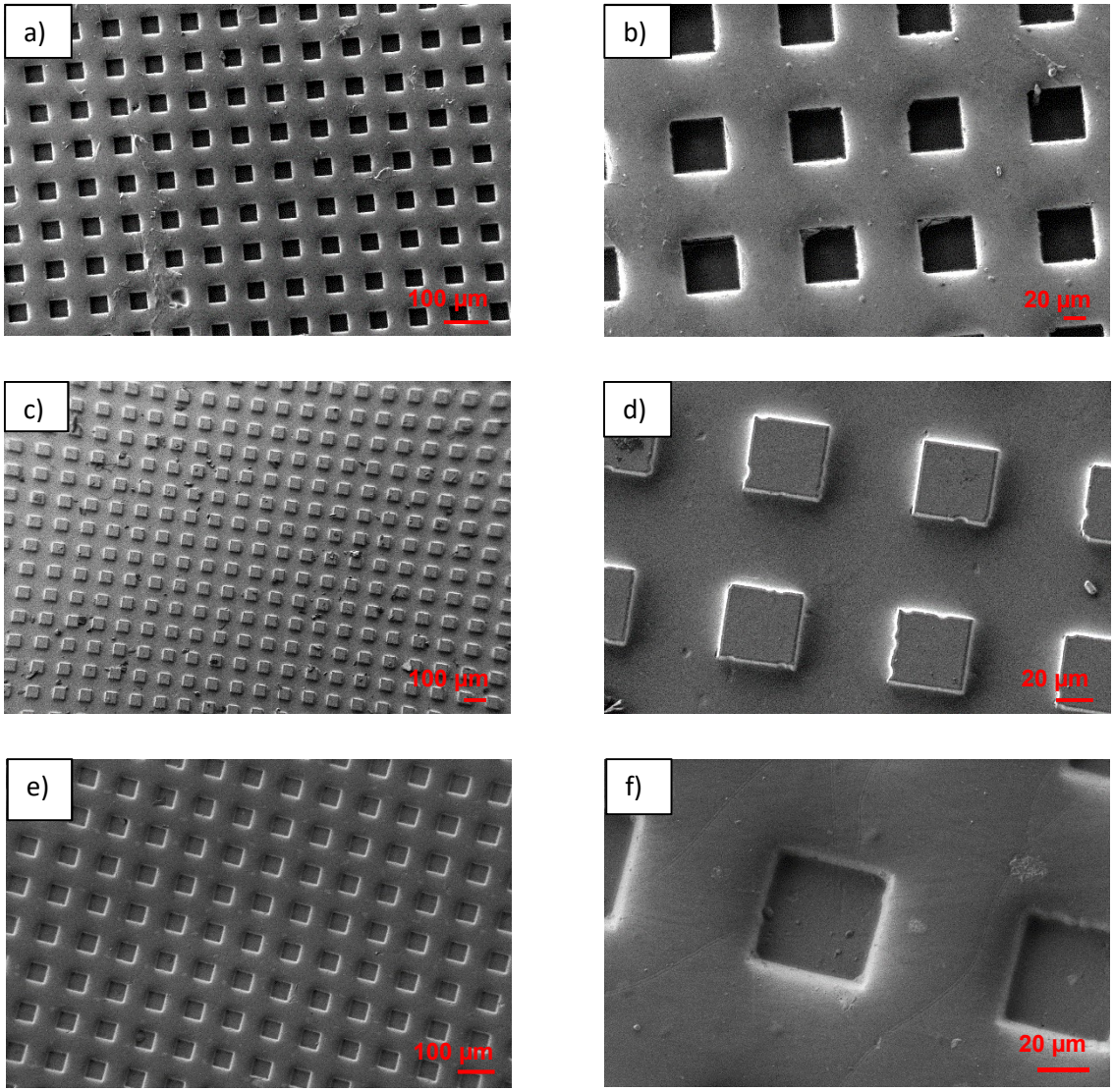


***Figure 4.16**: SEM images at different magnifications of a) and b) starting Kapton based microwells; c) and d) PDMS stamp 1 showing micropillars; e) and f) PDMS stamp 2 showing microwells.*

This is an example of PDMS stamp fabrication starting from Kapton based microwells. The as-obtained PDMS microwells are the perfect replica of the Kapton microwells having a dimension of 50x50x40 μm. We also used PDMS stamp obtained from Silicon master, as described in Paragraph 3.4.1, showing round micropillars with height and diameter from 5 to 10 μm and we started fabricating microchambers using precisely this kind of stamps.

### 4.4.1 FABRICATION OF MICROCHAMBERS BY THE LAYER-BY-LAYER TECHNIQUE

Since we want to activate the release with an electric stimulus, we explored conducting polymers as building blocks of the drug containers. We tried to make the chambers using polyaniline (PANI) combined with PSS and PEDOT:PSS combined with PEI, as described in Paragraph 3.4.3. The SEM characterization of (PANI-PSS) freestanding microchambers is reported in **Figure 4.17**.

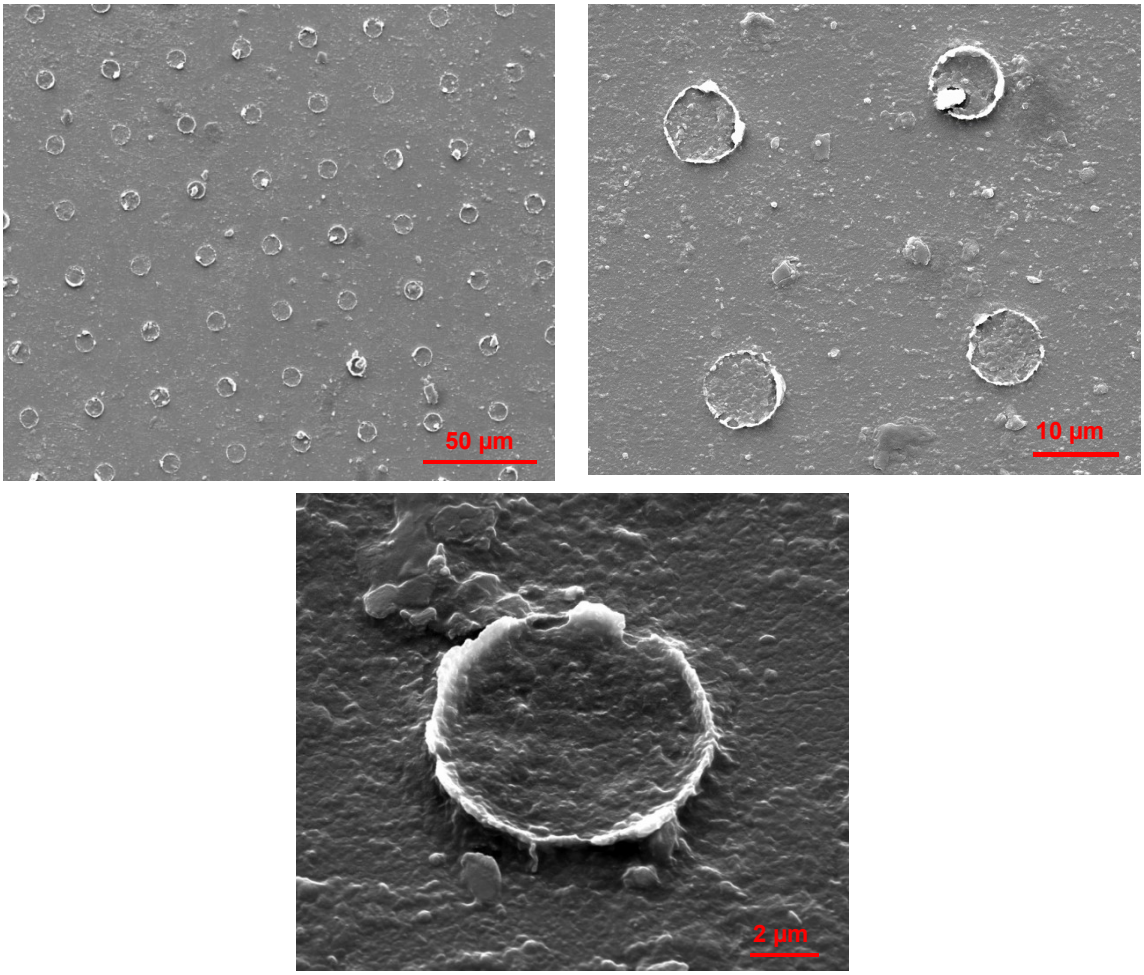


***Figure 4.17**: SEM images of (PANI-PSS) microchambers at different magnifications.*

The surface of the sample appears to be not smooth but with a high roughness that is most likely due to the presence of particles in the polyaniline solution. As previously described, the protocol to prepare the water solution of PANI involves the repeated filtration of the PANI solution in dimethylacetamide (DMAC) prior to the dilution in acidic water. Probably, the filtrations are not enough to remove completely PANI particles, thus making the obtained result not optimal. Furthermore, the number of layers deposited to create the chambers walls can affect the chambers morphology and roughness and it is in principle possible to decrease the number of layers in order to improve PANI microchambers features. Nevertheless, together with these drawbacks one should also take into account that the procedure to prepare a water solution of PANI is time consuming and that the as prepared solution expires in 3 day. All together it becomes possible only to perform a reduced number of experiments before restarting the whole process. On the basis of these considerations, we focused our work on the fabrication of microcontainers made of PEDOT:PSS in combination with PEI, since we have already demonstrated the possibility of creating both flat and 3D systems with these materials.

The formation of ordered microchambers arrays can be detected by light diffraction patterns. **Figure 4.18** shows an example of such patterns obtained from our samples.

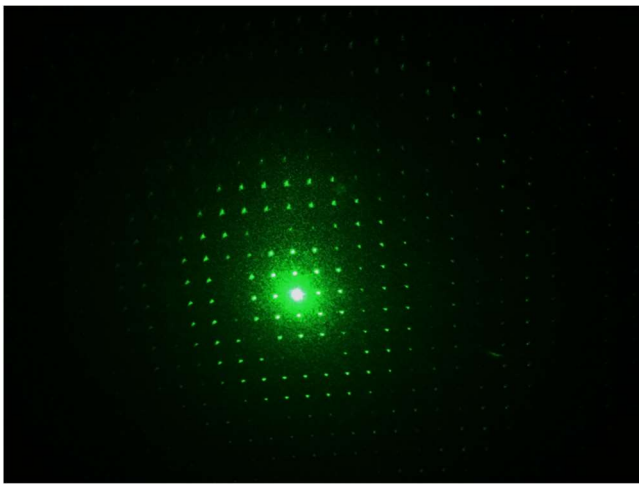

***Figure 4.18**: Light diffraction pattern of ordered PEI-PEDOT:PSS microchambers array.*

The PEI-PEDOT:PSS microchambers were also studied and characterized by SEM. **Figure 4.19** shows the typical characteristics of our arrays of microchamebers.

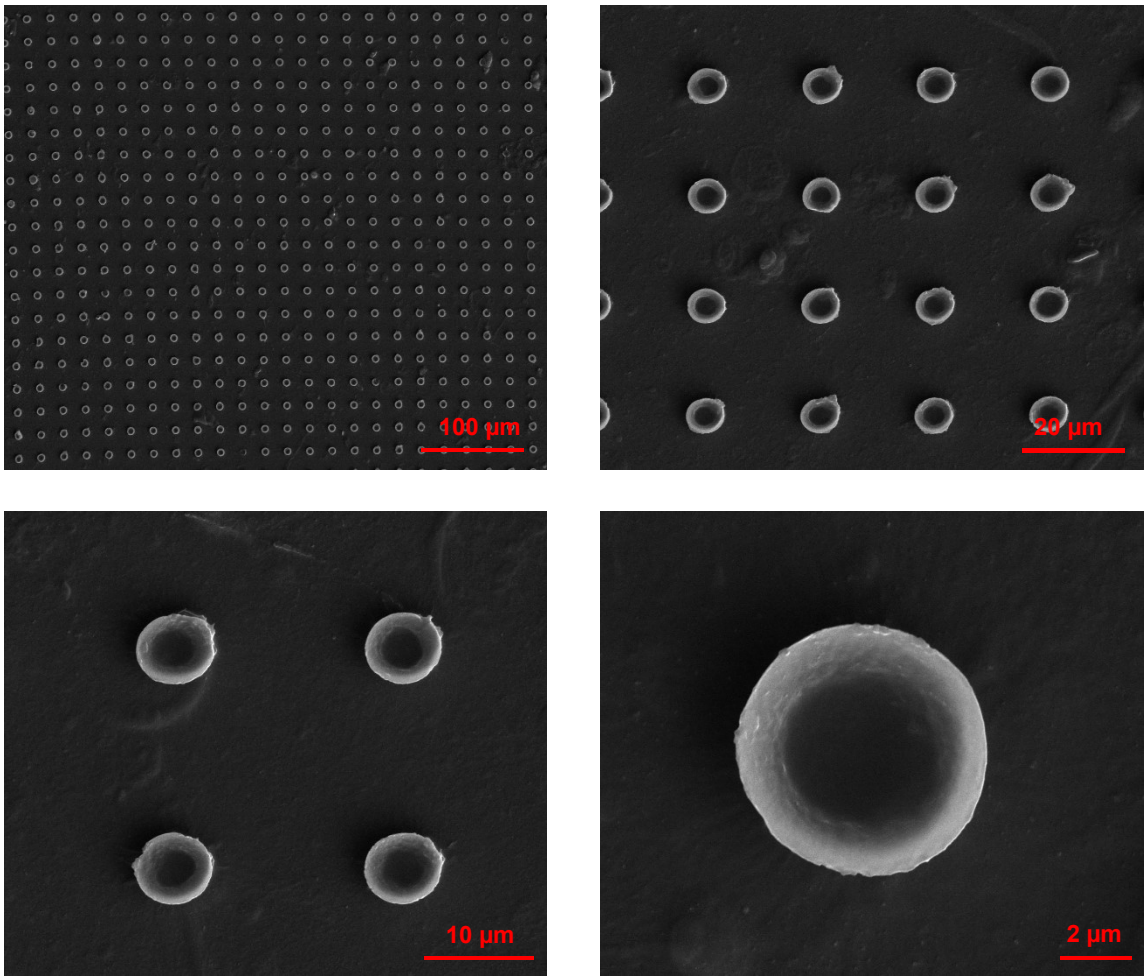


***Figure 4.19**: SEM images of PEI-PEDOT:PSS microchambers at different magnifications.*

The microchambers arrays of PEI-PEDOT:PSS are quite well ordered. The whole surface of the samples appears much smoother compared to the one made of PANI-PSS, but it seems that the inner part of the cap of the chambers collapses somehow inside the chambers themselves. Probably this effect could be avoided loading the chambers with chemicals in solid form, such as particles or crystals, before sealing the chambers. However, we did not yet further investigate this aspect, because even though these polyelectrolytes multilayer-based systems have a high potential as drug delivery systems, for the present aims of this specific project we need containers that can host small hydrophilic drugs and that are robust enough. That's why we explored other materials and another fabrication process.

### 4.4.2 FABRICATION OF MICROCHAMBERS BY ONE-STEP DIP COATING TECHNIQUE

In the process of achieving microchambers possessing all the needed properties and feautures we hence explored the possibility to make freestanding microchambers arrays made of polymers that are hydrophobic, biocompatible, biodegradable and approved by the Food and Drug Administration. This last aspect is mandatory in the case of applications in the biomedical field. The technique we used is the one-step dip coating technique and the procedure we followed is described in details in Paragraph 3.4.4. We explored different polymers such as polylactic acid (PLA, $T_g$=60-65°C, $T_m$= 173-178°C), poly-ε-caprolactone (PCL, $T_g$= -60°C, $T_m$=56-64°C, 60°C lit.), polyhydroxybutyrate (PHB, $T_g$=2°C, $T_m$= 175°C) and poly lactic-co-glycolic acid (PLGA, $T_g$=40-60°C, $T_m$= 72-77°C).

Freestanding microchambers have been fabricated using PDMS stamps showing small rounded microwells with a diameter of 5-10 μm. Polymers were dissolved in chloroform at the concentration of 2 % w/w except for PLGA the solution of which was prepared at 5% w/w because in previous attempts we noticed that it was not possible to build chambers made of PLGA at lower concentrations.

SEM characterization of small round microchambers made of PHB, PLGA and PLA are shown in **Figure 4.20**.

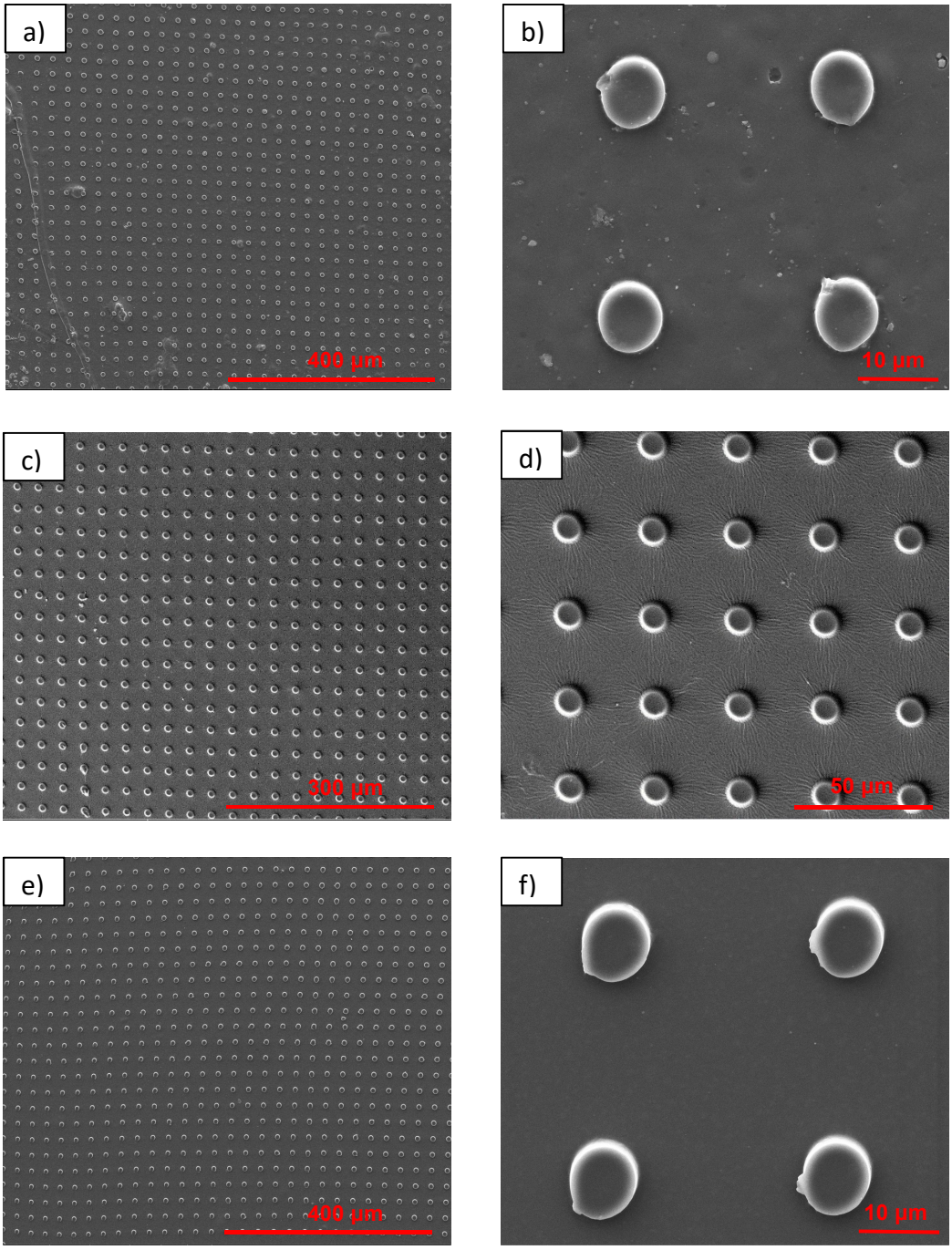


***Figure 4.20**: SEM images of microchambers made of one-step dip coating technique of a) and b) PHB (2%w/w), c) and d) PLGA (5% w/w), e) and f) PLA (2% w/w) at different magnifications.*

As mentioned before (see Paragraph 3.4.4) we fabricated microchambers also using PCL. In this case, we build small round microchambers with different polymer concentrations in chloroform, 1, 2 and 3 % w/w. We evaluated the morphology depending on the concentration with Scanning Electron Microscopy. The results are reported in the **Figure 4.21.**

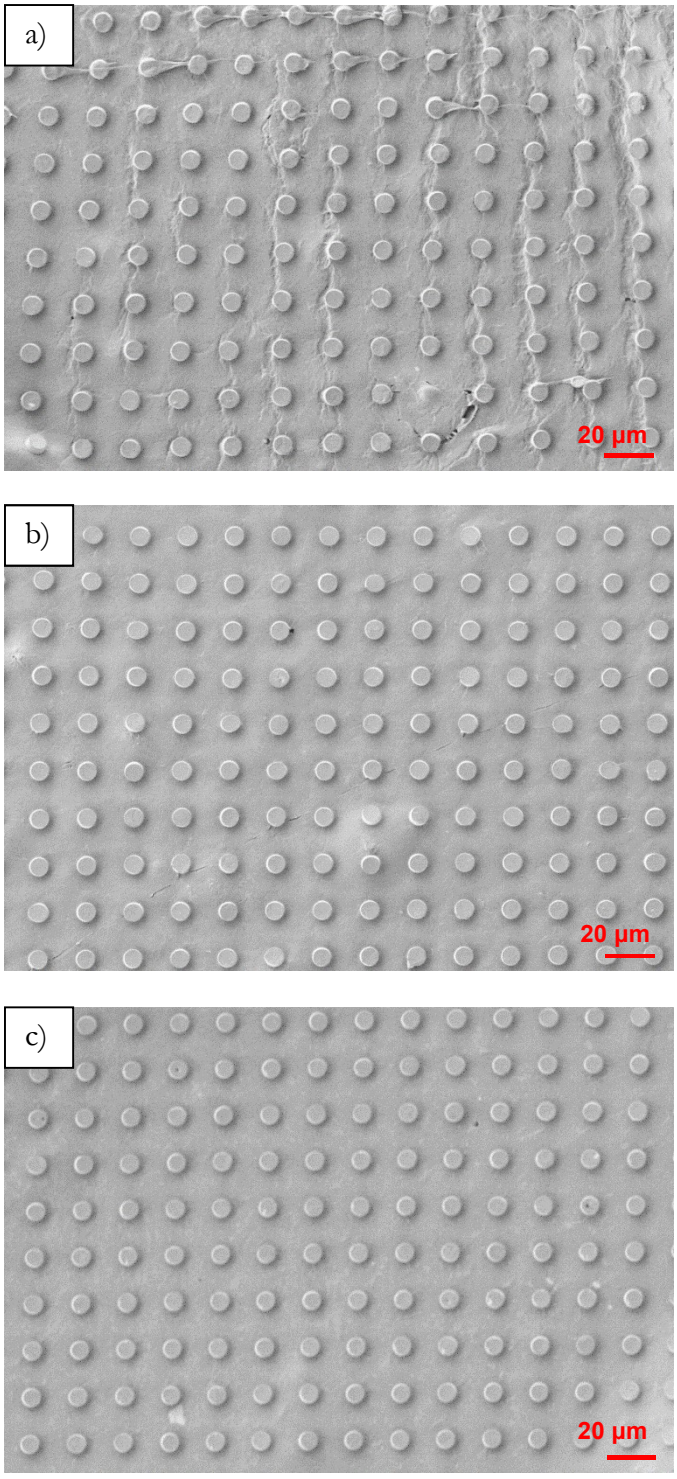


***Figure 4.21**: SEM images of freestanding microchambers made of PCL at the concentration of a) 1% w/w, b) 2% w/w and c) 3% w/w.*

Decreasing the concentration of polymer, the morphology gets worst and wrinkles are evident in the chambers fabricated with the concentration of 1% w/w. Some inhomogeneities are visible also in the sample produced with the concentration 2% w/w. Therefore, from these results we concluded that the best concentration of PCL in chloroform is the 3% w/w to build round chambers with diameters of 5-10 µm.

Among all the biopolymers that we explored to fabricate freestanding microchambers, we focused on PLA and PCL. PLA because it is very easy to handle and it is known from literature that it is stable, robust and it can host small hydrophilic molecules [17, 106, 114, 177]. Unfortunately, PLA could give some problems in the release mechanism that we want to achieve, that is the melting of the polymer induced by electric trigger. In fact in literature only High Intensity Focused Ultrasound (HIFU) and Near Infrared laser beams have been successfully used to open PLA chambers.[106, 114] Instead, PCL even though is stable enough, it could provide an easier solution for the opening of microchambers, since its melting temperature of about 60°C is much lower than the one of PLA that is about 175°C.

Using PLA and PCL we fabricated chambers using stamps showing larger and squared microwells of 50 x 50 μm, in order to maximize the drug loading and simultaneously optimize the geometry. The SEM characterization of these PLA squared microchambers is reported in **Figure 4.22**.

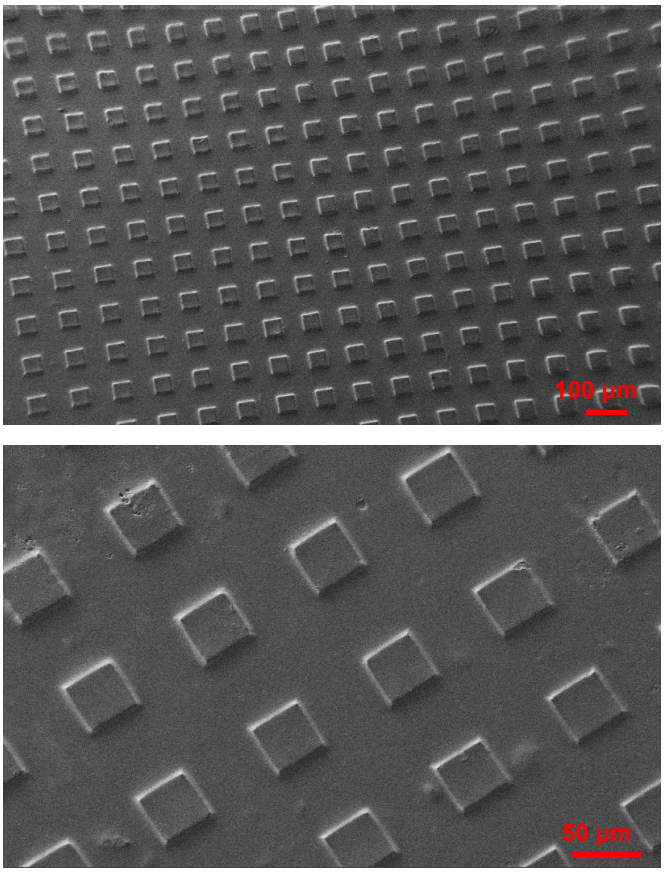


***Figure 4.22**: SEM images of freestanding big microchambers made of PLA at different magnifications.*

The SEM images confirm the high quality of the wells in terms of shape, reproducibility, surface homogeneity and least amount of defects.

In a similar way we proceeded with PCL and we studied the morphology of the samples as a function of the polymer concentration. **Figure 4.23** shows some typical results.

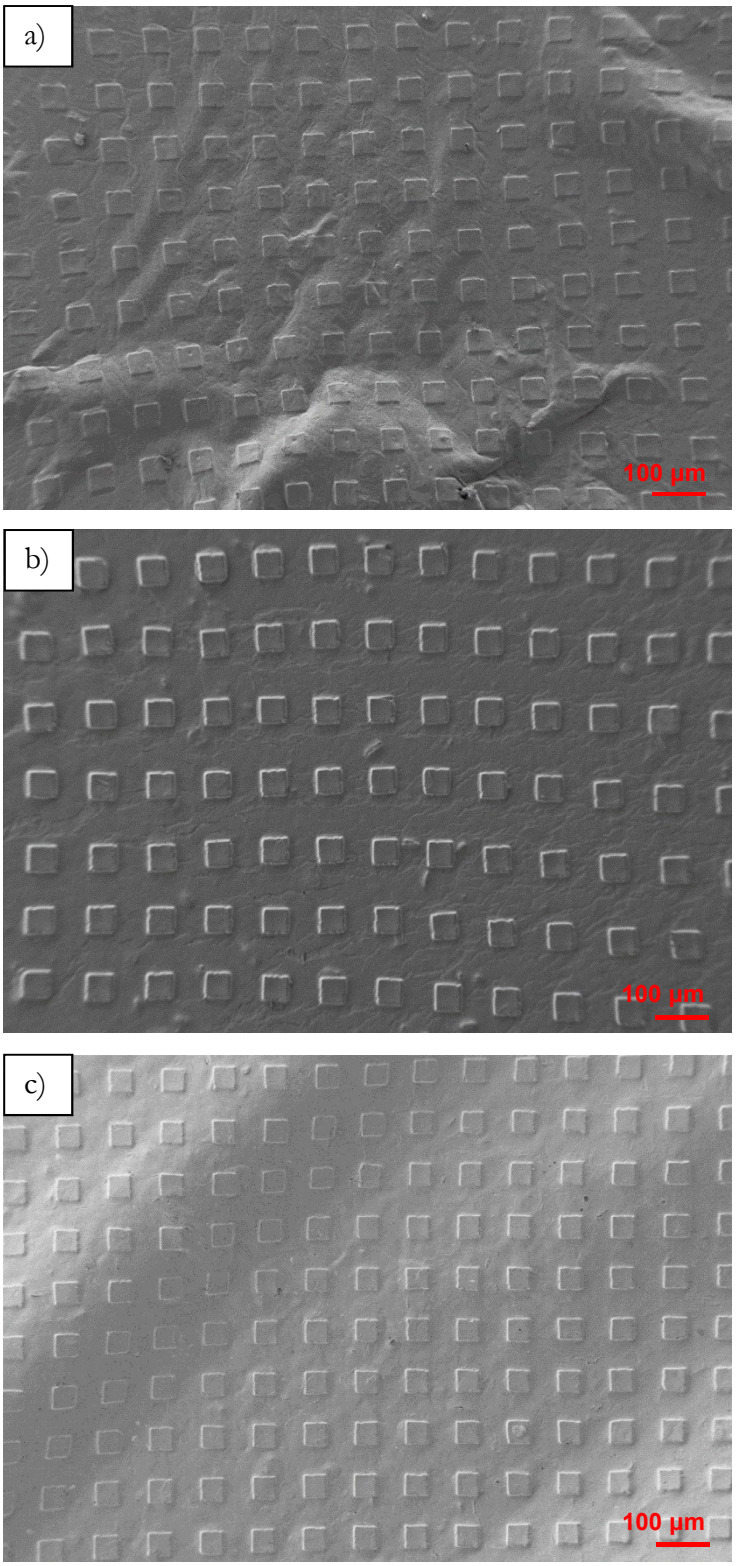


***Figure 4.23**: SEM images of freestanding PCL microchambers fabricated at the concentration of a) 1% w/w, b) 2% w/w and c) 3%w/w.*

In the case of the large chambers made of PCL, all the samples show defects. The smoothest surface seems to be obtained with the concentration of PCL 3% w/w but also in this case some folded areas are visible. At the concentration of PCL 2% w/w the sample seems quite homogenous but the roughness is quite high. Finally, as in the case of small microchambers, the worst sample is obtained with the concentration of PCL 1% w/w where cracks and wrinkles are most pronounced.

From all these experiments we could finally demonstrate for the first time the feasibility of fabricating large, stable and well defined microchambers made of polymers that are biocompatible, biodegradable, hydrophobic and FDA approved, even though further work is needed to optimize the process to fabricate large microchambers made of PCL.

These polymeric freestanding microchambers are very promising as drug delivery systems and for fine release control. However, since our final device has to be handled by a surgeon, we decided to focus our work on the other architecture where the microchambers array and the sealing film are made of materials with different characteristics: a robust substrate in which the microchambers are made, and a softer polymer just for sealing the microchambers. This approach is sketched in **Figure 4.24**.

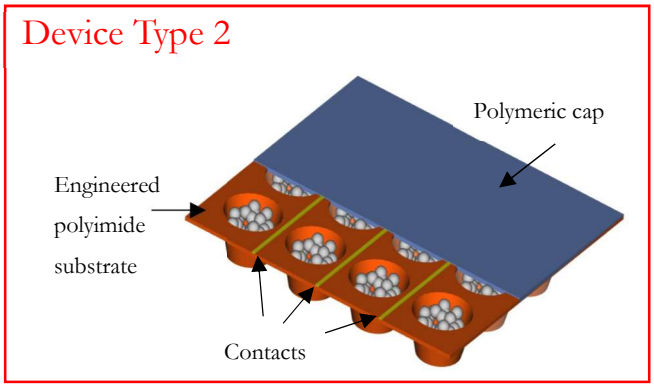


***Figure 4.24**: Basic architecture of the device Type 2.*

In order to achieve the final working device, we had to face several steps. First of all, we had to engineer the substrate in order to make the right patterned microwells with a geometry that optimizes the density and maximizes the volumes of drugs that can be loaded. Then, we had to develop and possibly optimize the processes of loading the drug and sealing the microchambers. Finally we had to reach the major aim of the project that is the electric activation of the drug release which could be only achieved if all the other processes would give the proper functionalities and compatibilities.

## 4.5 SUBSTRATE ENGINEERING

We chose to use polyimide to develop the substrate since it shows several favourable properties including flexibility, high tensile strength, transparency and biocompatibility. In particular, polyimide is USP Class VI compliant, meaning that no harmful reactions or long-term bodily effects are caused by the material. Moreover, it meets ISO 10993 biocompatibility requirements for a Class III device.[178] In most cases it has been used for implants mainly as a protective layer for implantable electrodes or as a substrate with different shapes (such as needle-like, cylindrical) for recording neural signals but also for retina implants or in contact with endothelial cells.[179-183]

### 4.5.1 SUBSTRATE ENGINEERING FROM A LIQUID PRECURSOR

We first explored the possibility of creating polyimide microwells from a liquid precursor. As described in Paragraph 3.5.1, we firstly created a silicon negative master by standard lithography that shows squared wells 20 μm apart, with dimensions of 50x50x40 μm. Then a positive PDMS master showing squared pillars was obtained from the Si negative master. Finally, the polyimide replica was obtained by casting the liquid polyamic acid precursor and activating the imidization process as described in Chapter 3. **Figure 4.25** shows from left to right the images of the Si master, the PDMS master and the polyimide replica respectively.

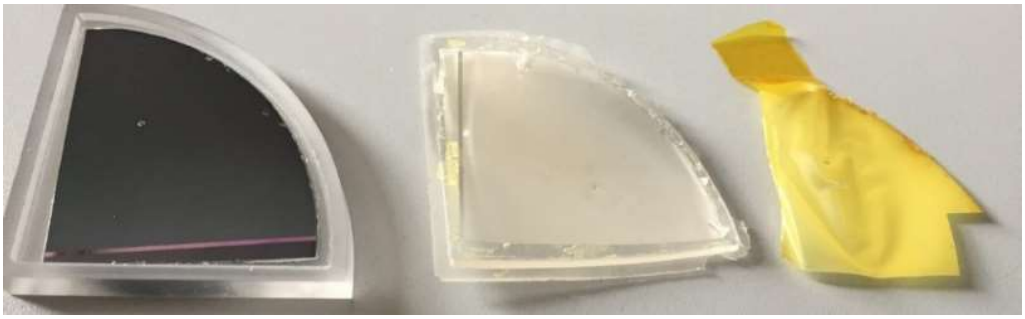

***Figure 4.25**: From left to right: Si negative master, PDMS master and polyimide replica.*

The as-obtained polyimide replica was investigated by optical and 3D Measuring Laser Microscope and the results are reported in the **Figure 4.26** and **Figure 4.27**.

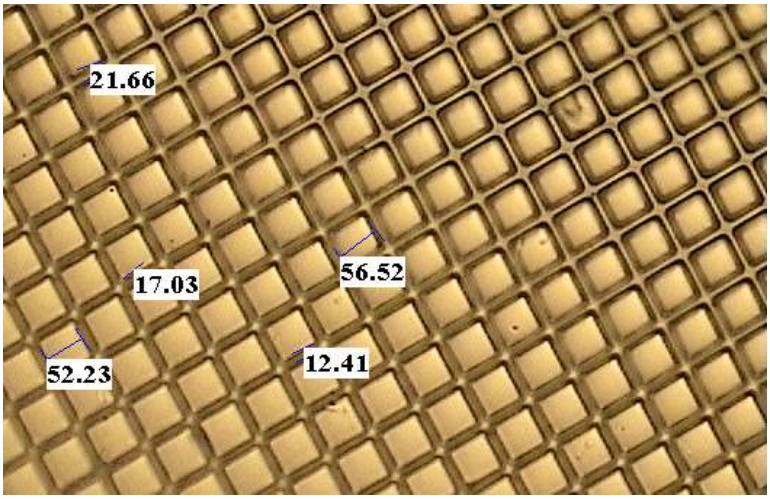


***Figure 4.26**: Optical image of polyimide replica obtained starting from a liquid precursor. The dimensions of some wells and the thickness of some walls are reported.*

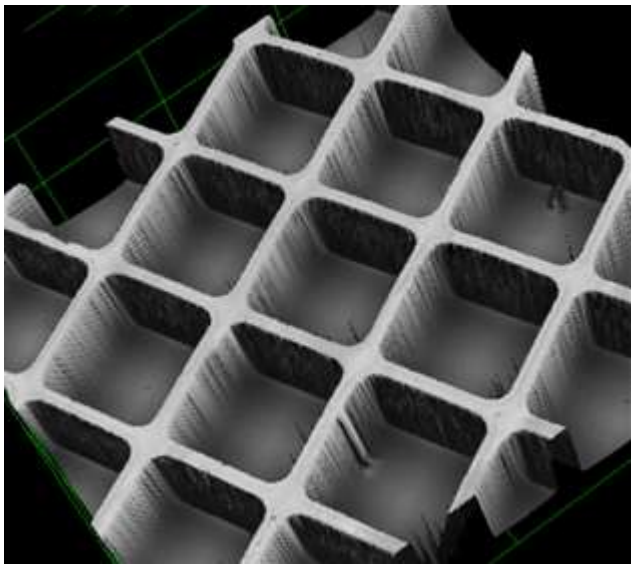

***Figure 4.27**: Polyimide microwells fabricated starting from a liquid precursor, observed with 3D Laser Measuring Microscope.*

This method of fabricating polyimide microwells from liquid precursor is particularly well suited because it gives the possibility of obtaining large density of wells that is very important to maximize the volumes of drug that can be hosted in the final device. Unfortunately, this method involves the use of chemicals to synthesize the liquid precursor and the chemical residues in the final replica are difficult to control and would require a systematic and careful study to minimize or eliminate their unwanted presence. In fact, these residues could introduce problems for biomedical applications where the presence of even traces of chemicals that are not already clinically tested would require long-lasting and cumbersome studies. Even though this line of research will be possibly pursued, we decided to explore another microwells fabrication technique that is safer from the point of view of the final application because it could guarantee the maximum purity and control of the materials: the patterning of the microwells on a Kapton foil by a hot-embossing technique.

### 4.5.2 SUBSTRATE ENGINEERING BY HOT-EMBOSSING TECHNIQUE

For the final application, we hence chose a commercial polyimide sheet (Kapton) as substrate to be engineered. As mentioned before, the glass transition temperature of Kapton is very high (>300°C) and we needed specific precautions to reach those temperatures. This is the reason why we tested the hot-embossing by making experiments onto Cyclic Olefin Copolymer (COC, Topas, 5013). The result is reported in **Figure 4.28**.

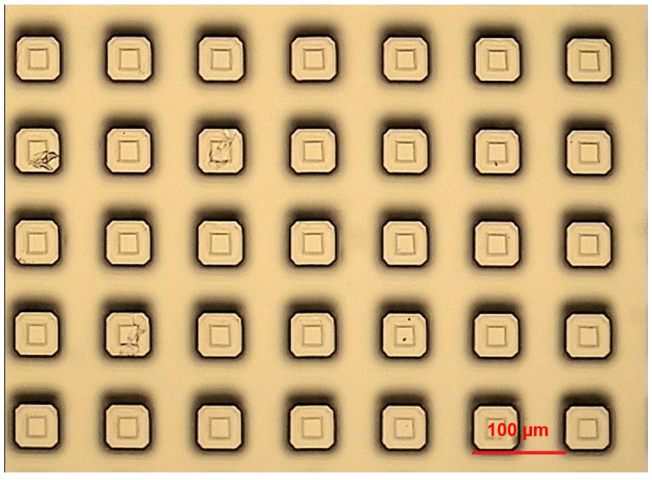


***Figure 4.28**: Optical image of hot-embossed COC.*

For our final application we selected in particular Kapton NH sheet from DuPont, 25 µm thick; as described in Paragraph 3.5.2, we engineered the Kapton sheet by a specifically tailored hot-embossing process. The moulded substrate has been characterized by optical

microscope and Scanning Electron Microscope (SEM). The results are reported below in **Figure 4.29** and **Figure 4.30**.

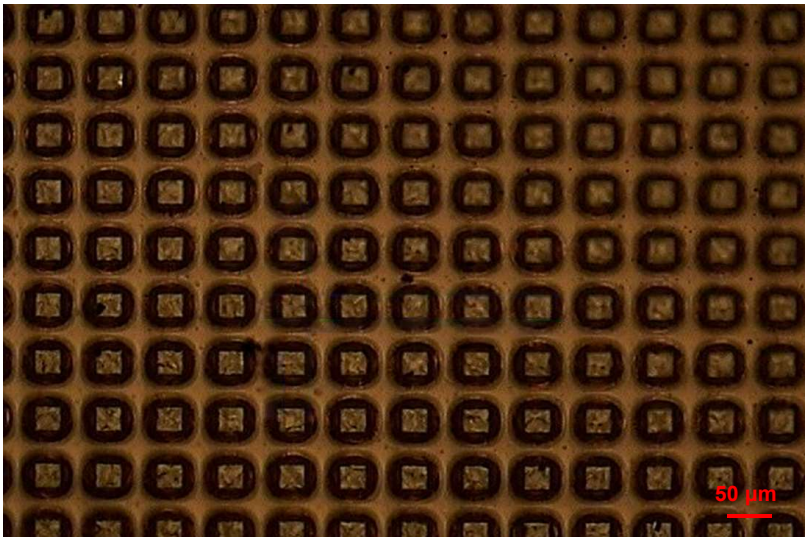


***Figure 4.29**: Optical image of polyimide microwells fabricated by hot-embossing a commercially available Kapton sheet.*

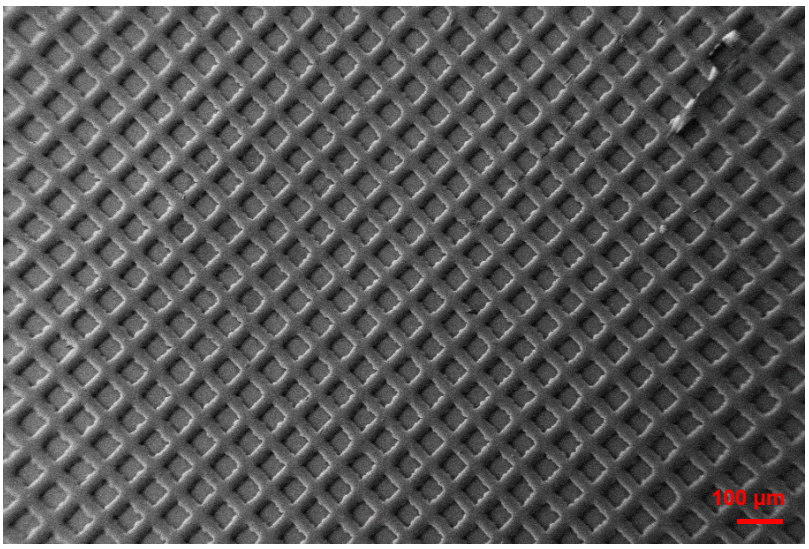


***Figure 4.30**: SEM image of polyimide microwells fabricated by hot-embossing a commercially available Kapton sheet.*

The results show a perfect microwells array. As in the previous case of substrate engineered from a liquid precursor, the density of wells is quite large. Considering the drawbacks correlated to potential chemical residues that the first method has, we decided to employ the hot-embossing technique to create the final substrate.

## 4.6 LOADING

After the substrate engineering, we had to face the development of a reliable process for the drug loading. We first studied a process for the loading of chemicals in form of crystals.

### 4.6.1 LOADING OF DRUGS IN FORM OF CRYSTALS

We used two different model agents, sodium chloride and Rhodamine B. We chose the first one because it creates big crystals, and hence it is easily recognizable, and the second one because it is a fluorescent dye so it is easily observable. To load crystals inside the wells, we used a process based on the sonication of the substrate inside the model agent solution, to remove the air bubbles and to allow the drug solution to enter easier into the wells. After the solvent evaporation, we effectively got drug crystals inside the microwells, as demonstrated by Scanning Electron Microscopy (SEM) in the case of sodium chloride (**Figure 4.31**) and fluorescence optical microscopy in the case of Rhodamine B (**Figure 4.32**).

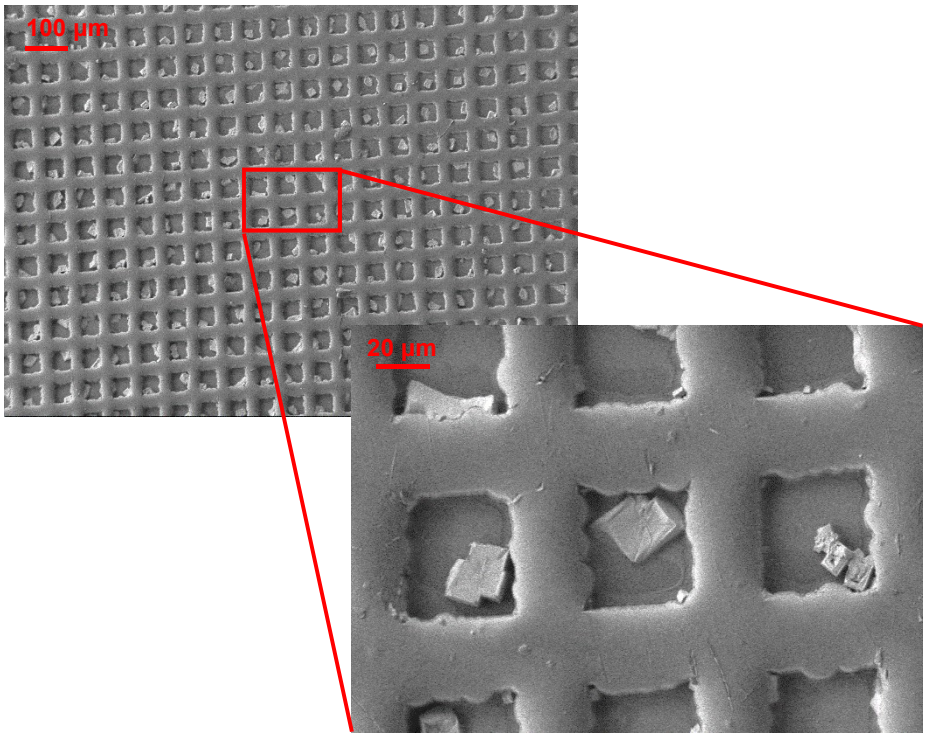


***Figure 4.31**: SEM images of NaCl crystals loaded inside microwells obtained by Kapton hot-embossing.*

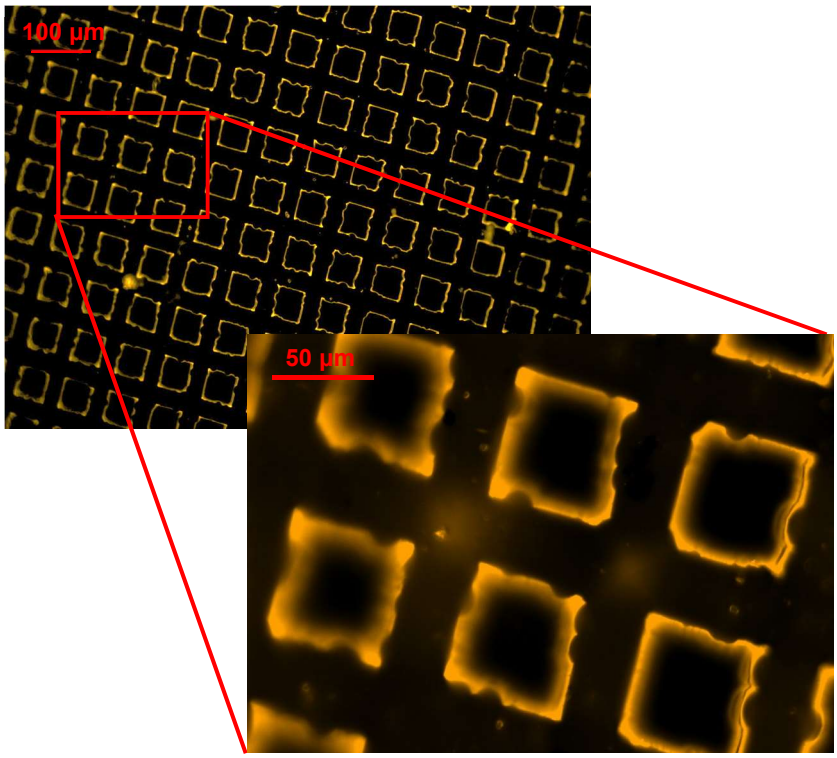


***Figure 4.32**: Fluorescence optical images of Rhodamine B crystals loaded inside microwells obtained by Kapton hot-embossing.*

As shown in **Figure 4.31** and **Figure 4.32**, model agent crystals are exclusively inside the microwells. Regarding Rhodamine B crystals, the fluorescence indicates that they are at the edge of the microchambers and this is very likely due to the solvent evaporation process combined with the defects, including the edges, produced by hot-embossing technique.

These experiments demonstrate that the processes that we have setup are well suited for loading model agents in form of crystals inside the microwells. Since the final device requires likely the load of pharmaceutical formulations in liquid form, we developed another technique for loading drugs in liquid form and the results will be discussed in the next few paragraphs since it involves the simultaneous loading and sealing processes.

## 4.7 SEALING

We developed two different methods for sealing the microwells. The first one we called the "Ring method" while the second one is the "Blanket coverage method". The *Ring method* can be used to seal microchambers already loaded with drugs crystals, while the *Blanket coverage method* is specifically designed to load drugs in liquid form.

### 4.7.1 SEALING BY THE "RING METHOD"

As described in more details in Paragraph 3.5.4.1, this method consists in fabricating a freestanding biopolymer film inside a ring that can be pressed onto the already loaded microwells patterned substrate. The feasibility experiments were carried out using empty microwells and the sealing film was made of poly-ε-caprolactone (PCL). The result is shown in the **Figure 4.33**, where a comparison between an empty, not sealed substrate and a sealed substrate is shown.

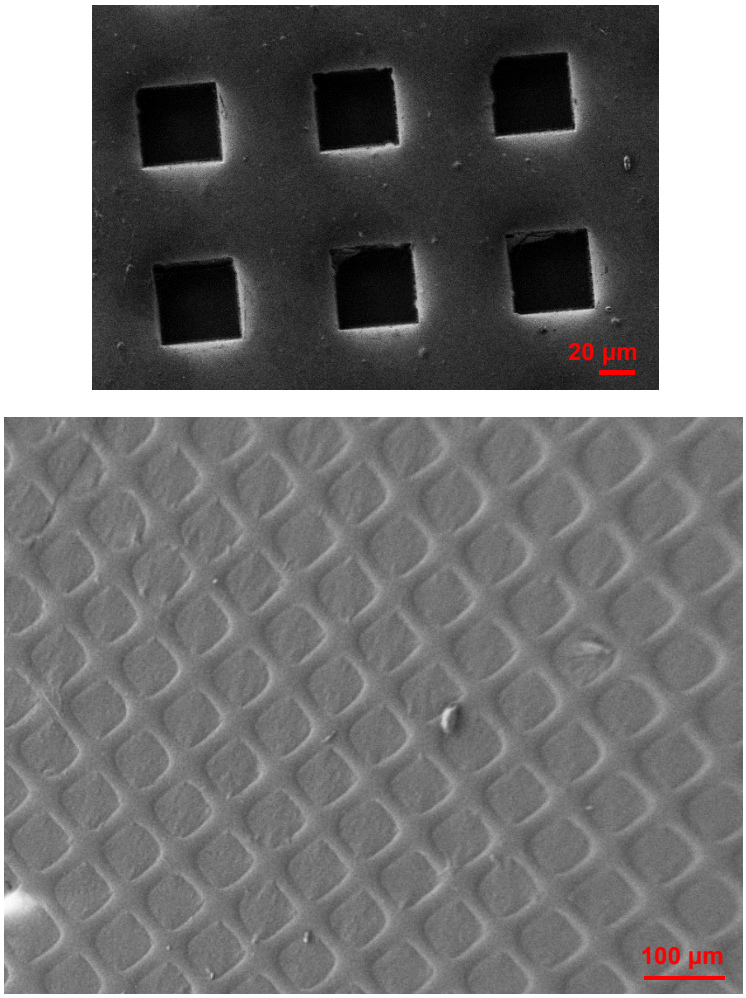


***Figure 4.33**: SEM images of a not sealed array of microwells in the Kapton substrate (top) and the PCL (1% w/w, 80µl) sealed by "Ring method" substrate (bottom).*

The SEM micrographs reported in the figure clearly demonstrated that with the *Ring method* we could reliably perfectly seal the polyimide microchambers. This method is hence viable for the sealing of the devices even though it requires a process with a certain manual skill and there is a need of automatization.

### 4.7.2 SEALING BY THE "BLANKET COVERAGE METHOD"

We developed this method in order to simultaneously load and seal the microchambers. This loading and sealing method is specifically designed for drugs in solution (liquids). The experiments were carried out as described in Paragraph 3.5.4.2 and to demonstrate the feasibility of the process we first tested it with pure water as subphase. The sealing result has been characterized by Scanning Electron Microscopy. **Figure 4.34** shows SEM micrographs of both empty microwells patterned substrate and the corresponding sealed array.

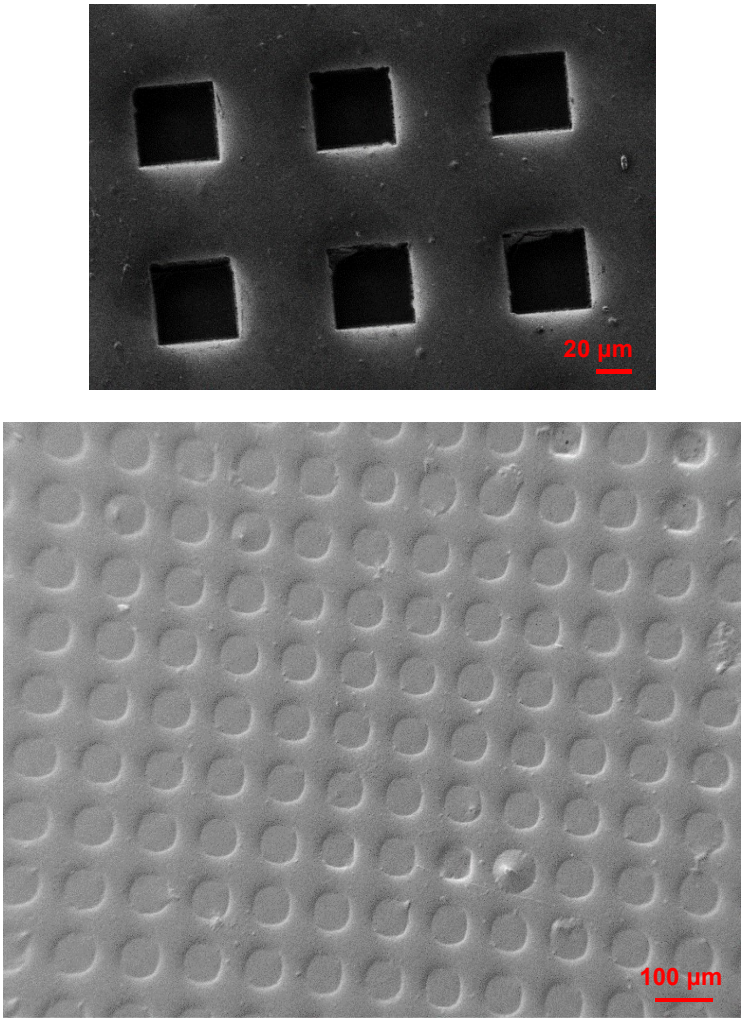


***Figure 4.34**: SEM images of not sealed (top) and PCL (1% w/w) sealed by the "Blanket coverage method" microwelles patterned substrate (bottom).*

Once the feasibility of the sealing by the *Blanket coverage method* has been demonstrated, we decided to upgrade the process to simultaneously load model agent in liquid form and seal the chambers.

#### 4.7.2.1 LOADING SUBSTRATE WITH LIQUID DRUG AND SEALING BY "BLANKET COVERAGE METHOD"

To perform this experiment, we chose fluorescein sodium salt solution (NaFluo) as model agent instead of previously used Rhodamine B. A choice motivated by the fact that it adsorbs and emits far from the orange range leading to an easier recognition of the dye itself (Kapton is orange and PCL absorbs even if slightly in the orange range as Rhodamine B). This upgrade of the *Blanket coverage method* involves a sonication step and the use of the model agent solution itself as subphase, with a process described in details in Paragraph 3.5.4.3. The result of the loading and sealing processes has been investigated by fluorescence optical microscopy. **Figure 4.35** shows a typical fluorescence image where the full microwells are clearly visible in green, the colour of the chosen dye.

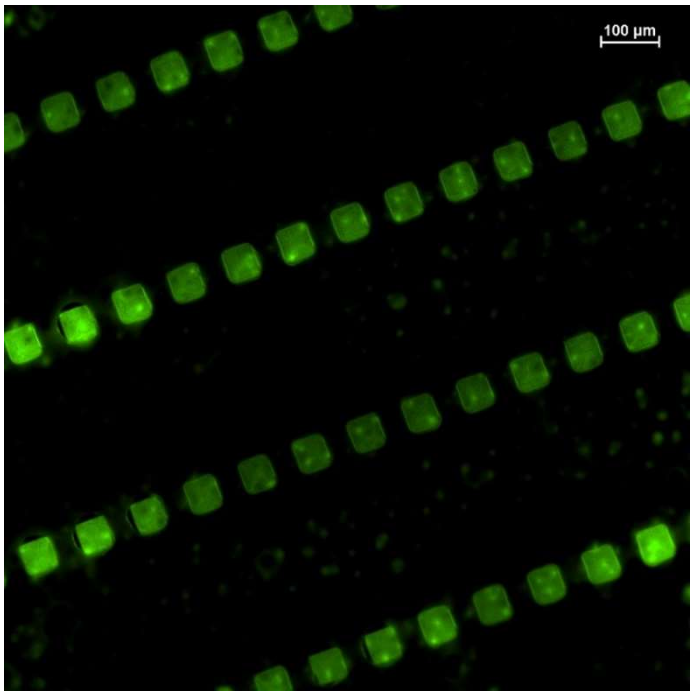


***Figure 4.35**: Fluorescence image of sealed chambers loaded with NaFluo observed with Nikon Eclipse Ni-E equipped with DS-Qi2 Camera.*

From the fluorescence image it is clear that the liquid fluorescein sodium salt is only inside the microwells as required. Therefore, we demonstrated that the developed process is ideally suitable for loading liquid drugs in the microwells array that could be then simultaneously and reliably sealed.

This represent a quite relevant accomplishment that was indispensable to be achieved for the final functionality of the device. A last but not least step to develop was hence the electrically actuated opening of the microwells that would give a reliable and controlled drug release in conditions compatible with the human body environment.

## 4.8 RELEASE ACTIVATION

The release activation represented a fundamental and at the same time critical step for achieving the final goal of our project that is the opening of the chambers triggered by an electric stimulus. To pursue this objective, we firstly deposited metallic contacts onto the substrate. As described in details in Paragraph 3.5.5, we deposited both gold and titanium contacts but with different layouts. The results of the contacts deposition are shown hereafter.

### 4.8.1 CONTACTS DEPOSITION

#### 4.8.1.1 GOLD CONTACTS DEPOSITION

In a first approach we deposited gold contacts on the sides of the microwells lines, as depicted in the layout reported in **Figure 3.20**, following different technological approaches described in more details in Paragraph 3.5.5.1. This layout was chosen on the basis of the idea of activating the release by opening chambers sealed by polyelectrolytes multilayers. In this case the electric field on the sides should induce an electrical stress on the layers formed of different charges that should lead to multilayer disintegration by electrical polarization up to the point of breaking the continuity of the film. To reduce the voltages needed and increase the internal stress into the material at a given voltage, we also studied the possibility of incorporating in between the polyelectrolytes layers particles of Prussian blue negatively charged, since the delamination of similar layers by changing the ionization of these particles was already reported in literature.[184-186]

We discuss in the following paragraphs four different gold contacts deposition strategies studied by optical microscopy, each of which presents some advantages and disadvantages.

1. Hot-embossing and evaporation through a shadow mask

In this approach, the Kapton sheet is firstly hot-embossed and then gold is deposited through a shadow mask. The result is shown in **Figure 4.36**.

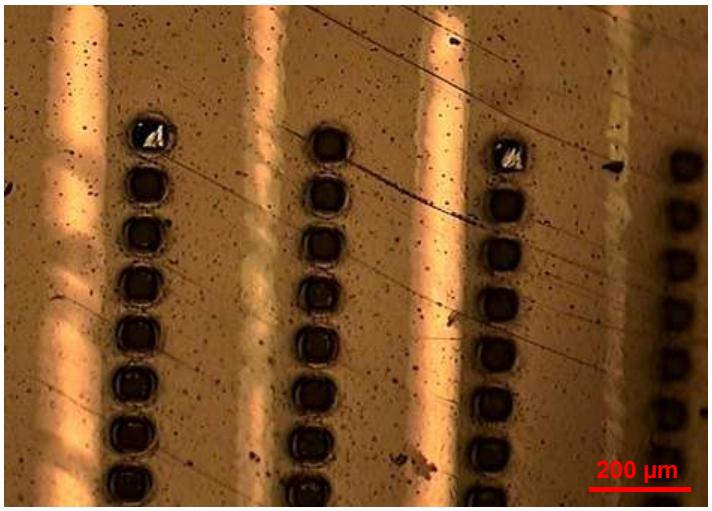


***Figure 4.36**: Optical image of gold contacts deposited through a shadow mask.*

The pros of this deposition strategy are that no photolithography is required and the process is efficient from time and cost points of view. However, this approach displays the undesired shadow effect and it requires a fine manual or mechanical alignment of the mask with the underlying microwells. As shown by the image in **Figure 4.36** we could not achieve a uniform and perfectly aligned series of contacts. This would make not fully reliable and uniform the opening of the microwells in different positions of the array.

2. Hot-embossing, evaporation, photolithography and etching

This approach involves first of all the hot-embossing of the Kapton sheet, the evaporation of gold on the whole substrate and finally photolithography and etching to obtain the final patterned contacts. A typical result is shown in **Figure 4.37**.

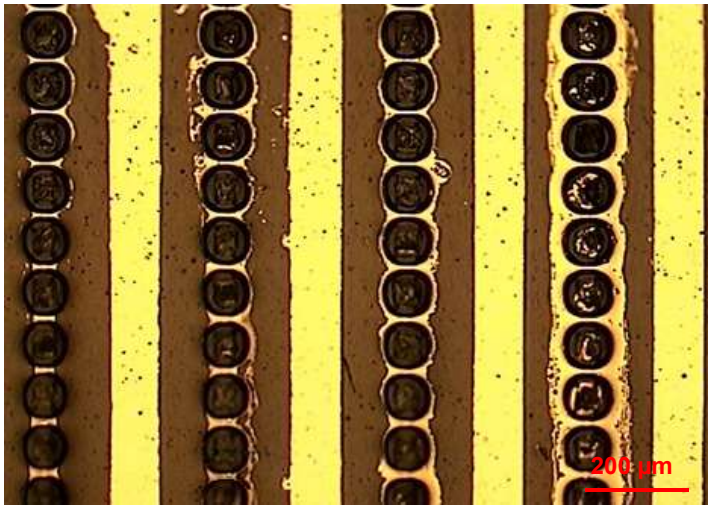


***Figure 4.37**: Optical image of gold contacts fabricated by photolithography and etching, after hot embossing and evaporation of gold.*

The advantage of using this technique is that it gives perfectly aligned and uniform contacts over the whole array but it is a quite time consuming approach and there are gold residues around the wells so that unwanted connections and cross talk between pads cannot be excluded.

3. Evaporation, hot-embossing, photolithography and etching

This contacts fabrication strategy in based on the gold evaporation on the flat Kapton sheet followed by hot-embossing. The contacts are hence obtained by photolithography and etching processes. A typical result is shown in **Figure 4.38**.

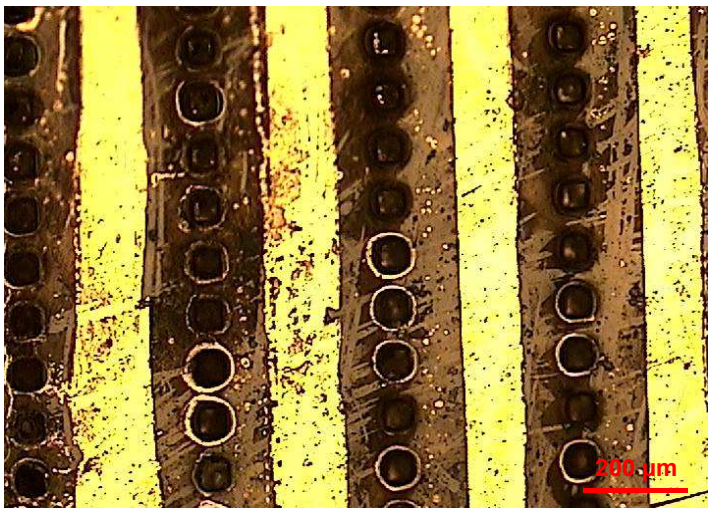


***Figure 4.38**: Optical image of gold contacts fabricated by photolithography and etching after evaporation and hot embossing processes.*

Again, the advantage of using this approach is the contacts alignment but as for the previous strategy, the cons are that it is time consuming, the presence of gold residues around the wells and the possible connection and cross talk between pads.

4. Evaporation, photolithography and etching, hot-embossing

This strategy involves first the evaporation of gold on the flat Kapton sheet followed by the gold contacts fabrication by means of photolithography and etching processes and finally the substrate engineering by hot-embossing. A typical result is shown in **Figure 4.39**.

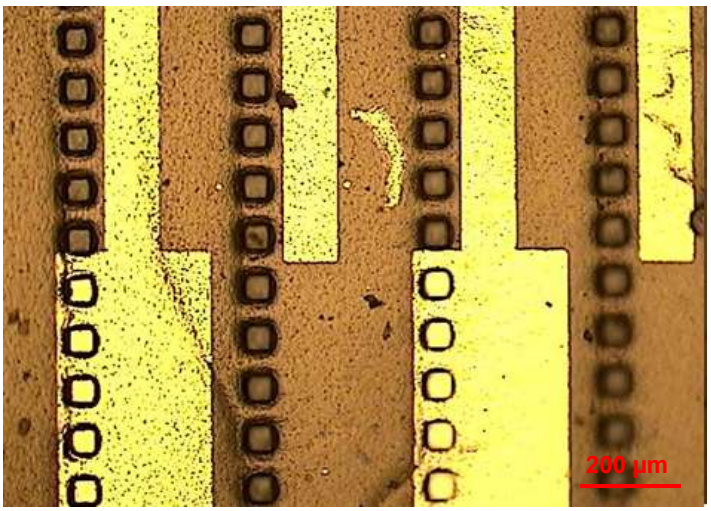


***Figure 4.39**: Optical image of gold contacts fabricated by photolithography and etching after gold evaporation and before hot-embossing.*

The main advantage of this approach is that no gold residues are detectable around the wells. However, this strategy is time consuming and the fine and critical manual or mechanical alignment of the master for proceeding with the hot-embossing makes it hard to have reliably contacts uniformly positioned over the array.

All these four technological approaches show advantages and disadvantages. As already mentioned, we began with the deposition of gold contacts between wells lines because we aimed at opening the microchambers disrupting the structure of the polymer by means of the local polarization stress induced by the electric field. Unfortunately, this activation mechanism could be pursued at reasonable voltages only on polyelectrolytes multilayers that we realized to be too much permeable to small hydrophilic compounds and hence permeable also to the type of drugs of interest for the project. Therefore since we decided to work on hydrophobic biopolymer as sealants we switched to study another release activation mechanism that is the melting of biopolymer by Joule effect induced by the current flow into the contacts by applying a reasonably low voltage. The heating within the

microwells, even though mild, would presumably produce a change of the volume of the liquid and of the vapour pressure within the microwells. Anyway the temperature range will be kept within the stability range of the drug, to avoid any side effects. All these effects would be synergic, cooperating towards the rupture of the sealing polymer over the microwell when heated by the current flow in the contacts. For this purpose, we decided to change the layout to the one described in more details in Paragraph 3.5.5.2 and furthermore we switched from gold to titanium deposition. We made this choice because titanium provides better adhesion to the substrate and a higher resistivity of the electrical lines with respect to gold and this could be useful for the electrically induced biopolymer melting.

#### 4.8.1.2 TITANIUM CONTACTS DEPOSITION

For the firsts opening tests, we deposited titanium contacts by sputtering onto the already hot-embossed substrate, followed by photolithography and etching. A typical resulting sample with titanium contacts is shown in **Figure 4.40**.

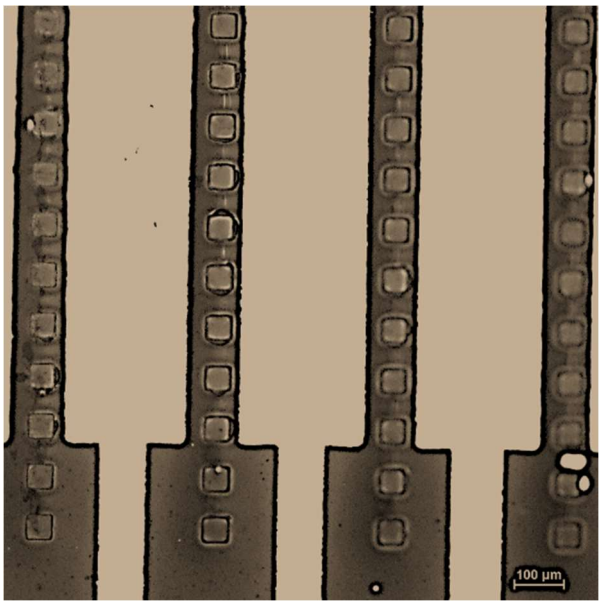


***Figure 4.40**: Optical image of Ti contacts (dark) deposited by sputtering.*

As it is clearly visible from the image, the alignment of titanium contacts with the wells lines is quite good and the contacts themselves seem homogeneous.

### 4.8.2 OPENING TESTS

Every single line can be addressed individually nonetheless for the first opening tests we worked in parallel on several lines as described in details in Paragraph 3.5.5.3 (Figure 3.27) so that we could apply the same voltage to a desired area of the sample to see a statistical response and hence the reliability of the opening simultaneously on several microwells. Furthermore we wanted to verify the presence of the cross-talking effect that could provoke the undesired opening of microchambers even though not directly biased. A picture of a sample with connected pads is reported in **Figure 4.41**.

***Figure 4.41**: Image of a sample with corto-circuited Ti contacts.*

All the opening tests were carried out on substrates sealed by the *Blanket coverage method* since it is the one selected for sealing our final device.
We first performed opening trials on a sealing cap made of 200 µl PCL 1% w/w. We applied 1V for 600s taking some images during the voltage application after 180s, 360s and 600s (see **Figure 4.42**).

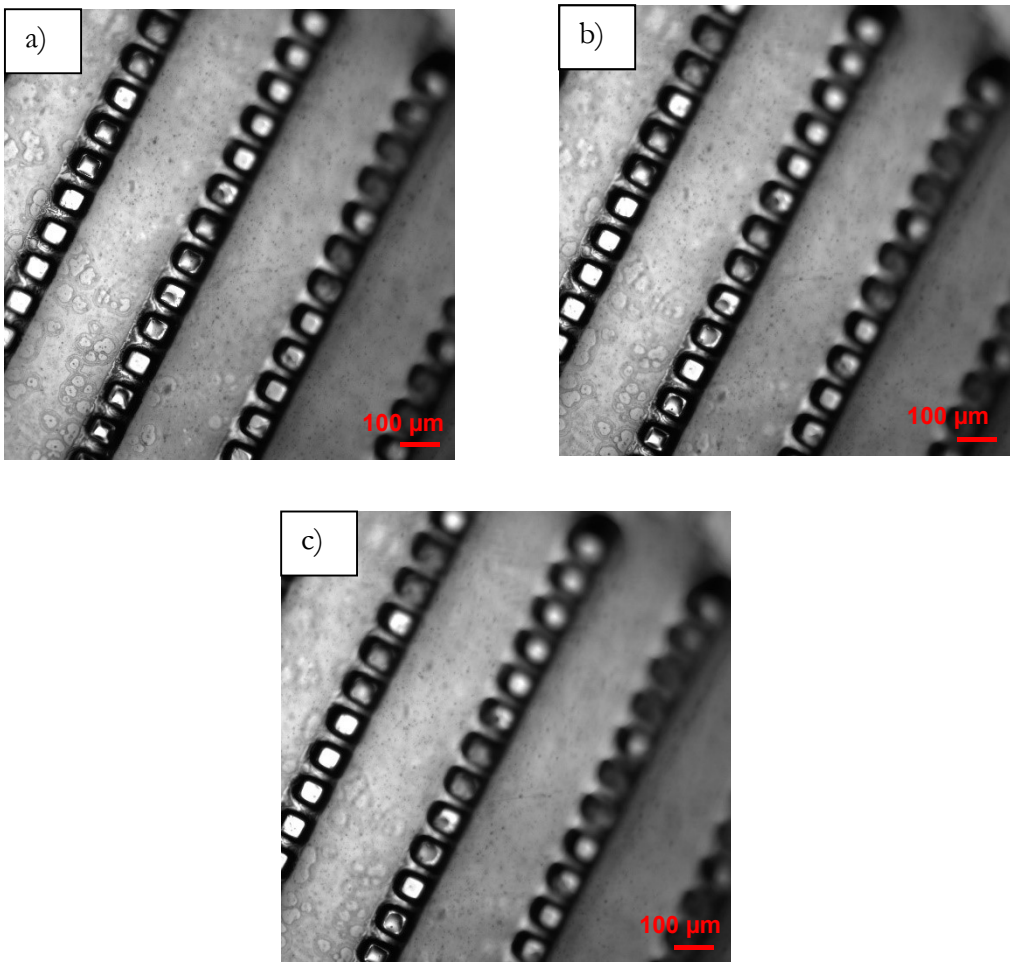


***Figure 4.42**: Optical images of a substrate sealed by 200 µl of PCL 1% w/w observed during the application of 1V. Images are taken at a) 180s, b) 360s and c) 600s.*

The optical images demonstrate that no clearly visible changes occur on the sealing film made of 200 µl of PCL 1% w/w during the application of 1V.

After that, we applied voltage from 0 to 10V in about 60 s and we took the optical image reported below in **Figure 4.43**.

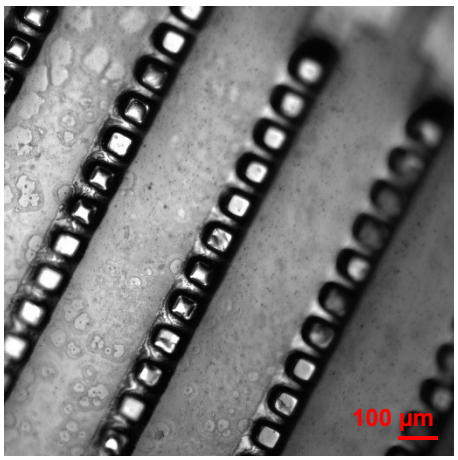


***Figure 4.43**: Optical image of a substrate sealed by 200 µl of PCL 1% w/w observed after the application of voltage from 0 to 10V in about 60 s.*

Again, no clear changes in the 200 µl PCL 1% w/w sealed film are visible.

We then focused the analysis on another area of the same sample by acquiring images after the application of 10V for 600s. The image observed just after the measurement is reported in **Figure 4.44**.

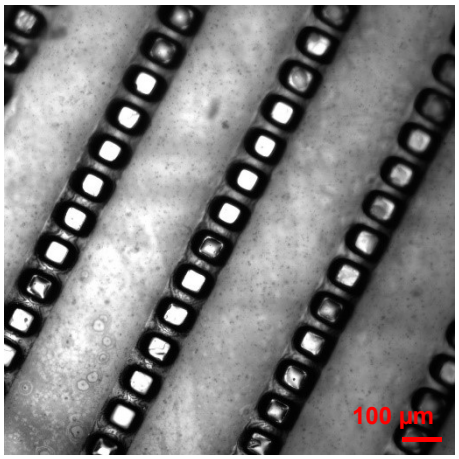


***Figure 4.44**: Optical image of a substrate sealed by 200 µl of PCL 1% w/w observed after the application of 10V for 600s.*

Since no trace of microchambers opening took place, we decided to further increase the voltage to 35V for 3 min, even though this voltage would be presumably incompatible with the operation of the final device. The idea was to observe any effect to have a starting point for optimizing the process. After this further voltage increase the sealing cap still stood intact, as demonstrated in the **Figure 4.45** shown below, indicating that the dissipated electrical power would not affect significantly the film properties.

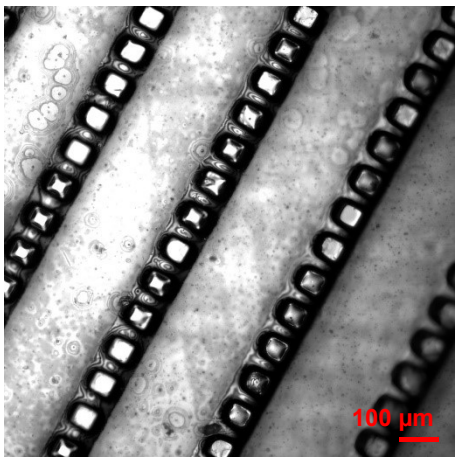


***Figure 4.45**: Optical image of a substrate sealed by 200 µl of PCL 1% w/w observed after the application of 35V for 180s.*

We ascribed the absence of film melting to the thickness of the sealing film obtained with 200 µl of PCL 1% w/w. The interplay between the power input to the layer, its thermal capacity and the dissipation of heat via the conductivity towards the outside and the other

parts of the device would not be adequate to produce the desired effect.
Hence, we prepared another sample consisting in an array of microwells covered by a much thinner film fabricated by using 50 µl of PLC 1% w/w.

We started the opening trials on a substrate sealed by 50 µl of PLC 1% w/w, applying 5V for 600s collecting images at 300s and 580s, as well as after 2, 10 and 15 min from the measurement ending time. Images showing the results are reported below in **Figure 4.46** and **Figure 4.47**.

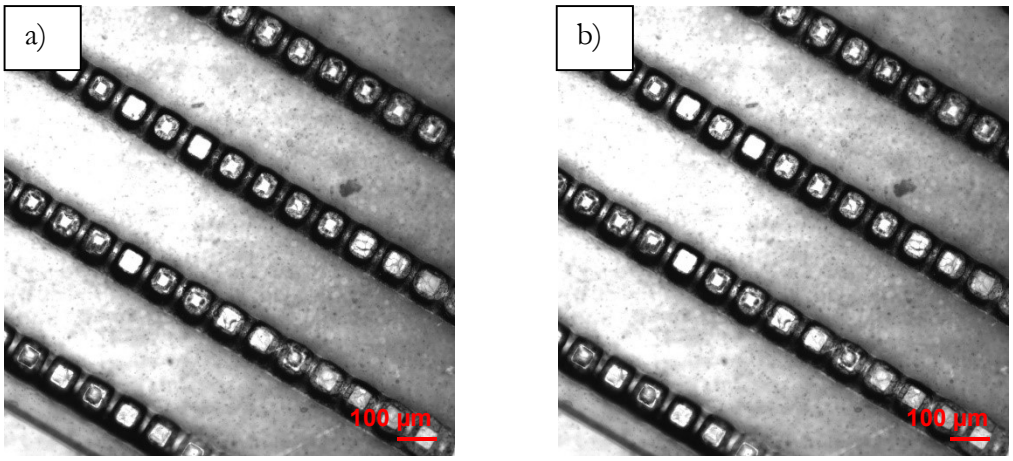


***Figure 4.46**: Optical images of a substrate sealed by 50 µl of PCL 1% w/w observed during the application of 5V. Images are taken at a) 300s and b) 580s.*

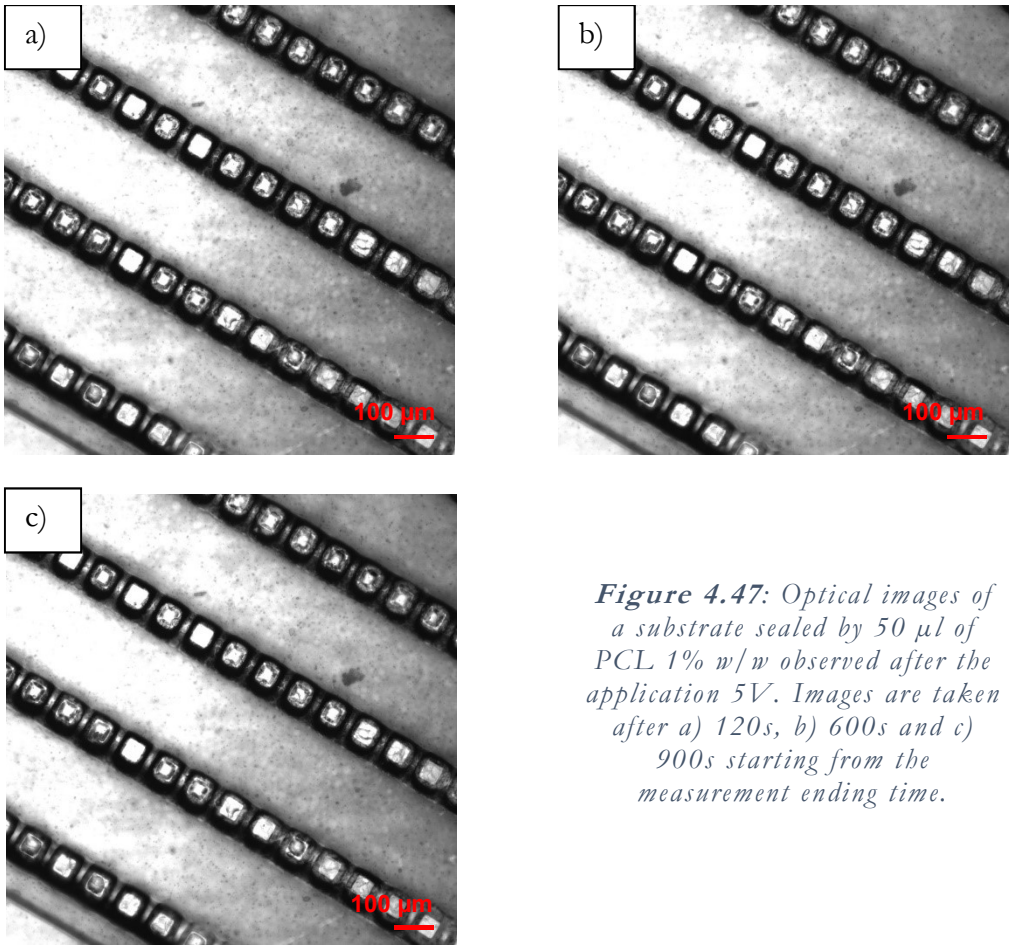


***Figure 4.47**: Optical images of a substrate sealed by 50 µl of PCL 1% w/w observed after the application 5V. Images are taken after a) 120s, b) 600s and c) 900s starting from the measurement ending time.*

No visible changes in the film structure were detected neither during voltage application (5V), nor after the measurement. Therefore, we decided to repeat the procedure by applying 15V for 600s, taking images at 300s and 580s during the measurements and after 3 and 10 min from the end of voltage application. **Figure 4.48** and **Figure 4.49** show some typical images of the results observed.

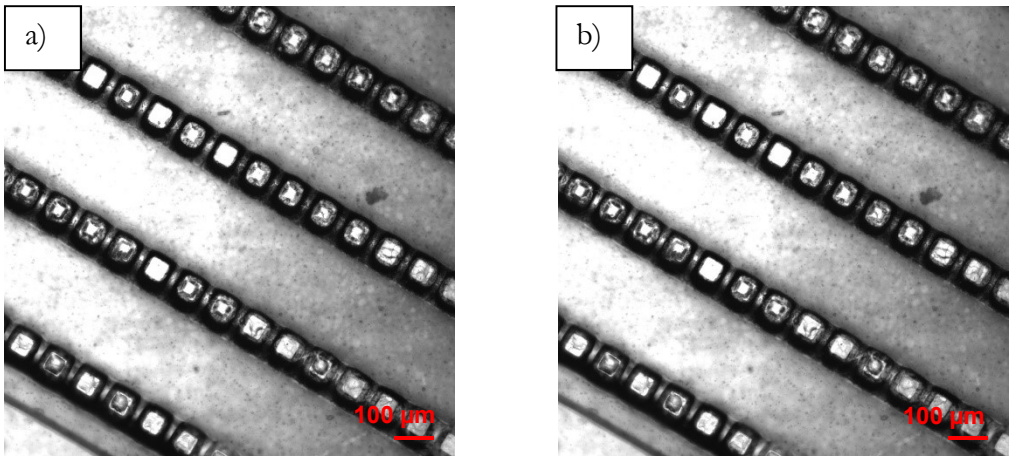


***Figure 4.48**: Optical images of a substrate sealed by 50 µl of PCL 1% w/w observed during the application of 15V. Images are taken after a) 300s and b) 580s.*

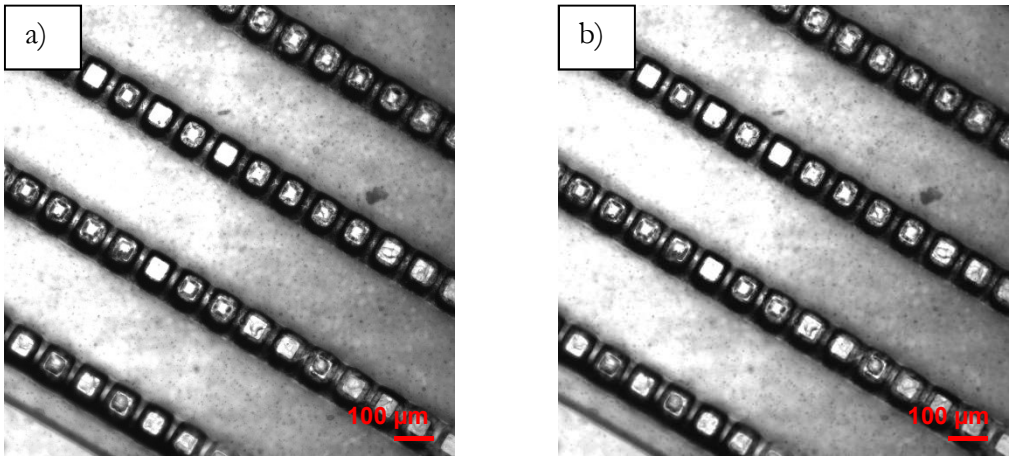


***Figure 4.49**: Optical images of a substrate sealed by 50 µl of PCL 1% w/w observed after the application of 15V. Images are taken after a) 180s and b) 600s starting from the measurement ending time.*

Again, no trace of opening appeared neither during nor after the supply of voltage (15V).

For this reason, we decided to change the protocol passing to the application of increasing step-like voltages with the aim of letting the power to be dissipated in defined and not abrupt steps, stabilizing the film heating process. In this experiment, we specifically applied the voltage from 0 to 40V with 1V as scan step and 5s as scan time. We took pictures of the film surface before, during (~ at 20V) and after the application of the voltage steps and a few selected images are reported in **Figure 4.50**.

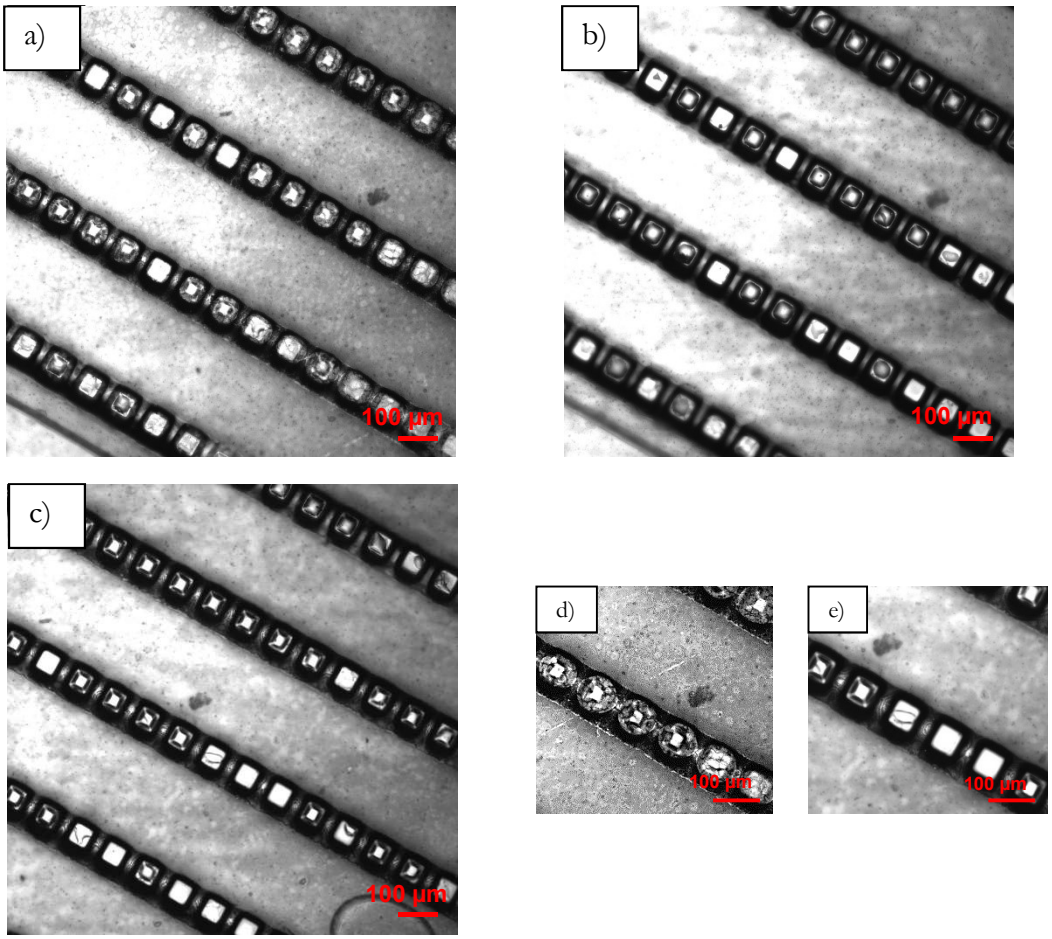


***Figure 4.50**: Optical images of a substrate sealed by 50 µl of PCL 1% w/w observed: a) and d) before; b) during (at about 20V) and c) and e) after the application voltage steps (scan from 0 to 40, scan step 1V, 5s).*

Finally, we achieved the opening of the chambers by inducing the melting of the sealing biopolymer film by Joule effect. Details of images shown in **Figure 4.50** *d)* and *e)* represent the sealed chambers before the voltage supply and the corresponding open chambers after the voltage supply, respectively. The onset opening estimated power was 270 mW corresponding to about 18V.

The microchambers opening has been confirmed by post process analysis performed by Scanning Electron Microscopy. The SEM images are reported in **Figure 4.51** below.

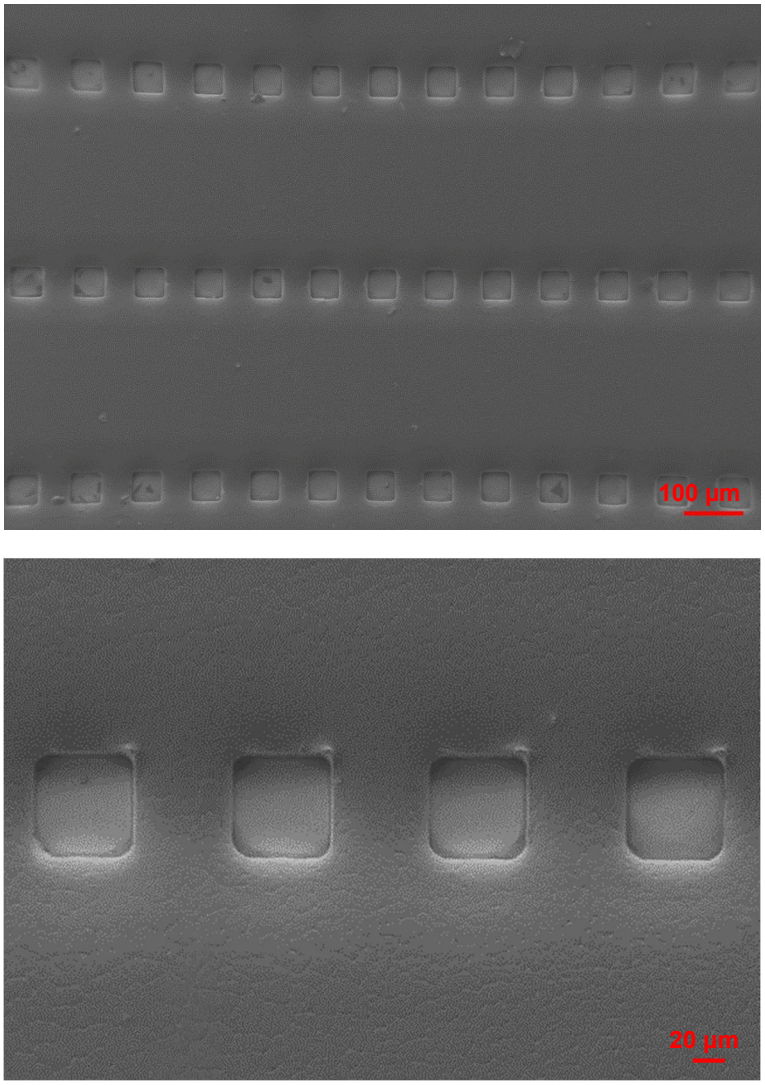


***Figure 4.51**: SEM images of opened microchambers at different magnifications, after voltage application from 0 to 40 V, scan step 1V and scan time 5s.*

As demonstrated with the SEM characterization, all the chambers are opened while the film is still visible on the flat area of the substrate. This is important for the final application since the device will be placed inside the human body. The fact that the insulating biopolymeric film is stable on the contacts means that it will prevent the direct contact of the tissues with the metallic contacts guaranteeing a safer application.

For better visualizing the differences between closed and opened chambers, two corresponding SEM images are shown in **Figure 4.52**.

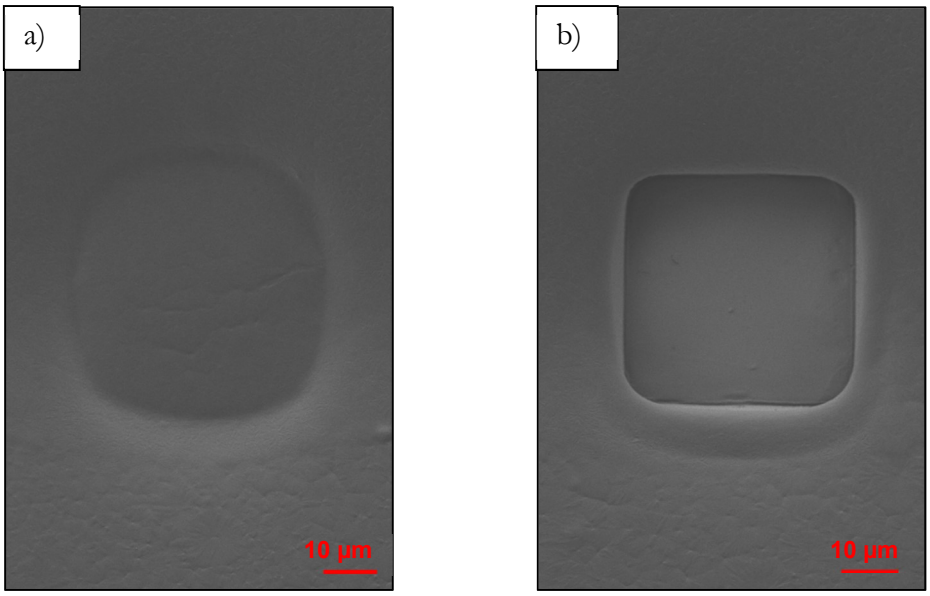


***Figure 4.52**: Comparison between SEM images of a) closed and b) opened chambers.*

In the image *a)* it is clearly visible the biopolymeric PCL film on the top of the chambers that seals it while in the image *b)* the film is no more sealing the chambers and it is possible to see the bottom of the opened microwell. It is also possible to see the melted biopolymer around the well edges, an a hillock surrounding the edge of the microwell that is not present in the sealed microwell. The opening is beautifully clean and complete.

Once we demonstrated the feasibility of the microchambers opening induced by the Joule effect by applying voltage to the system, we decided to perform further opening tests recording real time video with the optical microscope aiming at optimizing the process and possibly reduce the voltage and the power supply needed.

#### 4.8.2.1 OPENING TEST UP TO THE OPENING THRESHOLD

We performed the experiments employing again a substrate of microwells of Kapton sealed by *Blanket coverage method* with a film made of 50 µl of PCL 1% w/w and using pure water (stored at 4°C) as subphase. In the next experiment we decided to stop the voltage application at the opening threshold in order to have at the same time, closed, fully opened and partially opened chambers to better understand the opening mechanism. To this purpose, we applied voltage from 0 to 10V, with a scan step of 2V and scan time of 10 s, recording real time video during the measurement.

Some frames of the recorded real time videos are reported in **Figure 4.53**.

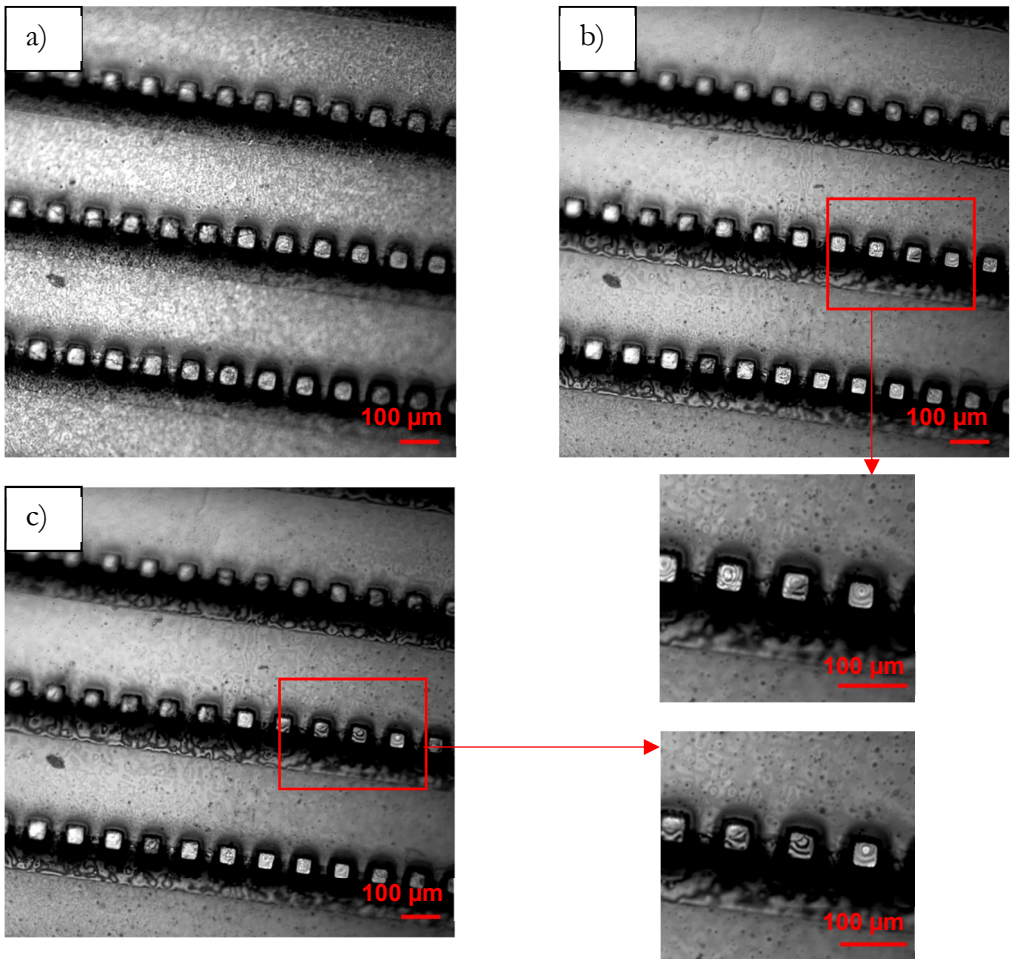


***Figure 4.53**: Frames of the real time video observed during application of voltage up to the threshold of opening (scan 0-10V, scan step 2V, scan time 10s). Frames are taken a) before and b) and c) during the measurement. Magnifications of the selected area are also reported.*

With the conditions of scan step and scan time used in this experiment, the estimated power at the opening onset at about 8V is about 45 mW.

From the single frames shown in the figure is not easy to recognize the opening of the wells. In the video instead, we could observe in real time the opening process that can be described as the sliding of a curtain that in a matter of seconds unveils the interior of the microwells. The video will be shown at the discussion meeting and will be made available. The very beautiful result is that is not the whole film covering the array of microwells but only on each single microwell that the PCL is being removed from its top by the process. This has been also demonstrated by the Scanning Electron Microscopy as it is shown in the images reported in **Figure 4.54**.

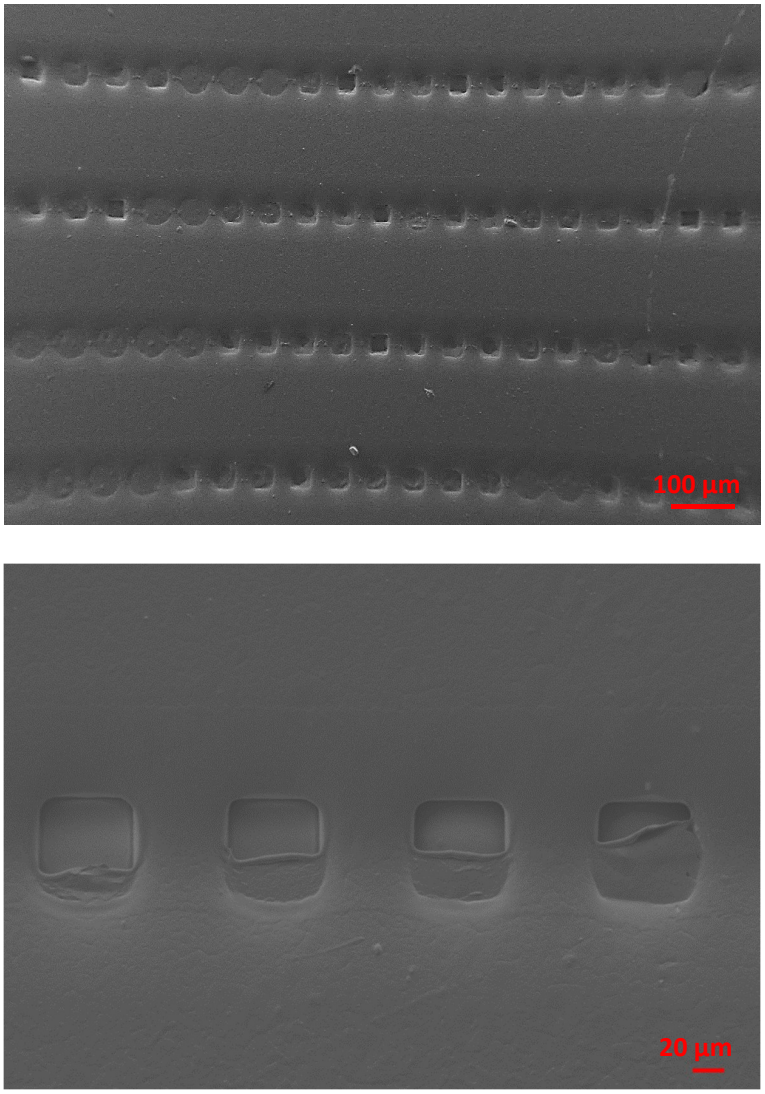


***Figure 4.54**: SEM images of substrate sealed by 50 µl of PCL 1% w/w after electric treatment up to the threshold of opening, at different magnifications.*

As already announced, this experiment gives a better understanding of the opening mechanism. As expected, by stopping the voltage supply just after the chambers begin to open we could prepare samples showing at the same time microwells closed, partially opened and fully opened. The SEM images indicate that the PCL film sealing the top of the chambers begins to break on one side of the chambers themselves and it withdraws like a "little curtain" towards the opposite side of the chambers.

Once the opening mechanism has been better understood, we performed the opening test up to the complete opening of the chambers.

#### 4.8.2.2 OPENING TEST UP TO THE COMPLETE OPENING OF THE CHAMBERS

In the following experiments on microwells patterned Kapton we kept adopting the *Blanket coverage method* with a film made of 50µl of PCL 1% w/w using pure water as subphase. We hence recorded real time video during the measurements that were carried out up to the complete opening of the chambers. The video will be made available and will be shown during the thesis discussion. In particular, we applied voltage from 0 to 25 V with scan step 1V and scan time 15s.

With the set parameters of scan step and scan time used to perform this experiment, the estimated power of the onset of opening is about 170 mW, corresponding at about 12 V. In **Figure 4.55**, SEM images of the resulting completely opened chambers are reported.

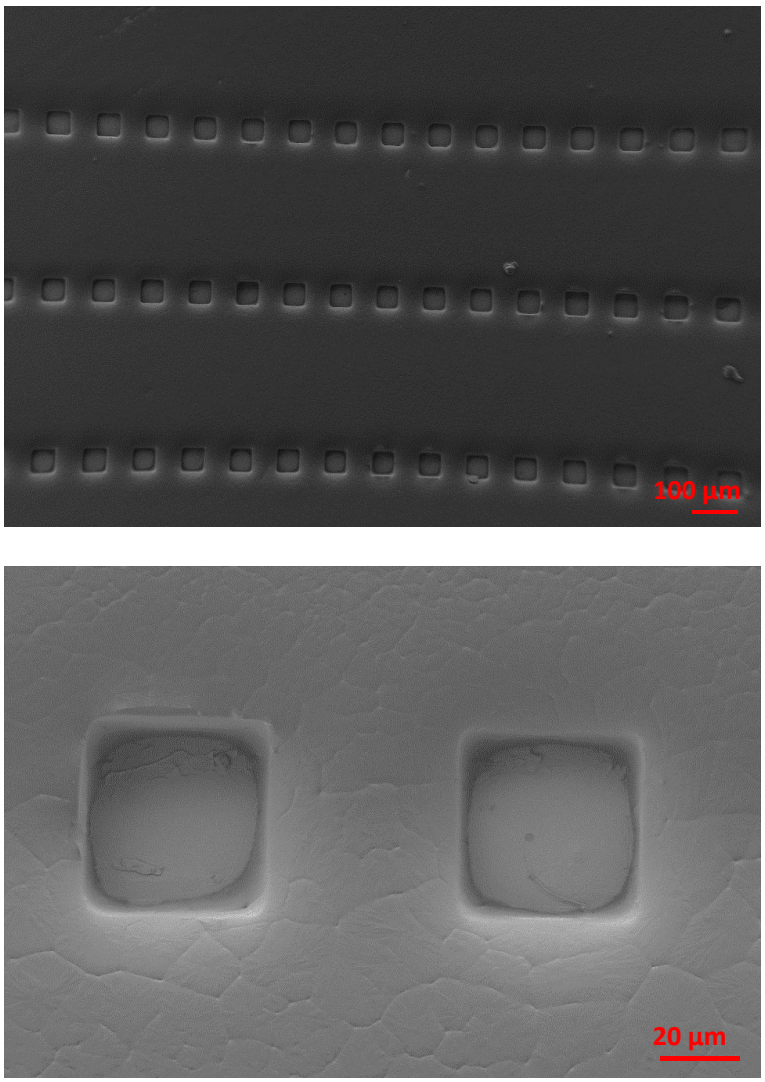


***Figure 4.55**: SEM images of substrate sealed by 50 µl of PCL 1% w/w after electric treatment up to the complete opening of the chambers, at different magnifications.*

As demonstrated by SEM characterization, all the chambers are opened.

With these opening tests, we finally demonstrated the feasibility of activating the release by application of electric stimuli that was the major aim of this PhD project. There is now a wide room for further optimization since we would like to minimize the voltage values and the power needed to open the chambers since the device will be placed inside the human body. The already achieved results make us very optimistic in a realistic large reduction of both.

All these experiments were carried out with the device facing the open air which is not the environment where they should finally work. To assess their functionality in the human body, where they should be placed and operate, we made a series of experiments starting with their immersion in liquid.

#### 4.8.2.3 OPENING TEST ON LOADED DEVICE, IN LIQUID

We performed opening tests on our device made of microwells patterned Kapton loaded with model agent and sealed by *Blanket coverage method* according to the procedure reported in details in Paragraph 3.5.4.3. The sealing film was made again of 50 μl of PCL 1% w/w and the subphase was the solution of fluorescein sodium salt 0.1 mg/ml. We performed the experiment under the optical microscope, recording real time video during the measurement. In particular, we applied a voltage ranging from 0 to 30V with a scan step of 1V and scan time 30s.

A quite interesting and favourable result is that the opening of the chambers in the liquid environment takes place at lower voltages (2-4V) and much lower power (about 4 mW) compared to the previous experiments performed in air. We believe that the reduction of required voltage and power, could be ascribed to the combination of the heating of the fluorescein solution loaded inside the chambers that generates an increase of vapour pressure promoting the opening process cooperating synergically to the heating and possibly softening of the biopolymeric sealing film itself. A movie illustrating these findings is available and will be shown during the thesis presentation.
Even though further systematic work is in progress and it is really needed to better qualify the processes involved, as well as their reliability and statistical reproducibility, these experiments fully demonstrate that we designed and tested reliable processes performing the controlled opening of the microchambers.

## 4.9 OUTLOOK

During the thesis work we also carried out *in vivo* experiments on rats as preliminary work to the final assessment of the functionality of our devices. We hence evaluated the biocompatibility of the engineered substrate (hot-embossed Kapton) in collaboration with the Kazan University (**Figure 4.56**).

***Figure 4.56**: In vivo experimentation of plain substrate on rats, performed at the Institute of Fundamental Medicine and Biology (IFMB), Kazan University, Russian Federation.*

These preliminary *in vivo* experimentations have demonstrated that no embody of the substrate itself and no inflammatory reactions occur correlated to the substrate. We have already programmed trials to evaluate the stability of the biopolymer in bio-environment and in a wound, even though it is well known that PCL shows a slow rate of degradation that is much larger than the expected resident time of the device in the wound (3-4 days).

We have also programmed the work needed to evaluate the overall toxicity and inflammatory response as well as the drug release efficacy.

# CONCLUSIONS

With the overall research work carried out with this PhD we demonstrated the feasibility of a novel type of devices that could be fruitfully used in the post-operative pain treatment by delivering locally much reduced quantities of drugs. All the main features needed for a successful application of the envisaged devices have been demonstrated including the biocompatibility, the ability of loading the drug and sealing and the mechanism of delivery actuated by electrical signals that could be eventually easily controlled remotely.

To reach these goals we studied different strategies for developing the drug containers. We firstly explored the fabrication of drug microcontainers completely made of soft polymers using both some standard technique, such as the widely investigated layer-by-layer method and the relatively new one-step dip-coating technique. With the first technique we explored and studied the deposition of both conventional and unconventional polyelectrolytes and hence we successful created multilayers films, capsules and freestanding microchambers well suited as drug containers. We realized that polyelectrolytes multilayers-based systems, even though very promising for other drug release devices, since they are permeable to small molecules they cannot be used in the specific case of pain-controlling drugs that are often relatively small molecules. We then explored several polymers among the hydrolytically biodegradable ones in order to ensure the possibility of encapsulating small hydrophilic drugs. We hence implemented successfully the one-step dip-coating technique to develop and study the fabrication of freestanding microchambers achieving the realization of reliable and well performing processes.

The other strategy we have successfully pursued to fabricate drug microcontainers has been the fabrication of the microwells on a polymeric substrate much more robust but flexible, engineered by patterning on it the microwells. The developed process could be finely tuned to fabricate a large density of microwells in a very reliable and scalable way. We hence chose this device architecture for the final device prototype that could be in this way much more robust since it will protect the drug payload and will ensure an easy handling by the surgeon, at the same time. To develop this final architecture, we engineered the polyimide substrate starting from a liquid precursor or by hot-embossing a commercially available polyimide sheet. In both cases, we got quite good and promising results; we selected the hot-

embossing process since it is safer from the biomedical point of view and would not require further studies concerning purity of the materials used. Once having engineered the substrate, we have developed different methods for loading the microwells with chemical compounds. We demonstrated that with our processes we could reliably load model agents both in form of crystals and in liquid form. This is a very important achievement since the local anaesthetic will be loaded in the currently available pharmaceutical formulations that are liquid. The next critical step was to develop processes that would guarantee the sealing of the microwells that would be compatible with all the other processes involved in the fabrication and use of the devices, including their aperture by an electrical signal to produce the drug release. We hence developed two methods with which we are able to seal chambers both if they are already loaded with crystals and if they have to be loaded with liquid solutions. For the liquid case, the loading and sealing processes take place at the same time. For the sealing film, we chose polycaprolactone among the others biodegradable polymers since it is the one with the lowest melting temperature. This parameter turned out to be responsible for the release activation mechanism that we achieved by direct electrical triggering.

In conclusion we have developed a novel class of devices that could efficiently carry out remotely controlled drug release demonstrating all the fundamental functionalities needed. A summary of the developed steps is reported in **Table 2**.

***Table 2**: Summary of the developed steps.*

| | | |
|---|---|---|
| 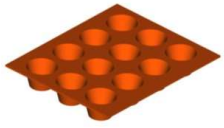 | Substrate engineering (see Par. 4.5) | • Liquid precursor<br>• Hot-embossing |
| 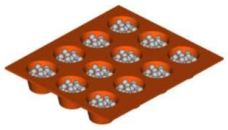 | Loading (see Par. 4.6) | Model agents in form of:<br>• Crystals<br>• Liquid |
| 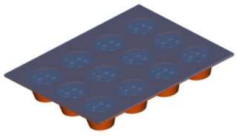 | Sealing (see Par. 4.7) | • Ring Method<br>• Blanket Coverage Method |
| 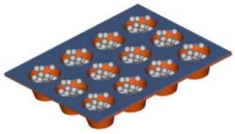 | Electrically driven release (see Par. 4.8) | • In air<br>• In liquid |

Further fundamental steps will concern the performance of the device in clinical applications starting from experiment on model animals, already used in literature for response to pain control. The efficacy of the devices should be tested by optimizing their architectures, the minimum drug load required, and their positioning within the wound. Another critical aspect subject of future work will concern the engineering of the mechanism for the device removal after the treatment aiming at minimizing any residual tissue damage. Finally the compatibility and the optimization of the device for different drugs even for other different applications will be investigated.

The activity has required frontier research on different materials and on the developing of processes and devices that were critical to the final achievements. We believe that all this research work will have a much wider impact on the development in micro-nano medicine and in particular in local drug release.

# BIBLIOGRAPHY


1. Katz, N., *The impact of pain management on quality of life.* Journal of pain and symptom management, 2002. **24**(1): p. S38-S47.
2. Kasper, D., et al., *Harrison's principles of internal medicine.* 19th ed. 2015: McGraw-Hill Education.
3. *Node of Ranvier.* https://www.britannica.com/science/node-of-Ranvier#/media/1/417103/66781, 2012.
4. Purves, D., et al., *Neuroscience, 2008.* De Boeck, Sinauer, Sunderland, Mass, 2014.
5. Tracey, I. and P.W. Mantyh, *The cerebral signature for pain perception and its modulation.* Neuron, 2007. **55**(3): p. 377-391.
6. Garland, E.L., *Pain processing in the human nervous system: a selective review of nociceptive and biobehavioral pathways.* Primary Care: Clinics in Office Practice, 2012. **39**(3): p. 561-571.
7. Bonnet, F. and E. Marret, *Postoperative pain management and outcome after surgery.* Best Practice & Research Clinical Anaesthesiology, 2007. **21**(1): p. 99-107.
8. Rawal, N., *Organization, function, and implementation of acute pain service.* Anesthesiology Clinics, 2005. **23**(1): p. 211-225.
9. Málek, J., P. Ševčík, and D. Bejšovec, *Postoperative pain management.* Mlada fronta: Prague, 2017.
10. Mercadante, S., *La gestione del dolore postoperatorio. Linee guida di trattamento. Con CD-ROM.* 2007: Elsevier srl.
11. Younger, J.W., et al., *Prescription opioid analgesics rapidly change the human brain.* PAIN®, 2011. **152**(8): p. 1803-1810.
12. Allegri, M., et al., *Continuous wound infusion with chloroprocaine in a pig model of surgical lesion: drug absorption and effects on inflammatory response.* Journal of pain research, 2017. **10**: p. 2515.
13. Lavand'homme, P., *From preemptive to preventive analgesia: time to reconsider the role of perioperative peripheral nerve blocks?* Regional anesthesia and pain medicine, 2011. **36**(1): p. 4-6.
14. Lavand'homme, P., *Improving postoperative pain management: continuous wound infusion and postoperative pain.* European Journal of Pain Supplements, 2011. **5**(2): p. 357-363.
15. Gupta, A., et al., *A meta - analysis of the efficacy of wound catheters for post - operative pain management.* Acta Anaesthesiologica Scandinavica, 2011. **55**(7): p. 785-796.
16. Ariga, K., et al., *Layer-by-layer self-assembled shells for drug delivery.* Advanced drug delivery reviews, 2011. **63**(9): p. 762-771.
17. Kiryukhin, M.V., et al., *Individually Addressable Patterned Multilayer Microchambers for Site - Specific Release - On - Demand.* Macromolecular rapid communications, 2013. **34**(1): p. 87-93.
18. Zafar Razzacki, S., *Integrated microsystems for controlled drug delivery.* Advanced Drug Delivery Reviews, 2004. **56**(2): p. 185-198.
19. Slowing, II, et al., *Mesoporous silica nanoparticles as controlled release drug delivery and gene transfection carriers.* Adv Drug Deliv Rev, 2008. **60**(11): p. 1278-88.
20. Webster, J., *Goodman and Gilman's the pharmacological basis of therapeutics.* British Medical Journal, 1992. **305**(6844): p. 65-66.

21. Pastorino, L., S. Erokhina, and V. Erokhin, *Smart nanoengineered polymeric capsules as ideal pharmaceutical carriers.* Current Organic Chemistry, 2013. **17**(1): p. 58-64.
22. Siemann, D.W., *The unique characteristics of tumor vasculature and preclinical evidence for its selective disruption by tumor-vascular disrupting agents.* Cancer treatment reviews, 2011. **37**(1): p. 63-74.
23. Kalyane, D., et al., *Employment of enhanced permeability and retention effect (EPR): Nanoparticle-based precision tools for targeting of therapeutic and diagnostic agent in cancer.* Materials Science and Engineering: C, 2019.
24. Maier-Hauff, K., et al., *Efficacy and safety of intratumoral thermotherapy using magnetic iron-oxide nanoparticles combined with external beam radiotherapy on patients with recurrent glioblastoma multiforme.* Journal of neuro-oncology, 2011. **103**(2): p. 317-324.
25. Bazile, D., et al., *Stealth Me. PEG - PLA nanoparticles avoid uptake by the mononuclear phagocytes system.* Journal of pharmaceutical sciences, 1995. **84**(4): p. 493-498.
26. Suk, J.S., et al., *PEGylation as a strategy for improving nanoparticle-based drug and gene delivery.* Advanced drug delivery reviews, 2016. **99**: p. 28-51.
27. Razzacki, S.Z., et al., *Integrated microsystems for controlled drug delivery.* Advanced drug delivery reviews, 2004. **56**(2): p. 185-198.
28. Hossen, S., et al., *Smart nanocarrier-based drug delivery systems for cancer therapy and toxicity studies: A review.* Journal of advanced research, 2019. **15**: p. 1-18.
29. Donath, E., et al., *Novel hollow polymer shells by colloid - templated assembly of polyelectrolytes.* Angewandte Chemie International Edition, 1998. **37**(16): p. 2201-2205.
30. Donath, E., et al., *Hollow polymer shells from biological templates: fabrication and potential applications.* Chemistry–A European Journal, 2002. **8**(23): p. 5481-5485.
31. Lasic, D.D., *Liposomes: from physics to applications.* 1993: Elsevier Science Ltd.
32. Zhao, Q. and B. Li, *pH-controlled drug loading and release from biodegradable microcapsules.* Nanomedicine: Nanotechnology, Biology and Medicine, 2008. **4**(4): p. 302-310.
33. Iler, R., *Multilayers of colloidal particles.* Journal of colloid and interface science, 1966. **21**(6): p. 569-594.
34. Decher, G. and J.D. Hong. *Buildup of ultrathin multilayer films by a self - assembly process, 1 consecutive adsorption of anionic and cationic bipolar amphiphiles on charged surfaces.* in *Makromolekulare Chemie. Macromolecular Symposia.* 1991. Wiley Online Library.
35. Decher, G. and J.D. Hong, *Buildup of ultrathin multilayer films by a self - assembly process: II. Consecutive adsorption of anionic and cationic bipolar amphiphiles and polyelectrolytes on charged surfaces.* Berichte der Bunsengesellschaft für physikalische Chemie, 1991. **95**(11): p. 1430-1434.
36. Decher, G., J. Hong, and J. Schmitt, *Buildup of ultrathin multilayer films by a self-assembly process: III. Consecutively alternating adsorption of anionic and cationic polyelectrolytes on charged surfaces.* Thin solid films, 1992. **210**: p. 831-835.
37. Blodgett, K.B., *Monomolecular films of fatty acids on glass.* Journal of the American Chemical Society, 1934. **56**(2): p. 495-495.
38. Blodgett, K.B. and I. Langmuir, *Built-up films of barium stearate and their optical properties.* Physical Review, 1937. **51**(11): p. 964.
39. Lee, H., et al., *Adsorption of ordered zirconium phosphonate multilayer films on silicon and gold surfaces.* The Journal of Physical Chemistry, 1988. **92**(9): p. 2597-2601.
40. Decher, G., *Fuzzy nanoassemblies: toward layered polymeric multicomposites.* science, 1997. **277**(5330): p. 1232-1237.

41. Portnov, S., et al., *An automated setup for production of nanodimensional coatings by the polyelectrolyte self-assembly method.* Instruments and experimental techniques, 2006. **49**(6): p. 849-854.
42. Serizawa, T., M. Yamaguchi, and M. Akashi, *Time - controlled desorption of ultrathin polymer films triggered by enzymatic degradation.* Angewandte Chemie International Edition, 2003. **42**(10): p. 1115-1118.
43. Zhou, L., et al., *Toxicity Screening by electrochemical detection of DNA damage by metabolites generated in situ in ultrathin DNA− enzyme films.* Journal of the American Chemical Society, 2003. **125**(5): p. 1431-1436.
44. Rusling, J.F., et al., *Biochemical applications of ultrathin films of enzymes, polyions and DNA.* Chemical Communications, 2008(2): p. 141-154.
45. Srivastava, S. and N.A. Kotov, *Composite layer-by-layer (LBL) assembly with inorganic nanoparticles and nanowires.* Accounts of chemical research, 2008. **41**(12): p. 1831-1841.
46. Neto, A.I., et al., *Nanostructured polymeric coatings based on chitosan and dopamine - modified hyaluronic acid for biomedical applications.* Small, 2014. **10**(12): p. 2459-2469.
47. De Villiers, M.M., et al., *Introduction to nanocoatings produced by layer-by-layer (LbL) self-assembly.* Advanced drug delivery reviews, 2011. **63**(9): p. 701-715.
48. Johnston, A.P., E.S. Read, and F. Caruso, *DNA multilayer films on planar and colloidal supports: sequential assembly of like-charged polyelectrolytes.* Nano letters, 2005. **5**(5): p. 953-956.
49. Cai, K., et al., *Polysaccharide-protein surface modification of titanium via a layer-by-layer technique: characterization and cell behaviour aspects.* Biomaterials, 2005. **26**(30): p. 5960-5971.
50. Sukhorukov, G.B., et al., *Layer-by-layer self assembly of polyelectrolytes on colloidal particles.* Colloids and Surfaces A: physicochemical and engineering aspects, 1998. **137**(1-3): p. 253-266.
51. Elsner, N., F. Dubreuil, and A. Fery, *Tuning of microcapsule adhesion by varying the capsule-wall thickness.* Physical Review E, 2004. **69**(3): p. 031802.
52. Déjugnat, C. and G.B. Sukhorukov, *pH-responsive properties of hollow polyelectrolyte microcapsules templated on various cores.* Langmuir, 2004. **20**(17): p. 7265-7269.
53. Shenoy, D.B., et al., *Layer-by-layer engineering of biocompatible, decomposable core− shell structures.* Biomacromolecules, 2003. **4**(2): p. 265-272.
54. Volodkin, D.V., et al., *Matrix polyelectrolyte microcapsules: new system for macromolecule encapsulation.* Langmuir, 2004. **20**(8): p. 3398-3406.
55. Petrov, A.I., D.V. Volodkin, and G.B. Sukhorukov, *Protein—calcium carbonate coprecipitation: a tool for protein encapsulation.* Biotechnology progress, 2005. **21**(3): p. 918-925.
56. Itoh, Y., et al., *Preparation of biodegradable hollow nanocapsules by silica template method.* Chemistry letters, 2004. **33**(12): p. 1552-1553.
57. Adalsteinsson, T., W.-F. Dong, and M. Schönhoff, *Diffusion of 77 000 g/mol dextran in submicron polyelectrolyte capsule dispersions measured using PFG-NMR.* The Journal of Physical Chemistry B, 2004. **108**(52): p. 20056-20063.
58. Schneider, G. and G. Decher, *From functional core/shell nanoparticles prepared via layer-by-layer deposition to empty nanospheres.* Nano Letters, 2004. **4**(10): p. 1833-1839.
59. De Villiers, M.M. and Y.M. Lvov, *Nanoshells for drug delivery.* Nanotechnologies for the Life Sciences: Online, 2007.
60. Neu, B., et al., *Biological cells as templates for hollow microcapsules.* Journal of microencapsulation, 2001. **18**(3): p. 385-395.

61. Moya, S., et al., *Polyelectrolyte multilayer capsules templated on biological cells: core oxidation influences layer chemistry.* Colloids and Surfaces A: Physicochemical and Engineering Aspects, 2001. **183**: p. 27-40.
62. Delcea, M., H. Möhwald, and A.G. Skirtach, *Stimuli-responsive LbL capsules and nanoshells for drug delivery.* Advanced drug delivery reviews, 2011. **63**(9): p. 730-747.
63. Radtchenko, I.L., et al., *Assembly of alternated multivalent ion/polyelectrolyte layers on colloidal particles. Stability of the multilayers and encapsulation of macromolecules into polyelectrolyte capsules.* Journal of Colloid and Interface Science, 2000. **230**(2): p. 272-280.
64. Voigt, A., et al., *Membrane filtration for microencapsulation and microcapsules fabrication by layer-by-layer polyelectrolyte adsorption.* Industrial & engineering chemistry research, 1999. **38**(10): p. 4037-4043.
65. Gao, C., et al., *The decomposition process of melamine formaldehyde cores: the key step in the fabrication of ultrathin polyelectrolyte multilayer capsules.* Macromolecular Materials and Engineering, 2001. **286**(6): p. 355-361.
66. Antipov, A.A., et al., *Polyelectrolyte multilayer capsule permeability control.* Colloids and Surfaces A: Physicochemical and Engineering Aspects, 2002. **198**: p. 535-541.
67. Antipina, M.N., et al., *Micropackaging via layer-by-layer assembly: microcapsules and microchamber arrays.* International materials reviews, 2014. **59**(4): p. 224-244.
68. Skirtach, A.G., A.M. Yashchenok, and H. Moehwald, *Encapsulation, release and applications of LbL polyelectrolyte multilayer capsules.* Chemical Communications, 2011. **47**(48): p. 12736-12746.
69. Antipov, A.A., G.B. Sukhorukov, and H. Möhwald, *Influence of the ionic strength on the polyelectrolyte multilayers' permeability.* Langmuir, 2003. **19**(6): p. 2444-2448.
70. Gao, C., H. Möhwald, and J.C. Shen, *Enhanced biomacromolecule encapsulation by swelling and shrinking procedures.* ChemPhysChem, 2004. **5**(1): p. 116-120.
71. Lvov, Y., et al., *Urease encapsulation in nanoorganized microshells.* Nano Letters, 2001. **1**(3): p. 125-128.
72. Steitz, R., et al., *Temperature-induced changes in polyelectrolyte films at the solid–liquid interface.* Applied Physics A, 2002. **74**(1): p. s519-s521.
73. Ahrens, H., et al. *Poly (styrene sulfonate) self - organization: electrostatic and secondary interactions.* in *Macromolecular Symposia.* 2004. Wiley Online Library.
74. Ibarz, G., et al., *Controlled permeability of polyelectrolyte capsules via defined annealing.* Chemistry of Materials, 2002. **14**(10): p. 4059-4062.
75. Déjugnat, C., et al., *Membrane densification of heated polyelectrolyte multilayer capsules characterized by soft X - ray microscopy.* Advanced Materials, 2007. **19**(10): p. 1331-1336.
76. Shchukin, D.G., D.A. Gorin, and H. Möhwald, *Ultrasonically induced opening of polyelectrolyte microcontainers.* Langmuir, 2006. **22**(17): p. 7400-7404.
77. Skirtach, A.G., et al., *Ultrasound stimulated release and catalysis using polyelectrolyte multilayer capsules.* Journal of materials chemistry, 2007. **17**(11): p. 1050-1054.
78. Lu, Z., et al., *Magnetic switch of permeability for polyelectrolyte microcapsules embedded with Co@ Au nanoparticles.* Langmuir, 2005. **21**(5): p. 2042-2050.
79. Skirtach, A.G., et al., *Remote activation of capsules containing Ag nanoparticles and IR dye by laser light.* Langmuir, 2004. **20**(17): p. 6988-6992.
80. Radt, B., T.A. Smith, and F. Caruso, *Optically addressable nanostructured capsules.* Advanced Materials, 2004. **16**(23 - 24): p. 2184-2189.
81. Skirtach, A.G., et al., *Reversibly permeable nanomembranes of polymeric microcapsules.* Journal of the American Chemical Society, 2008. **130**(35): p. 11572-11573.

82. Bédard, M., A.G. Skirtach, and G.B. Sukhorukov, *Optically driven encapsulation using novel polymeric hollow shells containing an azobenzene polymer.* Macromolecular rapid communications, 2007. **28**(15): p. 1517-1521.
83. Erokhina, S., et al., *Light-driven release from polymeric microcapsules functionalized with bacteriorhodopsin.* Journal of the American Chemical Society, 2009. **131**(28): p. 9800-9804.
84. De Geest, B.G., et al., *Intracellularly degradable polyelectrolyte microcapsules.* Advanced materials, 2006. **18**(8): p. 1005-1009.
85. Kamphuis, M.M., et al., *Targeting of cancer cells using click-functionalized polymer capsules.* Journal of the American Chemical Society, 2010. **132**(45): p. 15881-15883.
86. Pastorino, L., F.C. Soumetz, and C. Ruggiero. *Nanofunctionalisation for the treatment of peripheral nervous system injuries.* in *IEE Proceedings-Nanobiotechnology*. 2006. IET.
87. Grayson, A.C.R., et al., *Electronic MEMS for triggered delivery.* Advanced drug delivery reviews, 2004. **56**(2): p. 173-184.
88. Santini Jr, J.T., M.J. Cima, and R. Langer, *A controlled-release microchip.* Nature, 1999. **397**(6717): p. 335.
89. Stuart, M.A.C., et al., *Emerging applications of stimuli-responsive polymer materials.* Nature materials, 2010. **9**(2): p. 101.
90. Slowing, I.I., et al., *Mesoporous silica nanoparticles as controlled release drug delivery and gene transfection carriers.* Advanced drug delivery reviews, 2008. **60**(11): p. 1278-1288.
91. Ricci, V., et al., *Hyaluronated mesoporous silica nanoparticles for active targeting: influence of conjugation method and hyaluronic acid molecular weight on the nanovector properties.* Journal of colloid and interface science, 2018. **516**: p. 484-497.
92. Hamidi, M., A. Azadi, and P. Rafiei, *Hydrogel nanoparticles in drug delivery.* Advanced drug delivery reviews, 2008. **60**(15): p. 1638-1649.
93. Colilla, M., M. Manzano, and M. Vallet-Regí, *Recent advances in ceramic implants as drug delivery systems for biomedical applications.* International journal of nanomedicine, 2008. **3**(4): p. 403.
94. Mamedov, A.A. and N.A. Kotov, *Free-standing layer-by-layer assembled films of magnetite nanoparticles.* Langmuir, 2000. **16**(13): p. 5530-5533.
95. Jiang, C., S. Markutsya, and V.V. Tsukruk, *Compliant, robust, and truly nanoscale free - standing multilayer films fabricated using spin - assisted layer - by - layer assembly.* Advanced Materials, 2004. **16**(2): p. 157-161.
96. Nolte, M., et al., *Filled microcavity arrays produced by polyelectrolyte multilayer membrane transfer.* Advanced Materials, 2005. **17**(13): p. 1665-1669.
97. Nolte, M. and A. Fery. *Freestanding polyelectrolyte multilayers as functional and construction elements.* in *IEE Proceedings-Nanobiotechnology*. 2006. IET.
98. Kiryukhin, M.V., et al., *Fabrication and mechanical properties of microchambers made of polyelectrolyte multilayers.* Soft Matter, 2011. **7**(14): p. 6550-6556.
99. Kiryukhin, M.V., et al., *Peculiarities of polyelectrolyte multilayer assembly on patterned surfaces.* Langmuir, 2011. **27**(13): p. 8430-8436.
100. Jackman, R.J., et al., *Fabricating large arrays of microwells with arbitrary dimensions and filling them using discontinuous dewetting.* Analytical chemistry, 1998. **70**(11): p. 2280-2287.
101. Yin, Y. and Y. Xia, *Self - assembly of monodispersed spherical colloids into complex aggregates with well - defined sizes, shapes, and structures.* Advanced Materials, 2001. **13**(4): p. 267-271.
102. Kiryukhin, M.V., et al., *Adhesion of polyelectrolyte multilayers: Sealing and transfer of microchamber arrays.* Langmuir, 2012. **28**(13): p. 5678-5686.

103. Ariga, K., J.P. Hill, and Q. Ji, *Biomaterials and biofunctionality in layered macromolecular assemblies.* Macromolecular bioscience, 2008. **8**(11): p. 981-990.
104. De Cock, L.J., et al., *Polymeric multilayer capsules in drug delivery.* Angewandte Chemie International Edition, 2010. **49**(39): p. 6954-6973.
105. Moya, S., et al., *Microencapsulation of organic solvents in polyelectrolyte multilayer micrometer-sized shells.* Journal of colloid and interface science, 1999. **216**(2): p. 297-302.
106. Gai, M., et al., *Polylactic acid nano-and microchamber arrays for encapsulation of small hydrophilic molecules featuring drug release via high intensity focused ultrasound.* Nanoscale, 2017. **9**(21): p. 7063-7070.
107. Gao, H., et al., *In situ synthesis of fluorescent carbon dots/polyelectrolyte nanocomposite microcapsules with reduced permeability and ultrasound sensitivity.* ACS nano, 2016. **10**(10): p. 9608-9615.
108. P Pawar, R., et al., *Biomedical applications of poly (lactic acid).* Recent patents on regenerative medicine, 2014. **4**(1): p. 40-51.
109. Jamshidian, M., et al., *Poly - Lactic Acid: production, applications, nanocomposites, and release studies.* Comprehensive reviews in food science and food safety, 2010. **9**(5): p. 552-571.
110. Hamad, K., et al., *Properties and medical applications of polylactic acid: A review.* Express Polymer Letters, 2015. **9**(5).
111. Rancan, F., et al., *Investigation of polylactic acid (PLA) nanoparticles as drug delivery systems for local dermatotherapy.* Pharmaceutical research, 2009. **26**(8): p. 2027-2036.
112. Sukhorukov, G.B., et al., *Physical chemistry of encapsulation and release.* Physical Chemistry Chemical Physics, 2004. **6**(16): p. 4078-4089.
113. Li, W., et al., *Polyelectrolyte multilayer microchamber-arrays for in-situ cargo release: Low frequency vs. medical frequency range ultrasound.* Colloids and Surfaces A: Physicochemical and Engineering Aspects, 2018. **547**: p. 19-27.
114. Gai, M., et al., *Polylactic acid sealed polyelectrolyte complex microcontainers for controlled encapsulation and NIR-Laser based release of cargo.* Colloids and Surfaces B: Biointerfaces, 2019. **173**: p. 521-528.
115. Zykova, Y., et al., *Free-standing microchamber arrays as a biodegradable drug depot system for implant coatings.* European Polymer Journal, 2019. **114**: p. 72-80.
116. Kopach, O., et al., *Polymer microchamber arrays for geometry-controlled drug release: a functional study in human cells of neuronal phenotype.* Biomaterials science, 2019. **7**(6): p. 2358-2371.
117. Husseini, G.A., W.G. Pitt, and A.M. Martins, *Ultrasonically triggered drug delivery: breaking the barrier.* Colloids and Surfaces B: Biointerfaces, 2014. **123**: p. 364-386.
118. Schroeder, A., J. Kost, and Y. Barenholz, *Ultrasound, liposomes, and drug delivery: principles for using ultrasound to control the release of drugs from liposomes.* Chemistry and physics of lipids, 2009. **162**(1-2): p. 1-16.
119. Repacholi, M.H., M. Gandolfo, and A. Rindi, *Ultrasound: medical applications, biological effects, and hazard potential.* 2012: Springer Science & Business Media.
120. Boissenot, T., et al., *Ultrasound-triggered drug delivery for cancer treatment using drug delivery systems: from theoretical considerations to practical applications.* Journal of Controlled Release, 2016. **241**: p. 144-163.
121. Sindeeva, O.A., et al., *Effect of a Controlled Release of Epinephrine Hydrochloride from PLGA Microchamber Array: In Vivo Studies.* ACS applied materials & interfaces, 2018. **10**(44): p. 37855-37864.

122. Makadia, H.K. and S.J. Siegel, *Poly lactic-co-glycolic acid (PLGA) as biodegradable controlled drug delivery carrier.* Polymers, 2011. **3**(3): p. 1377-1397.
123. Houchin, M. and E. Topp, *Physical properties of PLGA films during polymer degradation.* Journal of applied polymer science, 2009. **114**(5): p. 2848-2854.
124. Williams, D.F., *On the nature of biomaterials.* Biomaterials, 2009. **30**(30): p. 5897-5909.
125. Ulery, B.D., L.S. Nair, and C.T. Laurencin, *Biomedical applications of biodegradable polymers.* Journal of polymer science Part B: polymer physics, 2011. **49**(12): p. 832-864.
126. Lloyd, A.W., *Interfacial bioengineering to enhance surface biocompatibility.* Medical device technology, 2002. **13**(1): p. 18-21.
127. Ceonzo, K., et al., *Polyglycolic acid-induced inflammation: role of hydrolysis and resulting complement activation.* Tissue engineering, 2006. **12**(2): p. 301-308.
128. Otto, J., et al., *Large-pore PDS mesh compared to small-pore PG mesh.* Journal of Investigative Surgery, 2010. **23**(4): p. 190-196.
129. Suuronen, R., et al., *A 5-year in vitro and in vivo study of the biodegradation of polylactide plates.* Journal of Oral and Maxillofacial Surgery, 1998. **56**(5): p. 604-614.
130. Tang, L., et al., *Preparation, antibacterial properties and biocompatibility studies on vancomycin-poly (D, L)-lactic loaded plates.* International orthopaedics, 2010. **34**(5): p. 755-759.
131. Middleton, J.C. and A. Tipton, *Synthetic biodegradable polymers as medical devices.* Medical Plastic and Biomaterials, 1998. **5**: p. 30-39.
132. Miller, R.A., J.M. Brady, and D.E. Cutright, *Degradation rates of oral resorbable implants (polylactates and polyglycolates): rate modification with changes in PLA/PGA copolymer ratios.* Journal of biomedical materials research, 1977. **11**(5): p. 711-719.
133. Zhijiang, C. and W. Zhihong, *Preparation of biodegradable poly (3-hydroxybutyrate)(PHB) and poly (ethylene glycol)(PEG) graft copolymer.* Journal of materials science, 2007. **42**(14): p. 5886-5890.
134. Laeger, T., C.C. Metges, and B. Kuhla, *Role of β-hydroxybutyric acid in the central regulation of energy balance.* Appetite, 2010. **54**(3): p. 450-455.
135. Ahmed, T., et al., *Polyhydroxybutyrate and its copolymer with polyhydroxyvalerate as biomaterials: influence on progression of stem cell cycle.* Biomacromolecules, 2010. **11**(10): p. 2707-2715.
136. Kubein-Meesenburg, D., et al., *Changes in insulin like growth factors, myostatin and vascular endothelial growth factor in rat musculus latissimus dorsi by poly-3-hydroxybutyrate implants.* Journal of Physiology and Pharmacology, 2009(60 Suppl 3): p. 77-81.
137. Pouton, C.W. and S. Akhtar, *Biosynthetic polyhydroxyalkanoates and their potential in drug delivery.* Advanced Drug Delivery Reviews, 1996. **18**(2): p. 133-162.
138. Patlolla, A., G. Collins, and T.L. Arinzeh, *Solvent-dependent properties of electrospun fibrous composites for bone tissue regeneration.* Acta biomaterialia, 2010. **6**(1): p. 90-101.
139. Darney, P.D., et al., *Clinical evaluation of the Capronor contraceptive implant: preliminary report.* American Journal of Obstetrics & Gynecology, 1989. **160**(5): p. 1292-1295.
140. Sun, H., et al., *The in vivo degradation, absorption and excretion of PCL-based implant.* Biomaterials, 2006. **27**(9): p. 1735-1740.
141. He, S., et al., *Synthesis of biodegradable poly (propylene fumarate) networks with poly (propylene fumarate)–diacrylate macromers as crosslinking agents and characterization of their degradation products.* Polymer, 2001. **42**(3): p. 1251-1260.
142. Young, S., et al., *Dose effect of dual delivery of vascular endothelial growth factor and bone morphogenetic protein-2 on bone regeneration in a rat critical-size defect model.* Tissue Engineering Part A, 2009. **15**(9): p. 2347-2362.

143. Hacker, M., et al., *Biodegradable fumarate - based drug - delivery systems for ophthalmic applications.* Journal of Biomedical Materials Research Part A: An Official Journal of The Society for Biomaterials, The Japanese Society for Biomaterials, and The Australian Society for Biomaterials and the Korean Society for Biomaterials, 2009. **88**(4): p. 976-989.
144. Chen, W., et al., *pH-Sensitive degradable polymersomes for triggered release of anticancer drugs: a comparative study with micelles.* Journal of Controlled Release, 2010. **142**(1): p. 40-46.
145. Lee, S., et al., *Polyketal microparticles: a new delivery vehicle for superoxide dismutase.* Bioconjugate chemistry, 2007. **18**(1): p. 4-7.
146. Ekholm, M., et al., *A histological and immunohistochemical study of tissue reactions to solid poly (ortho ester) in rabbits.* International journal of oral and maxillofacial surgery, 2006. **35**(7): p. 631-635.
147. Zhang, Z., et al., *The in vivo and in vitro degradation behavior of poly (trimethylene carbonate).* Biomaterials, 2006. **27**(9): p. 1741-1748.
148. Bonzani, I.C., et al., *Synthesis of two-component injectable polyurethanes for bone tissue engineering.* Biomaterials, 2007. **28**(3): p. 423-433.
149. Weikel, A.L., et al., *Miscibility of choline-substituted polyphosphazenes with PLGA and osteoblast activity on resulting blends.* Biomaterials, 2010. **31**(33): p. 8507-8515.
150. Verret, V., et al., *Influence of degradation on inflammatory profile of polyphosphazene coated PMMA and trisacryl gelatin microspheres in a sheep uterine artery embolization model.* Biomaterials, 2011. **32**(2): p. 339-351.
151. Ulery, B.D., L.S. Nair, and C.T. Laurencin, *Biomedical Applications of Biodegradable Polymers.* J Polym Sci B Polym Phys, 2011. **49**(12): p. 832-864.
152. Wakizaka, D., et al., *Hole transport in conducting ultrathin films of PEDOT/PSS prepared by layer-by-layer deposition technique.* Polymer, 2004. **45**(25): p. 8561-8565.
153. Okutan, M. and H. Deligöz, *Effect of external salt addition on the structural, morphological and electrochemical properties of flexible PEDOT: PSS based LbL multilayered films.* Colloids and Surfaces A: Physicochemical and Engineering Aspects, 2019. **580**: p. 123695.
154. Ling, H., et al., *Layer-by-layer assembly of PEDOT: PSS and WO3 nanoparticles: enhanced electrochromic coloration efficiency and mechanism studies by scanning electrochemical microscopy.* Electrochimica Acta, 2015. **174**: p. 57-65.
155. Sakai, N., et al., *Layer-by-layer assembled TiO2 nanoparticle/PEDOT-PSS composite films for switching of electric conductivity in response to ultraviolet and visible light.* Chemistry of materials, 2006. **18**(16): p. 3596-3598.
156. Knowles, K.R., et al., *Layer-by-layer assembled multilayers of polyethylenimine-stabilized platinum nanoparticles and PEDOT: PSS as anodes for the methanol oxidation reaction.* ACS applied materials & interfaces, 2012. **4**(7): p. 3575-3583.
157. DeLongchamp, D. and P.T. Hammond, *Layer - by - layer assembly of PEDOT/polyaniline electrochromic devices.* Advanced Materials, 2001. **13**(19): p. 1455-1459.
158. Ward, M.D. and D.A. Buttry, *In situ interfacial mass detection with piezoelectric transducers.* Science, 1990. **249**(4972): p. 1000-1007.
159. Maiorova, L.A., et al., *Encapsulation of vitamin B12 into nanoengineered capsules and soft matter nanosystems for targeted delivery.* Colloids and Surfaces B: Biointerfaces, 2019. **182**: p. 110366.
160. Gai, M., et al., *Polylactic acid nano- and microchamber arrays for encapsulation of small hydrophilic molecules featuring drug release via high intensity focused ultrasound.* Nanoscale, 2017. **9**(21): p. 7063-7070.

161. Cheung, J., W. Stockton, and M. Rubner, *Molecular-level processing of conjugated polymers. 3. Layer-by-layer manipulation of polyaniline via electrostatic interactions.* Macromolecules, 1997. **30**(9): p. 2712-2716.
162. Gai, M., et al., *Patterned microstructure fabrication: polyelectrolyte complexes vs polyelectrolyte multilayers.* Scientific reports, 2016. **6**: p. 37000.
163. Gai, M., et al., *Micro-contact printing of PEM thin films: effect of line tension and surface energies.* RSC Advances, 2015. **5**(64): p. 51891-51899.
164. Cheng, J.L., et al. *Synthesis and imidization of polyamic acid.* in *Advanced Materials Research.* 2011. Trans Tech Publ.
165. Marasso, S., et al., *A novel graphene based nanocomposite for application in 3D flexible micro-supercapacitors.* Materials Research Express, 2016. **3**(6): p. 065001.
166. Senturia, S.D., *Microsystem design.* 2007: Springer Science & Business Media.
167. Chen, K.-S., et al., *Effect of process parameters on the surface morphology and mechanical performance of silicon structures after deep reactive ion etching (DRIE).* Journal of Microelectromechanical Systems, 2002. **11**(3): p. 264-275.
168. Liu, P. and L. Zhang, *Hollow nanostructured polyaniline: Preparation, properties and applications.* Critical Reviews in Solid State and Materials Sciences, 2009. **34**(1-2): p. 75-87.
169. Park, M.-K., et al., *Self-assembly and characterization of polyaniline and sulfonated polystyrene multilayer-coated colloidal particles and hollow shells.* Langmuir, 2003. **19**(20): p. 8550-8554.
170. Sukhorukov, G.B., et al., *Hollow polyelectrolyte shells: exclusion of polymers and donnan equilibrium.* The Journal of Physical Chemistry B, 1999. **103**(31): p. 6434-6440.
171. De Geest, B.G., et al., *Polyelectrolyte microcapsules for biomedical applications.* Soft Matter, 2009. **5**(2): p. 282-291.
172. De Geest, B.G., et al., *Release mechanisms for polyelectrolyte capsules.* Chemical Society Reviews, 2007. **36**(4): p. 636-649.
173. De Geest, B.G., G.B. Sukhorukov, and H. Möhwald, *The pros and cons of polyelectrolyte capsules in drug delivery.* Expert opinion on drug delivery, 2009. **6**(6): p. 613-624.
174. De Koker, S., et al., *Polymeric multilayer capsules delivering biotherapeutics.* Advanced drug delivery reviews, 2011. **63**(9): p. 748-761.
175. Sukhorukov, G.B., et al., *pH - controlled macromolecule encapsulation in and release from polyelectrolyte multilayer nanocapsules.* Macromolecular Rapid Communications, 2001. **22**(1): p. 44-46.
176. Charcosset, C. and J.-C. Bernengo, *Comparison of microporous membrane morphologies using confocal scanning laser microscopy.* Journal of membrane science, 2000. **168**(1-2): p. 53-62.
177. Gai, M., et al., *Polylactic acid sealed polyelectrolyte multilayer microchambers for entrapment of salts and small hydrophilic molecules precipitates.* ACS applied materials & interfaces, 2017. **9**(19): p. 16536-16545.
178. McKeen, L.W., *The effect of sterilization on plastics and elastomers.* 2018: William Andrew.
179. de la Oliva, N., X. Navarro, and J. del Valle, *Time course study of long - term biocompatibility and foreign body reaction to intraneural polyimide - based implants.* Journal of Biomedical Materials Research Part A, 2018. **106**(3): p. 746-757.
180. Löffler, S., et al., *Long term in vivo stability and frequency response of polyimide based flexible array probes.* Biomedical Engineering/Biomedizinische Technik, 2012. **57**(SI-1 Track-S): p. 104-107.

181. Pothof, F., et al., *Chronic neural probe for simultaneous recording of single-unit, multi-unit, and local field potential activity from multiple brain sites.* Journal of neural engineering, 2016. **13**(4): p. 046006.
182. Lee, Y.J., et al., *Characterization of nerve-cuff electrode interface for biocompatible and chronic stimulating application.* Sensors and Actuators B: Chemical, 2016. **237**: p. 924-934.
183. Heo, D.N., et al., *Flexible and highly biocompatible nanofiber-based electrodes for neural surface interfacing.* ACS nano, 2017. **11**(3): p. 2961-2971.
184. DeLongchamp, D.M. and P.T. Hammond, *High - contrast electrochromism and controllable dissolution of assembled Prussian blue/polymer nanocomposites.* Advanced Functional Materials, 2004. **14**(3): p. 224-232.
185. Schmidt, D.J., J.S. Moskowitz, and P.T. Hammond, *Electrically triggered release of a small molecule drug from a polyelectrolyte multilayer coating.* Chemistry of Materials, 2010. **22**(23): p. 6416-6425.
186. Wood, K.C., et al., *Electroactive controlled release thin films.* Proceedings of the National Academy of Sciences, 2008. **105**(7): p. 2280-2285.

# ACKNOWLEDGMENTS

First of all I want to thank my supervisor Dr. Salvatore Iannotta and my co-supervisor Dr. Victor Erokhin from the Institute of Materials for Electronics and Magnetism who gave me the opportunity to study and work in the field of drug delivery. I want to thank you for your continuous support, motivation and knowledge. Thank you for having guided me throughout my PhD program and during the writing of this work.

I would like to thank the other people from IMEM that contributed to my PhD in different extent and ways: Dr. Svetlana Erokhina, Dr. Pasquale D'Angelo, Dr. Tatiana Berzina, Dr. Simone Marasso, Dr. Matteo Cocuzza, Dr. Giovanna Trevisi.

A huge thank goes to Theras Group, in the persons of Cristiano Ferrari, Federico Ferrari e Maria Bobbi, for having believed and contributed in/to the project and for the stimulating suggestions in the various meetings.

I really would like to thank also Prof. Gleb Sukhorukov of the School of Engineering and Materials Science of Queen Mary University of London, for giving me the opportunity to join his team for a while and giving me the access to the laboratory and research facilities. My time in London has been a great experience both in terms of work and personal life.

A very huge thank you goes to Dr. Silvia Battistoni for her time, support and patience and for having suffered all my schicchiricchi.

I want to thank all my lab mates and friends Davide, Carlotta, Regina, Roman, Adeliia for their support and laughs in and outside the lab and in the case of Davide, also for eating all my leftover food. I want also to thank Elena and Ifeany.
I would like to thank also my *Parmigiane pentite* friends Ceci and Carmen, Clari and my *Baby* Viola for being an important part of my life during this experience.

Finally, I want to thank my family and Pier for the unconditional support and love.